Title
Matrix Attachment Therapy for Cancer

Author
Park, Joshua Inshik

Publication Date
2008-06-03

Peer reviewed|Thesis/dissertation

Matrix Attachment Therapy for Cancer

by

Joshua Inshik Park

DISSERTATION

Submitted in partial satisfaction of the requirements for the degree of

DOCTOR OF PHILOSOPHY

in

PHARMACEUTICAL SCIENCES AND PHARMACOGENOMICS

in the

GRADUATE DIVISION

Dedicated to my wife Renee, my parents, and my sister Lois

For their unconditional love and support,

And to our friend JC

ACKNOWLEDGEMENTS

There are many individuals who gave their precious time and advice for me since I started graduate school--my thesis would be incomplete without their help. First and foremost, I thank Professor Frank Szoka for his guidance, research ideas, and many insightful advices as my thesis research advisor. I also thank Professor Dennis Deen for sharing his knowledge on enzyme-prodrug combination therapies for cancer, and giving me a big dose of encouragement when I started my thesis project as a former collaborator.

I thank my thesis committee members, Professor Deanna Kroetz and Professor Robert Stern, for reviewing my thesis dissertation and giving me helpful suggestions. I also thank Professor Patsy Babbitt and Professor Emil Lin for kindly serving in my qualifying exam committee with my thesis committee members.

I thank Dr. Bob Stull and Dr. Jeff Sperinde for constructing early versions of bacteria expression vectors for TSG-6Link, CD, and LinkCD fusion protein; Dr. Limin Cao who helped me with modifying LinkCD constructs for different fusion tags; Dr. Zhaohua Huang for creating tri-NTA molecule for improved immobilization of His-tagged proteins on Biacore chip, and for obtaining hyaluronan binding activity of LinkCD; Virginia Platt for hyaluornan oligomers for Biacore experiments; Dr. Peter Hwang for his helpful advice for operating Biacore instruments; Dr. Weijun Li, Allan Graves, and Neema Salimi for their technical guidance on circular dichroism; Dr. Eric Johansen for ESI-MS; Justin Blethrow for MALDI; Jenn Yokoyama for creating a functional mutant of the CD enzyme that lacks enzymatic activity; Ed Dy, Nikki Macaraeg, and Kat Jerger for *in vivo* experiments. It was my pleasure to work with all other members of the Szoka group: Dr. Andrew MacKay, Rich Cohen, Doug Watson, Kareen Riviere, Dr. Grace Huynh, Laura Serwer, Emily Watson, Dr. Marieke van der Aa, Leanna Lapacan, Gabriel Reyes, Dr. Bo Chen, Dr. Oana Martin, Dr. Norased Nasongkla, Dr. Dipali Ruhela, Dr. Mahmoud Jaafari, Dr. Mark Rashkin, Dr. Vladimir Sidarov, Dr. Xin Wen, Michael Hicks, Michael Mysinger, and Louisa Stern.

Also, I thank Dr. Greg Frost, Dr. Lou Bookbinder, and Dr. Gilbert Keller at Halozyme Therapeutic for their special interest in my thesis project and industry support for UC Discovery Grant.

Lastly, I thank my previous research mentors who encouraged pursuing a scientific career: Professor Chan Jung at the State University of New York at Buffalo, and Professor Arleen Rifkind at Weill Medical College of Cornell University.

This work was supported by NIH R01-CA107268 and UC Discovery Grant.

Matrix Attachment Therapy for Cancer

by Joshua Inshik Park

Abstract

The hypothesis of my thesis project was that targeting the extracellular matrix of a solid tumor for a local generation of a cytotoxic drug could inhibit tumor growth and progression. To test this hypothesis of the matrix attachment therapy (MAT), a gene therapy and recombinant protein therapy were pursued. For the gene therapy, I cloned a mammalian expression vector containing the extracellular domain of CD44 (sCD44), yeast cytosine deaminase (CD), and *E.coli* uracil phosphoribosyltransferase (UPRT) genes to transfect tumor cells *in vitro*. The sCD44::CD::UPRT fusion gene construct was designed to secrete the expressed fusion protein and generate cytotoxic drugs to cause cell deaths in the presence of the prodrug 5-fluorocytosine (5-FC). This gene therapy strategy did not result in a potent cytotoxic effect on cells that expressed the fusion gene due to low expression of the fusion genes in transfected cells.

For the protein therapy, a recombinant fusion protein containing TSG-6 Link (Link) and the CD enzyme was expressed in *E.coli* and purified to characterize the functions of the LinkCD fusion protein. LinkCD exhibits K_m of 0.33 mM and V_{max} of 14 μM/min/μg for the conversion of 5-FC to 5-FU. LinkCD can bind to a hyaluronan oligomer (12-mer) at a K_D of 55 μM at pH 7.4 and a K_D of 5.32 μM at pH 6.0 measured using surface plasmon resonance (SPR). To evaluate the anti-tumor effect of LinkCD/5-FC combination

therapy *in vivo*, mice received intratumoral injections of LinkCD on days 11 and 14 after C26 tumor implantation and drinking water containing 10 mg/mL of 5-FC starting on day 11. Animals that received LinkCD/5-FC treatment showed significant tumor size reduction and increased survival compared to the CD/5-FC treatment group. Other treatment groups that were unable to produce 5-FU had no effect on the tumor growth despite receiving the fusion protein that contained the Link domain. The results strongly suggest that a treatment regime consisting of a fusion protein containing the Link domain, the active CD enzyme, and the prodrug 5-FC are required to produce an anti-tumor effect. Intravenous administration of LinkCD to animals tumored with C26 that received 5-FC in the drinking water did not result in a therapeutic effect, possibly due to a short circulation time of LinkCD. I created chimeras of the CD44 Link domain *in silico* that could potentially be used to increase the circulation time of LinkCD in the blood. Thus, MAT is a promising alternative to antibody-directed prodrug enzyme therapy approach for cancer treatment.

TABLE OF CONTENTS

PRELIMINARY PAGES

LIST OF TABLES

LIST OF FIGURES

LIST OF ABBREVIATIONS

5-FC	5-fluorocytosine
5-FdUMP	5-fluoro-2'-deoxyuridine-monophosphate
5-FU	5-fluorouracil
5-FUMP	5-fluorouridine-5'-monophosphate
ADEPT	antibody-directed enzyme prodrug therapy
CD	cytosine deaminase, yeast
ECM	extracellular matrix
EPR	enhanced permeability and retention
GDEPT	gene-directed enzyme prodrug therapy
GST	glutathione-s-transferase
HA	Hyaluronan
His	histitine(×6)-tag
LinkCD	TSG-6Link-cytosine deaminase fusion protein
Link-mtCD	TSG-6Link-mutant cytosine deaminase (E64A) fusion protein
MAT	matrix attachment therapy
MMP	matrix metalloproteinase
mtCD	mutant cytosine deaminase (E64A)
MTT	3-(4,5-dimethylthiazol-2-yl)-2,5-diphenyl tetrazolium bromide
Mw	molecular weight
NTA	nitriloacetic acid
ORF	open reading frame
PEG	polyethylene glycol
PEI	polyethyleneimine
PSI-BLAST	position-specific iterative basic local alignment tool
RMSD	room mean squared deviation
SPR	surface plasmon resonance
TS	thymidylate synthase
TSG-6	tumor necrosis factor-α stimulated gene-6
UPRT	uracil phosphoribosyltransferase

CHAPTER 1

Targeting Extracellular Matrix for Cancer Therapy

1.1 Introduction

Ideal chemotherapeutic drugs against cancer would target and eradicate malignant cells while leaving normal cells intact, thus minimizing unwanted side effects of the treatment. Small molecule-based chemotherapeutic drugs are usually non-targeted because the drug can be absorbed either passively or by drug transporters in both normal and cancer cells. Therefore, the drug effect in normal tissues always results in adverse side effects from the chemotherapy treatment, which ultimately limits the dose that can be given to a patient. Cancer cells become more resistant to drug treatment when they over-express drug transporters that pump the drug out of the cells, thereby reducing the intracellular drug concentration (reviewed in Gillet et al 2007). In such situations, a logical course of treatment is to increase the drug dose. Although increasing the dose of chemotherapeutic drug(s) may overcome the drug resistance to certain limits, such a tactic often leads to severe systemic toxicities that may even be fatal. Therefore, targeted therapy that could deliver cytotoxic agents to the tumor, while minimizing its effect on normal tissue, is the hallmark of successful cancer therapy.

Recent developments in targeted therapies include monoclonal antibodies against growth factor receptors to prevent cancer progression (reviewed in Zafir-Lavie et al 2007). While these target specific antibody drugs bring higher hopes for better disease management, only a small number of selected patients benefit from these treatments.

This is because not all patients express the target proteins at high enough levels in tumors for the antibody-based therapies to be effective.

Unlike small molecule drugs, macromolecules such as monoclonal antibodies, liposomes, and biocompatible polymers are too large to diffuse out of the blood through the capillary walls. However, these macromolecules can accumulate at sites where the architecture of the blood vasculature is compromised due to an abnormally high rate of angiogenesis, and macromolecules escape through the large gaps between the endothelial cells that make up blood vessels (reviewed in Greish 2007). This phenomenon is called the enhanced permeability and retention (EPR) effect (O'Conner and Bale 1984). Macromolecules that circulate with a long half-life can exploit this phenomenon to passively target solid tumors and sites of inflammations (reviewed in Allen and Cullis 2004).

Enzyme prodrug therapy is a targeted therapy strategy for treating cancer. A prodrug, by definition, is non-toxic to the body and must be metabolized by an enzyme to become an active drug. A prodrug designed so that it can only be converted to a cytotoxic drug by an exogenous enzyme is preferred for enzyme prodrug therapy. This approach employs a relatively non-toxic prodrug that can be activated into a cytotoxic drug only at the site where the enzyme partner is located. Gene Directed Enzyme Prodrug Therapy (GDEPT) and Antibody Directed Enzyme Prodrug Therapy (ADEPT) for targeted tumor therapy have been developed based on this enzyme prodrug strategy (Moolten 1987, and Bagshawe 1987). The delivery of therapeutic genes for GDEPT and antibody-enzyme

conjugates for ADEPT to the tumor site depend on the EPR effect for tumor targeting. Although there are many promising examples of GDEPT and ADEPT in animal studies, there are major impediments for moving them forward to successful clinical trials. For GDEPT, the safety and efficacy of gene delivery are the major issues that must be improved (Greco and Dachs 2001, and Portsmouth et al 2007). The major impediments for ADEPT are heterogenous expressions of tumor specific antigens and technical challenges of producing large quantities of antibody-enzyme conjugates (Senter and Springer 2001, and Asai et al 2005). To address some of the challenges of current enzyme prodrug strategies, my project focused on targeting hyaluronan in the tumor matrix by a fusion protein containing a hyaluronan binding domain and an enzyme to generate cytotoxic drug in the tumor microenvironment.

In this chapter, I summarize the recent preclinical studies and clinical trials based on GDEPT and ADEPT and describe the limitations of current enzyme prodrug therapy strategies. The enzyme/prodrug combinations used for GDEPT and ADEPT experiments, and the mechanisms of anti-tumor activity by activated drugs have been extensively reviewed elsewhere (Bagshawe 2006, and Portsmouth et al 2007). I also describe the influence of hyaluronan on tumor progression and metastasis to show that hyaluronan is an attractive target for matrix attachment therapy. Lastly, I introduce the matrix attachment therapy for treating cancer; targeting the extracellular matrix of solid tumor and generating a non-toxic drug into cytotoxic drug in the vicinity of tumor cells would potentially overcome many of the impediments of GDEPT and ADEPT for cancer treatment.

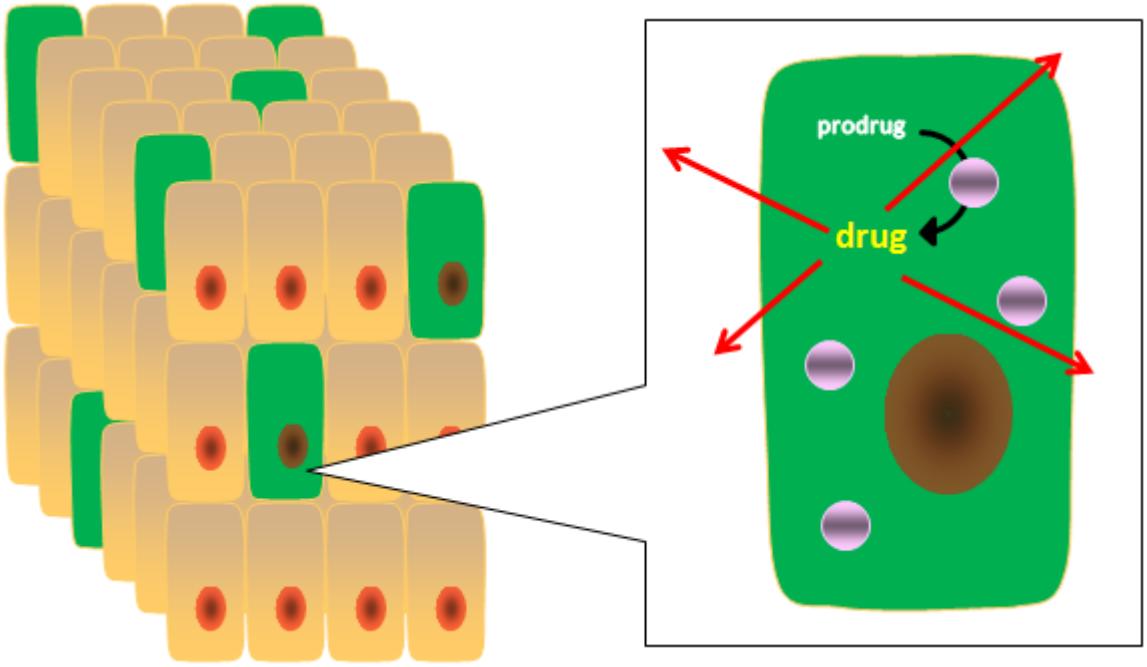

Figure 1-1. Gene-directed enzyme prodrug therapy
A prodrug converting enzyme gene is delivered to the tumor cells via viral or non-viral vectors. A subpopulation of the tumor cells is genetically modified to express the enzyme. These 'factory cells' (green) convert a prodrug to cytotoxic drug. The generated cytotoxic drug is released from the factory cells to cause a bystander effect to non-transfected tumor cells.

Table 1-1. Preclinical studies of gene-directed enzyme prodrug therapy

Enzyme	Prodrug	Active drug	Tumor model/animal	*In vivo* efficacy *	Reference
Carboxylesterase (human)	Irinotecan	SN-38	A549/mouse	Delayed tumor growth (30 d)	Kojima et al 1998
Carboxypeptidase G2 (*Pseudomonas*)	CMDA	Nitrogen mustard	MDA-MB361/mouse	Delayed tumor growth (110 d)	Stribbling et al 2000
Cytochrome P450 2B6 (human)	CPA	CPA-mustard	HT29 and MDA-MB231/mouse	Delayed tumor growth (21 d)	Kan et al 2001
Cytosine deaminase (*E.coli*)	5-FC	5-FU	HT29/mouse	Delayed tumor growth (24 d)	Hirschowitz et al 1995
Cytosine deaminase (yeast)	5-FC	5-FU	HT29/mouse	Delayed tumor growth (84 d), CR (6/13)	Kievit et al 1999
	5-FC	5-FU	U87/mouse	Delayed tumor growth, CR	Tai et al 2005
Nitroreductase (*E.coli*)	CB1954	Alkylating agents	SUIT2 and SKOV3/mouse	Delayed tumor growth (56 d), favorable survival (56 and 91 d)	McNeish et al 1998
Thymidine kinase (HSV-1)	GCV (and radiation)	Triphosphorylated GCV	K3T3/mouse	CR (52/55)	Moolten 1988

Cell lines – A549: human lung carcinoma, MDA-MB231/361: human breast carcinoma, HT29: human colon carcinoma, U87: human glioblastoma, SUIT2: human pancreatic carcinoma and SKOV3: human ovarian carcinoma, K3T3: murine sarcoma

CMDA: 4-[2-chloroethyl)(2-mesyloxyethyl)amino]benzoyl-L-glutamic acid, Nitrogen mustard: 4-[(2-chloroethyl)(2-mesyloxyethyl)amino]benzoic acid, CPA: cyclophosphamide, 5-FC: 5-fluorocytosine, 5-FU: 5-fluorouracil, CB1954: 5-(aziridin-1-yl)-2,4-dinitrobenzamide, GCV: ganciclovir
* d in parenthesis: last days of in vivo anti-tumor study, CR: complete response (no. survived/no. treatment group)

1.2 Gene-directed enzyme prodrug therapy (GDEPT)

GDEPT is based on a gene therapy approach, in which tumor cells are genetically modified with an exogenous enzyme gene to become 'factory cells'. These factory cells express an enzyme that can catalyze a prodrug into a cytotoxic drug (Figure 1-1). Since no other cells in the body express the enzyme, the prodrug will only be activated within these factory cells. A prodrug is designed so that it can diffuse into tumor cells relatively easily and to be converted to a cytotoxic drug by the expressed enzyme within the factory cells. Gene therapy studies evolved and branched out to develop GDEPT in the 1980's, and many enzyme/prodrug combinations have been investigated for GDEPT in laboratories to treat cancers (Table 1-1). Some of these combinations are also being investigated for ADEPT (Table 1-2).

An activated cytotoxic drug by a prodrug converting enzyme should be able to cause a 'bystander effect' in order to maximize the efficacy of GDEPT to eradicate tumors. A bystander effect of the prodrug activation is achieved when the generated cytotoxic drug within a factory cell diffuses into the neighboring cells that may not have been modified by the exogenous gene. Hence, GDEPT is synonymously called 'suicide gene therapy' because the cell that produces the prodrug converting enzyme is killed. The bystander effect of an enzyme prodrug partner is one of the salient features of GDEPT, because only a fraction of the tumor cell population can be genetically modified by the current gene delivery methods (reviewed in Glasgow et al 2006). Huber and his coworkers (1994) stably transfected WiDr cells (a human colon adenocarcinoma cell line) with the yeast CD gene, and mixed them with untransfected WiDr cells in various ratios to

examine the minimum percentage of the tumor cell population that is required for the bystander effect *in vivo*. They showed that only 2% of the transfected cells in the tumor population are required for significant tumor growth inhibition with 5-FC treatment, but also reported that there are no long-term survivors beyond 175 days. The findings of this study are useful for GDEPT investigators, but it is also misleading because: 1) gene delivery to the tumor cells will not be distributed evenly within a solid tumor; and 2) the drug sensitivity of tumor cells varies among tumor cell type.

Thymidine kinase from herpes simplex virus 1 (HSVtk) and ganciclovir (9-([2-hydroxy-1-(hydroxymethyl)ethoxy]methyl) guanine, or GCV) combination showed promising results in the laboratory settings and moved on to clinical trials for treating patients with the malignant brain tumor glioblastoma multiforme (Ram et al 1997, Klatzmann 1998, and Shand et al 1999). However, the HSVtk/GCV combination therapy failed to demonstrate significantly longer survival and treatment responses in a controlled-Phase III clinical study for glioblastoma patients who received HSVtk/GCV and radiation treatments (Rainov 2000). The most common adverse effects of the GDEPT treatments on glioblastoma and glioblastoma multiformes were related to the prodrug treatment and progression of the disease, including: cranial hematomas, thromboembolic events, pneumothorax, thrombosis, leucopenia, and infections. HSVtk and its prodrugs were also used unsuccessfully in early clinical trials for prostate and ovarian cancers.

Other enzyme/prodrug combinations used in Phase I amd II clinical trials include: cytosine deaminase/5-fluorocytosine, nitroreductase/5-(aziridin-1-yl)-2,4-dinitrobenzam-

ide, and cytochrome P-450/cyclophosphamide for breast, melanoma, and head/neck cancers (Table 1-3). Common adverse side effects of these treatments were related to prodrug/gene vector administrations, which included pain, inflammation, and bleeding at the injection site; leucopenia, neutropenia, thrombocytopenia, neutropenia, and elevated pyruvic transaminases/alanine aminotrasferases. Although the side effects of the treatments seem to be somewhat less severe than that of GDEPT treatments for glioblastoma, none of these trials have yet to successfully move forward into Phase III.

A multi-cycle, replication-competent retroviral (RCR) vector seems be an effective viral vector for gene delivery (reviewed in Dalba et al 2007). A recent GDEPT study employed a murine leukemia virus (MLV) based RCR vector to increase the efficiency of transfecting tumor cells (Tai et al 2005). This study showed that an efficient gene transfer to tumor cells could be achieved *in vivo* using a multi-cycle RCR vector. Using the U87-MG human glioma model in mice, the study demonstrated that the *in vivo* gene transfection by a single intratumoral injection was highly efficient and tumor-selective. Furthermore, significant survival was observed (90% survival up to ~110 days) in the animals that received the cytosine deaminase gene via multi-cycle RCR vector and 5-FC, whereas all animals that received the cytosine deaminase gene via a single-cycle RCR vector and 5-FC died shortly after 70 days. Thus, the use of multi-cycle RCR vector for the delivery of a prodrug converting enzyme gene to tumor cells is certainly a promising approach for a viral-vector mediated GDEPT for cancer. The safety and efficacy for human use remain to be evaluated. Despite the efforts to enhance bystander effect and therapeutic efficacy in animal studies, the results of GDEPT clinical trials so far have

been disappointing (Table 1-3). The major impediments for moving gene therapy based approaches are the safety and efficacy of gene delivery (reviewed in Greco and Dachs 2001, and Portsmouth et al 2007). Unless there are technical breakthroughs in the current gene delivery methods that can overcome safety and efficacy issues for human use, it is improbable for GDEPT to become a successful cancer therapy.

1.3 Antibody-directed enzyme prodrug therapy (ADEPT)

The goal of ADEPT is to deliver an antibody-enzyme conjugate, which is designed to bind to a tumor specific antigen, to the tumor cell surface and in the presence of prodrug, generate active cytotoxic drug at the tumor site to kill tumor cells (Figure 1-2). The delivery of antibody-enzyme conjugate relies on the enhanced permeability and retention effect observed in the tumor vasculature (O'Conner and Bale 1984). There are many antibody-enzyme/prodrug combinations that have been developed and examined for potential cancer treatments in laboratories (Table 1-2). Detailed mechanisms of targeting and anti-tumor activities of antibody-enzyme/prodrug combinations are reviewed elsewhere (Senter and Springer 2001, and Bagshawe 2006).

Although the theoretical concept of ADEPT was conceived and laboratory experiments began in the mid-1980s (Bagshawe 1987, Bagshawe et al 1988, and Senter et al 1988), the efficacy of its use for cancer treatment has not yet been demonstrated in clinical trials (Table 1-3). Moreover, the number of preclinical animal studies of ADEPT is far less than that of GDEPT. Thus, there is no strong *in vivo* evidence to support that ADEPT is a promising cancer therapy. The difficulty of producing large enough quantity of an

antibody-enzyme conjugate for animal studies in an academic setting is one of the reasons ADEPT is not as extensively studied as GDEPT for preclinical development (Senter and Springer 2001, and Asai et al 2005). In the early stage of development, intact IgG antibodies against tumor specific antigens were chemically conjugated to prodrug converting enzymes (Senter et al 1988, Wallace and Senter 1989, Senter et al 1991). The intrinsic property of an IgG is a long circulation time in the blood, which can be an advantage for accumulation of the antibody-enzyme conjugate in the tumor site. However, it is also a major drawback since the long circulation half life of antibody-enzyme conjugate can possibly lead to systemic toxicities by converting the prodrug into the active drug in the blood. If this occurs, there is not a great therapeutic advantage over systemic drug treatment alone.

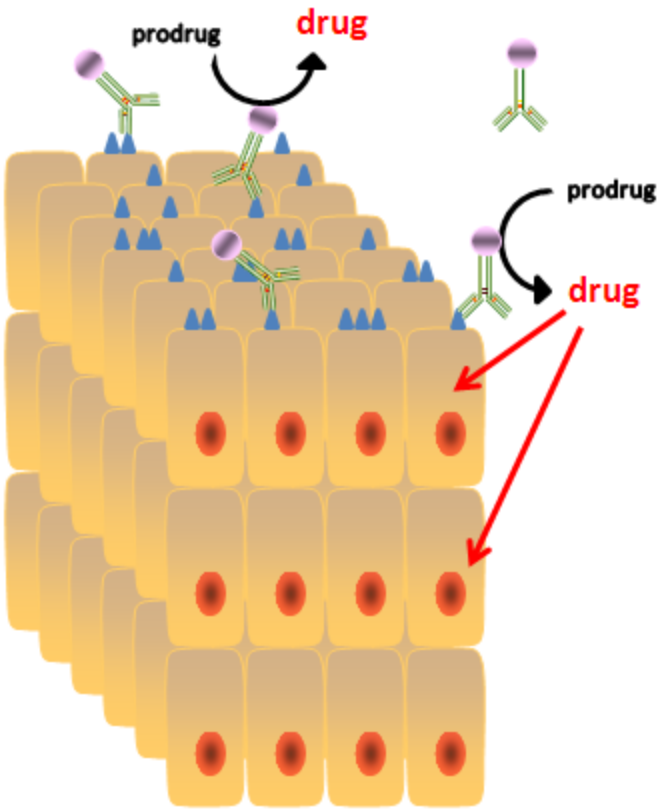

Figure 1-2. Antibody-directed enzyme prodrug therapy for cancer
ADEPT strategy employs an antibody-enzyme conjugate, which is designed to target tumor specific antigen and convert a non-toxic prorug into cytotoxic drug locally. The effectiveness of this strategy depends on the high level of tumor-specific antigen expression on the cell surface of tumor cells.

Table 1-2. Preclinical studies of antibody-directed enzyme prodrug therapy

Enzyme	Prodrug	Active drug	Tumor model/animal	*In vivo* efficacy *	Reference
Alkaline phosphatase	Etoposide phosphate	Etoposide	H3347/ mouse	CR (6/16), S (5/16), P(2/6)	Senter et al 1988
	Phenol mustard phosphate	Phenol mustard	H2981/mouse	Delayed tumor growth (42 d)	Wallace and Senter 1991
β-Lactamase	Cephalosporin sulfoxide	DAVLBHYD	LS174T and T380/ mouse	Delayed tumor growth (80 d)	Meyer et al 1993
	GS-Mel	Mel	LS174T/mouse	Delayed tumor growth (34 d)	Alderson et al 2006
Carboxypeptidase A1	Prodrugs of MTX, GW1031, and GW1843	MTX, GW1031, and GW1843	LS174T/mouse	No effect	Wolfe et al 1999
	Prodrug of MTX	MTX	PC-3m/mouse	Delayed tumor growth (42 d)	Hao et al 2006
Carboxypeptidase G2	CMDA	Nitrogen mustard	CC3/mouse	CR (9/12)	Springer et al 1991
Cytosine deaminase	5-FC	5-FU	H2981/mouse	No data on tumor growth	Wallace et al 1994

Cell lines: H2981, H3347, LS174T, T380 (human colon adenocarcinoma), PC-3 (human prostate cancer), CC3: human gestational choriocarcinoma
* d in parenthesis: last days of in vivo anti-tumor study, CR: complete response, S: stable, P: partial response (no. animals/total no. treatment group)

Phenol mustard: *p*-[*N*,*N*-bis(2-chloroethyl)amino]phenol, CMDA: 4-[2-chloroethyl)(2-mesyloxyethyl)amino]benzoyl-L-glutamic acid, DAVLBHYD: 4-desacetylvinblastine-3-carbohydrazide, GS-Mel: Glutaryl cephalosporin bis-diphenylmethyl ester, Mel: melphalan, MTX: methotrexate, GW1031: *N*-(2-fluoro-4(((1,2-dihydro-3-methyl-1-oxobenzo(*f*)quinazolin-9-yl) methyl)amino)benzoyl)-L-glutamic acid, GW1843: (*S*)-2-(5-(((1,2-dihydro-3-methyl-1-oxobenzo(*f*)quinazolin-9-yl)methyl)amino)-1-oxo-2-isoindolinyl)glutaric acid, Nitrogen mustard: 4-[(2-chloroethyl)(2-mesyloxyethyl)amino]benzoic acid, 5-FC: 5-fluorocytosine, 5-FU: 5-fluorouracil

Table 1-3. Summary of clinical trials of enzyme prodrug therapy for various cancer types

Therapy	Cancer	Enzyme	Prodrug	Additional Treatment	Phase	No. Patients	Survival Effect*	Adverse Effect	Reference
GDEPT	Glioblastoma	HSVtk (i.t.)	GCV	None	I	15	N/A	Moderate	Ram et al 1997
	Glioblastoma	HSVtk (i.t.)	GCV	None	I/II	12	N/A	Moderate to severe	Klatzmann et al 1998
	GBM	HSVtk (i.t.)	GCV	None	I/II	48	N/A	Moderate	Shand et al 1999
	GBM	HSVtk (i.t.)	GCV	Radiation	III	124	No effect	Moderate to severe	Rainov 2000
	Prostate	HSVtk (i.t.)	GCV	None	I	18	N/A	Mild to moderate	Herman et al 1999
	Prostate	HSVtk/CD (i.p.)	VCV/5-FC	Radiation	I	15	N/A	Mild to moderate	Freytag et al 2003
	Prostate	HSVtk (i.t.)	VCV	Radiation	I/II	59	N/A	Mild	Teh et al 2004
	Breast	CD (i.t.)	5-FC	None	I	12	N/A	Mild	Pandha et al 1999
	Breast and melanoma	CYP2B6 (i.t.)	CPA	None	I	12	N/A	Mild	Braybrooke et al 2005
	Ovarian	HSVtk (i.p.)	ACV	Topotecan	I	10	N/A	Mild	Hasenburg et al 2000
	Head/neck/esophagus	CD (i.t.)	5-FC	None	I	3	N/A	Mild to moderate	Nemunaitis et al 2003
	Liver	NR (i.t.)	CB1954	None	I	18	N/A	Mild	Palmer et al 2004
ADEPT	Colon	CPG2	CMDA	None	I	10	N/A	N/A	Martin et al 1997
	Colon	CPG2	ZD2767P	None	I	27	N/A	Mild to moderate	Mayer et al 2006

GBM: Glioblastoma multiform, HSVtk: Thymidine kinase (herpes simplex virus-1), CD: Cytosine deaminase (*E.coli*), CYP2B6: Cytochrome P-450 2B6 (human fibrosarcoma), NR: Nitroreductase (*E.coli*), CPG2: carboxypeptidase G2 (pseudomonas), ACV: acyclovir, GCV: gancyclovir, VCV: valcyclovir, 5-FC: 5-Fluorocytosine, CPA: cyclophosphamide, CB1954: 5-(aziridin-1-yl)-2,4-dinitrobenzamide, CMDA: 4-[2-chloroethyl)(2-mesyloxyethyl)amino]benzoyl-L-glutamic acid, ZD2767P: 4-{[bis(2-iodoethyl)amino]-phenyl} oxycarbonyl-L-glutamic acid; i.t.: intratumoral injection; i.p.: intraperitoneal injection

* Comparison between treatment and non-treatment groups

In an attempt to eliminate the long circulating antibody-enzyme conjugates from the blood, a secondary antibody was employed (Sharma et al 1990, and Kerr et al 1993). But the use of secondary antibodies to reduce circulation times complicated an already complex multi-step anti-cancer therapy based on ADEPT. Antibody fragments that have a shorter circulating half-life (e.g., $F(ab')_2$ and Fab) have been conjugated to prodrug converting enzymes (Bagshawe 1988). More recently, scFv fragments of antibodies have been employed for ADEPT (Deckert et al 2003, Alderson et al 2006, Hao et al 2006, and Coelho et al 2007). There are several advantages for using small fragments of antibody containing just the epitope binding domain: better tumor penetrations, faster clearance from the blood, and the recognition site can be identified using a phase display library and tailored to make recombinant antibody fragments that can be expressed in *E.coli* (Helfrich et al 2000). Despite many efforts to increase the anti-tumor therapeutic effect, ADEPT continue to struggle to advance from the laboratory to the clinic. Although there are reports of anti-tumor responses by ADEPT in preclinical studies, the limited number of *in vivo* survival data published so far is disappointing (Table 1-2).

Another major challenge for ADEPT is heterogeneous expression of tumor specific antigens. Several cell surface receptors are over-expressed in certain types of cancers, such as epidermal growth factor receptor (EGFR), Her-2/neu, and CD44. Advances in mAb technology for targeted therapy resulted in the development of Erbitux® (mAb against EGFR for metastatic colorectal cancer patients), Herceptin® (mAb against Her-2/neu receptor in breast cancer patients), and Rituxan® (mAb against CD20 for B-cell non-Hodgkin's lymphoma patients). Although antigen-specific mAbs are marketed, only

a small subset of cancer patients is qualified to receive these mAb treatments. For example, overexpression of the Her2/neu receptor is found in about 25% of all breast cancer patients (Slamon et al 1989). As a consequence, the remaining 75% of breast cancer patients are not suited for anti-Her2 mAb treatment. There is also an issue of immune response in some cases—patients who are allergic to murine species are not eligible to receive Rituxan® because the antibody is derived from the mouse. Therefore, a continuing challenge for the development of effective targeted therapy is to develop strategies to treat a greater number of patients. This is the impetus for focusing my project to targeting a tumor matrix component that is more ubiquitous, and yet tumor selective in terms of preferential accessibility of macromolecules into the tumor due to the EPR effect (Section 1.6).

1.4 Targeting tumor microenvironment for cancer therapy: hyaluronan and hyaluronan binding proteins

Cancer is caused by series of molecular events that perturb the balance between cell growth and apoptosis, and eventually lead to uncontrolled cell growth (reviewed Hanahan and Weinberg 2000). Therefore, intracellular mechanisms that transform normal tissue to cancer have been the central focus of cancer research.

The influence of the tumor microenvironment on tumor development has been gaining attention among cancer researchers, as carcinoma-associated stromal fibroblasts and over-expression of matrix-metalloproteinases (MMPs) are becoming major factors in the genesis of neoplastic cells (Olumi et al 1999, Tlsty 2001, Coussens et al 2002, and Joyce

2005). Recently, clinical observations revealed associations between tumor progression and the level of hyaluronan in the extracellular matrix of tumors (reviewed in Toole 2004). Hyaluronan is a glycosaminoglycan found in all vertebrate tissues and body fluids (Fraser et al 1997), and is composed of repeating N-acetyl-D-glucosamine and D-glucuronate disaccharide units, and its molecular weight ranges from 10^6 to 10^7. Hyaluronan synthases (Has-1, Has-2, and Has-3 in humans), which are transmembrane enzymes, are responsible for producing hyaluronan. The turnover rate in the body is high—less than 5 min in the blood, 1-2 days in the skin, and 1-3 weeks in cartilage. Hyaluronan is digested by hyaluronidases (Hyals) that are found in circulating blood and tissues, and digested hyaluronan fragments can act as signaling molecules—high molecular weight hyaluronan can trigger anti-angiogenic and anti-inflammatory responses and low molecular weight hyaluronan (~20 kDa) can induce cytokine synthesis, whereas lower molecular weight hyaluronan (< 20 kDa) can activate dendritic cells and antigen-presenting cells (reviewed in Stern 2004).

Perturbations in hyaluronan regulation influence tumor invasiveness, migration, and progression (Toole 2004). Elevated levels of hyaluronan are found in various malignant tumors, including melanoma, and cancers of ovaries, breast, lung, and bladder. In breast and ovarian cancers, high hyaluronan levels are a prognostic factor associated with poor patient survival (Ropponen et al 1998, Anttila et al 2000, and Auvinen et al 2000). In addition, anchorage-independent growth and tumorigenicity were observed in hyaluronan synthase 2 (HAS-2) transfected human fibrosarcoma cells, which were associated with overproduction of hyaluronan (Itano et al 1999, Kosaki et al 1999). Although it is

unclear how Has or Hyal activities are altered to accumulate high hyaluronan levels in many cancers, these clinical observations suggest that hyaluronan is an attractive target for cancer therapy.

A natural ligand for hyaluronan can be used to target hyaluronan in the tumor matrix. There are many hyaluronan-binding proteins that are localized in the extracellular matrix of mammalian tissues (Fraser et al 1997). These proteins are grouped into two categories: the Link module and non-Link module superfamilies (Day and Prestwich 2002). The Link module is a unit of a hyaluronan binding domain, which is about 100 amino acid residues long and contains 4 conserved cysteine residues that form 2 disulfide bonds. Aggrecan, versican, CD44, and TSG-6 are some of the major Link module superfamily proteins. Non-Link module superfamily proteins are capable of binding to hyaluronan, but they do not contain the Link domain. Instead, some of these proteins contain BX_7B motif (B for Lys or Arg, and X for any non-acidic amino acid), which may be involved in the interaction with hyaluronan (Day and Prestwich 2002). Receptor for hyaluronan mediated mobility (RHAMM) is one of the major non-Link module proteins.

Of the known hyaluronan binding proteins, the hyaluronan binding domains of CD44 and TSG-6 are the most extensively characterized (Blundell et al 2005, and Higman et al 2007). CD44 is a major cell surface receptor for hyaluronan that is over-expressed in many cancer types, where elevated levels of hyaluronan are found (listed above). CD44 has been a target for hyaluronan-liposome mediated gene and drug delivery studies (Eliaz and Szoka 2001, and Peer and Margalit 2004). TSG-6 is another well-characterized

hyaluronan binding protein, and its expression is induced by a pro-inflammatory cytokine TNF-α (Lee et al 1992). Although the distribution of TSG-6 is limited to the inflamed tissues, the hyaluronan binding affinity is observed to be higher than that of CD44 (Lesley et al 2002). Interestingly, the optimum pH for the interaction between hyaluronan and the Link domains is found at pH 6 (Parkar et al 1998). Therefore, the binding interaction of hyaluronan and hyaluronan binding domain would be more favorable in the tumor microenvironment, where the pH is more acidic than the physiological pH due to higher metabolism by tumor cells than in the circulating blood.

1.5 Matrix Attachment Therapy (MAT) for cancer

Current enzyme prodrug strategies have technical limitations that are impeding their progress toward become successful cancer therapies. Targeting hyaluronan in the extracellular matrix of a solid tumor for local production of a cytotoxic drug near tumor cells may be able to overcome several key challenges of GDEPT and ADEPT. Hyaluronan-targeted matrix attachment therapy can also take advantage of the EPR effect for treatment of both solid tumors and inflammation. This way, the accumulation of the therapeutic protein at the target sites is more favored than that in the normal tissue, even though hyaluronan is a ubiquitous extracellular matrix polysaccharide and is widely distributed (Frasier 1997). Moreover, the level of hyaluronan does not have to be substantially higher at the tumor site as long as it has enough available binding sites for the therapeutic protein. This is a major advantage of matrix attachment therapy over GDEPT and ADEPT, which does not depend on the limited, heterogeneous expression of tumor specific antigens.

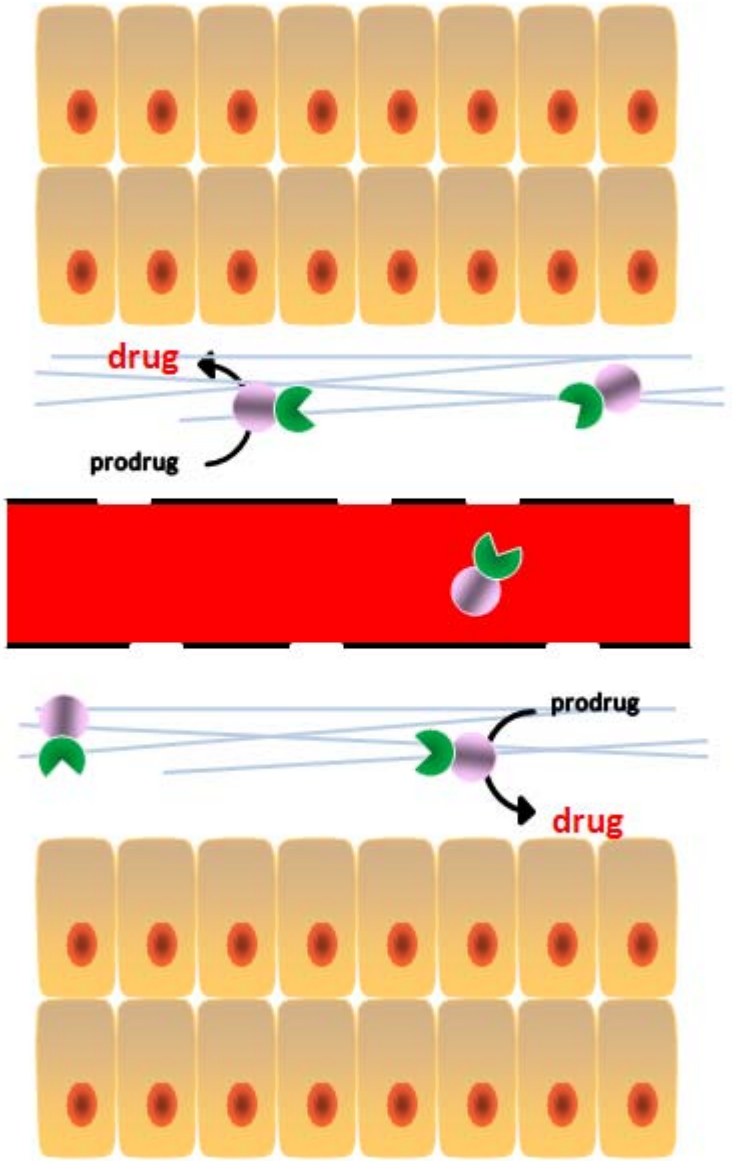

Figure 1-3. Matrix-attachment therapy for targeting cancer
A recombinant fusion protein containing tumor matrix targeting ligand and a prodrug converting enzyme can accumulate in the tumor matrix by taking advantage of the EPR effect, and generate cytotoxic drug locally at the tumor site in the presence of its prodrug.

My choice of enzyme/prodrug combination for testing the proof-of-concept for MAT was: yeast cytosine deaminase (CD)/5-fluorocytosine (5-FC). Many anti-tumor GDEPT and ADEPT experiments have used this combination, because 5-FC is an FDA-approved oral medication for antifungal treatment (under the name Ancobon^{TM}) that has a high bioavailability (Cutler et al 1978). The activated cytotoxic drug produced by the cytosine deaminase/5-FC combination is 5-fluorouracil (5-FU), one of the most widely used anti-cancer drugs worldwide.

In Chapter 2, I describe the construction of a mammalian expression vector containing the extracellular domain of CD44, the CD enzyme, and the uracil phosphoribosyltransferase (UPRT) genes to examine if 5-FC could cause a cytotoxic effect on the tumor cells expressing the CD44-CD-UPRT fusion protein *in vitro*. I also show the dose response cytotoxicities of 5-FU and 5-FC *in vitro* using human glioma and breast cancer cell lines. In Chapter 3, I show the construction of a bacterial expression vector containing TSG-6 Link and CD enzyme genes. The LinkCD recombinant fusion protein was expressed and purified using *E.coli*. Functional characterizations of the LinkCD fusion protein are described in this chapter. The anti-tumor effect of LinkCD/5-FC combination therapy and the preliminary results of pharmacokinetics and biodistribution of radioisotope labeled-LinkCD are described in Chapter 4. Finally, I describe a strategy to engineer the Link domain of CD44 via a rational design approach to create CD44 Link chimeras that are optimized for hyaluronan binding. These chimeras could potentially be employed to increase the circulation time of LinkCD *in vivo*.

CHAPTER 2

Gene-Directed Enzyme Prodrug Therapy: Cytotoxicity of 5-Fluorocytosine on Tumor Cells Containing Cytosine Deaminase-Uracil Phosphoribosyltransferase Fusion Gene

2.1 Introduction

Cytosine deaminase (CD) is a pyrimidine salvaging enzyme found in bacteria and fungi. The enzyme catalyzes the deamination of cytosine to uracil. GDEPT studies have employed this enzyme with a prodrug 5-fluorocytosine (5-FC) to generate cytotoxic 5-fluorouracil (5-FU) in the tumor cells that express the CD enzyme (reviewed in Greco and Dachs 2001). Since mammalian cells do not have the cytosine deaminase gene, the administered 5-FC is eliminated from the body unchanged, except in the gut where microflora convert 5-FC to 5-FU. 5-FC has a high oral-bioavailability (Cutler et al 1978), and is a FDA-approved drug for antimicrobial treatment.

5-FU is a classic anti-cancer drug, which was first synthesized by Heidelberger and his coworkers in the 1950's (Curreri et al 1958). Since then, 5-FU has become one of the widely used chemotherapy drugs for treating breast and colorectal cancers (reviewed in Novolanic and McCubrey 2005, and Board and Valle 2007). The mechanism of action by 5-FU had been extensively studied (reviewed in Diasio et al 1989 and Peters 2003). The anabolic pathway of 5-FU that leads to cytotoxicity is shown in Figure 2-1. 5-FU can readily diffuse across the lipid bilayer membrane and is metabolized into 5-fluoro-2'-deoxyuridine-5'-monophosphate (5-FdUMP) by endogenous intracellular enzymes. The

phosphorylated drug metabolite is unable to escape from the cell. 5-FdUMP is an irreversible inhibitor for thymidylate synthase (TS), the key enzyme for *de novo* synthesis of thymidine: FdUMP covalently binds to the active site of TS with its cofactor 5,10-methylene tetrahydrofolate. The irreversible inhibition of TS is the key inhibition of cell growth by 5-FU.

Although 5-FU is one of the widely used chemotherapeutic drugs, the drug response among cancer patients who receive 5-FU in their chemotherapeutic regime varies widely, from having no response to having severe toxicities from the treatment due to an enhanced sensitivity to the drug. Such a broad range of 5-FU responses has been a subject of many cancer pharmacogenetics studies (reviewed in Soong et al 2005, and Zhang and Diasio 2007). The lack of therapeutic response from the 5-FU treatment generally results from either 5-FU resistance by cancerous cells or rapid clearance of 5-FU from the circulation. Pharmacogenetics studies have revealed that elevated TS expression level and genetic polymorphisms on the TS gene are correlated with significantly less drug response from the 5-FU treatment (Johnston et al 1994, and Pullarkatet al 2001). Moreover, the genetic polymorphism of the methylene-tetrahydrofolate reducatase (MTHFR) gene that lead to attenuated 5,10-methylene-tetrahydrofolate production is another influential factor for the lack of 5-FU response (Martin et al 2006). To compensate for the lack of intracellular MTHF, current 5-FU chemotherapeutic treatment regimes for colon and breast cancer is supplemented with leucovorin, a non-toxic derivative of folate (reviewed in Peters 2003). Hyper-sensitivity to 5-FU that leads to severe drug toxicity is primarily due to the attenuation of 5-FU

degradation by dihydropyrimidine dehydrogenase, which is the first enzyme involved in the clearance of ~ 85% of administered 5-FU (Wei 1996). The enzyme activity and expression level of dihydropyrimidine dehydrogenase are influenced by genetic polymorphisms in the coding region and promoter region of the gene (reviewed in Zhang and Diasio 2007).

The 5-FU sensitivity varies among different tumor cell lines *in vitro*. The IC_{50} of 5-FU is reported to be 10 μM for the human glioma cell line U87-MG whereas the IC_{50} of 5-FU for a human pancreatic cancer cell line BxPC is 0.5 μM (Miller et al 2002). To increase the sensitivity of tumor cells to 5-FU, the uracil phosphoribosyltransferase (UPRT) gene was employed (Kanai et al 1998, and Kawamura et al 2000). UPRT is a bacterial pyrimidine salvaging enzyme that facilitates the metabolism of 5-FU to 5-FUMP (Figure 2-1). 5-FUMP is converted by intracellular enzymes to either 5-FdUMP to inhibit TS, or 5-FUTP to inhibit RNA synthesis (Figure 2-1). The UPRT enzyme was able to increase the 5-FU sensitivity of various human colorectal cancer cell lines (WiDr, PLC/PRF/5, MKN1, MKN28, and MKN 45) by 7 to 100-fold *in vitro* (Kanai et al 1998), and of the C26 murine colon carcinoma tumor model *in vivo* (Kawamura 2000). The CD::UPRT fusion gene was created to convert 5-FC to 5-FU by the CD enzyme, and to rapidly generate 5-FUMP in the tumor cells that express the CD::UPRT fusion protein (Adachi et al 2000 and Koyama et al 2000). The CD::UPRT/5-FC combination treatment has been effective against the 9L rat brain tumor model (Adachi et al 2000) and the HT29 human colon carcinoma model (Koyama et al 2000) with 5-FC treatment.

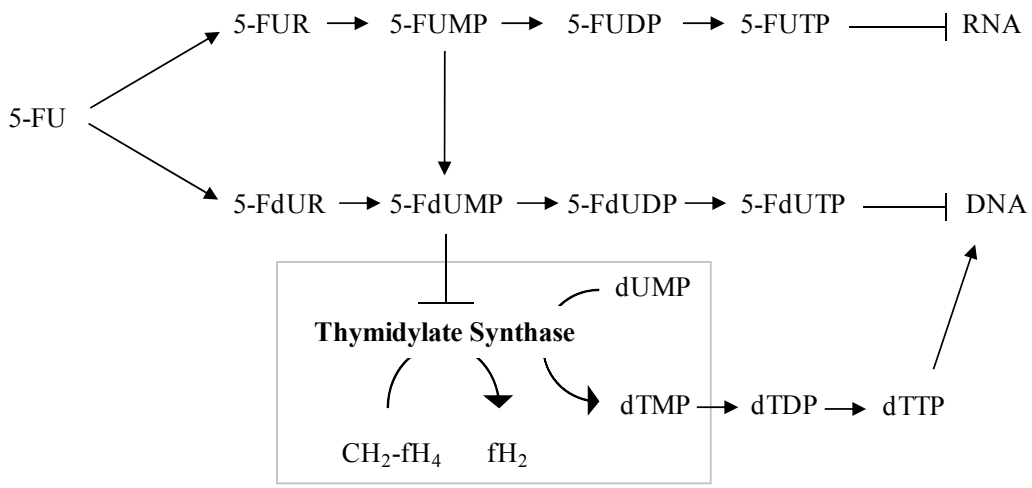

Figure 2-1. The mechanism of cytotoxicity by 5-FU. A schematic diagram of the anabolic pathway of 5-FU. The box highlights the irreversible inhibition of thymidylate synthase by 5-Fluoro-2'-deoxyuridine-5'-monophosphate (5-FdUMP) with the endogenous cofactor methylene tetrahydrofolate (CH_2-fH_4). The cell eventually die due to the lack of thymidine. The catabolic pathway of 5-FU that leads to the drug clearance is not shown.

I started my thesis project on MAT with the GDEPT approach *in vitro*. I wanted to see if the sCD44 (soluble CD44 containing the Link domain)::CD::UPRT fusion gene could be expressed in transiently transfected cancer cells and cause cytotoxicity in the presence of 5-FC *in vitro*. If the sCD44::CD::UPRT fusion protein could be successfully engineered to secrete out of the cells where it might bind to the extracellular-matrix, it would remain localized in the vicinity of tumor by attaching to hyaluronan, and convert 5-FC to 5-FU and 5-FUMP.

2.2 Methods

2.2.1 Cell culture

Human breast cancer cell line MCF-7, human glioma cell lines U87-MG and U251-MG, murine melanoma cancer cell line B16-F10, culture media, and fetal bovine serum (FBS) were obtained from the UCSF Cell Culture Facility. MCF-7 was maintained in the RPMI-1640 culture medium with 10% FBS. U87-MG, U251-MG, and B16-F10 were maintained in the MEM culture medium with 10% FBS. All cell lines were maintained in sterile T-75 flasks (Corning Life Sciences; Corning, NY) in a 37 ^{o}C incubator with 95% humidity and 5% CO_2. Asceptic techniques were used for all procedures.

2.2.2 Construction of pORF-sCD44::CD::UPRT fusion gene for mammalian expression

The pOTB7-CD44 plasmid containing the cDNA sequence of human CD44 (standard isoform) was purchased from American Type Culture Collection (Manassas, VA). The pORF5-Fcy::Fur plasmid containing the CD (Fur) and UPRT (Fur) fusion gene was purchased from Invivogen (San Diego, CA). The CD44 exons 1–5 (residues 1 – 223,

sCD44) containing the secretion signal peptide and the Link domain was amplified by PCR with the NcoI restriction enzyme site (5'-primer sequence: CCATGGACAAGTTTTGGTGG and 3'-primer sequence CCATGGTACTGGTAGCAGGGATTCTGTCTG). The sCD44 amplicon and pORF5-CD::UPRT plasmid were digested with 5 units of NcoI restriction enzyme at 37 ^{o}C overnight. After restriction enzyme digest with NcoI, the DNA fragments were gel-purified. The 5'-phosphate of the gel-purified and NcoI-cut plasmid was removed by 0.5 units of calf intestinal phosphatase (New England Biolabs; MA) at 37 ^{o}C for 1 hr to prevent self-ligation. The ligation reaction mixture containing the plasmid, insert, and 100 units of T4 DNA ligase (New England Biolabs; MA) in 5 μL of 1×T4 DNA ligase buffer were incubated at room temperature overnight. The ligation product was transformed into DH5α *E.coli* cells. The transformed *E.coli* cells were spread on a LB-agarose plate with carbenicillin and incubated at 37 ^{o}C overnight. Colonies were picked to screen for the positive clones that contain the sCD44 insert. The plasmid was purified from each colony for screenings by a restriction enzyme digest (NcoI and StuI) and PCR (using 5'-primer, which anneals to sCD44: *GCTAGCGTT*ATGGACAAGTTTTGGTGG and 3'primer, which anneals to CD: *TCTAGA*CTACTCCCCAATGTCCTCAAAC) to identify positive colonies with the sCD44 insert in the correct orientation with the ORF. The DNA sequence of the ORF containing the sCD44::CD::UPRT fusion gene was confirmed by DNA sequencing (Biomolecular Research Center, UCSF).

2.2.3 Preparation of transfection agent polyethyleneimine(PEI) for gene transfection experiments

PEI (Sigma; St. Louis, MO) is a polymeric transfection agent for gene transfer to mammalian cells. The average Mw of the reagent was 25,000 Da, and a dialysis was performed to remove small Mw PEI. First, PEI was dissolved in dH_2O at 200 mg/mL concentration in a boiling water bath. The pH of the dissolved PEI in dH_2O was adjusted to 7.4 by adding concentrated HCl. A Spectra/Por dialysis membrane tube (Spectrum Laboratories; Rancho Dominguez, CA) with 6–8,000 Da cut-off was prepared by boiling the membrane in 1% $NaHCO_3$ and 1 mM EDTA for 30 min. Then the membrane was washed with dH_2O. One end of the membrane tube was knotted and clipped, and then the PEI solution was transferred into the membrane tube. The other end was knotted and clipped to seal the dialysis membrane. The dialysis was performed in 2 L of 1 M NaCl solution for 2 days at 4 ^{o}C. Then the PEI solution was transferred to freshly prepared dialysis membrane tubes, and dialyzed in 4 L dH_2O at pH 7.4 for 24 hr at 4 ^{o}C (the pH of dH_2O was adjusted by adding NaOH). The PEI was dialyzed in fresh dH_2O at pH 7.4 for another 24 hr at 4 ^{o}C. After the second dialysis step in dH_2O, the PEI solution was transferred to pre-weighed 50-mL conical tubes and lyophilized. The amount of lyophilized PEI was determined by weighing each tube containing PEI and subtracting the weight of the tube previously measured prior to lyophilization. The lyophilized PEI was stored at -80 ^{o}C.

2.2.4 In vitro transient gene transfection and β -galactosidase reporter assay

5×10^3 cells (U251-MG, MCF-7, or B16-F10) were seeded per well in 96-well plates and started incubation at 37°C on the day before a transient gene transfection experiment. PEI was used to transfect cells with the pCMVβ-gal plasmid containing the β-galactosidase (β-gal) gene. The lyophilized PEI was dissolved in sterile dH_2O at 1 mg/mL, and filtered through a 0.2 μm membrane. The plasmid DNA and PEI were mixed in 1:1 w/w ratio in an appropriate culture medium without serum, from 0.1 μg up to 2 μg in serum free culture medium. The mixture was incubated at room temperature for 30 min. The gene transfection to the cells was performed by incubating the cells with 100 μL culture medium containing the plasmid/PEI complex at 37°C for 4 hr. At the end of incubation, the culture medium containing the plasmid/PEI complex was aspirated off, and the cells were gently washed with PBS twice. Then 200 μL of fresh culture medium containing 10% FBS was added to each well, and the plates were incubated at 37 °C for 48 hr.

After 48 hr incubation, the β-gal activity in the transfected cells was measured using β-Galactosidase Enzyme Assay System (Promega; Madison, WI). The cell culture medium from each well was aspirated by vacuum and washed with PBS. Then 50 μL of 1×Reporter Lysis Buffer (RLB) was added to each well and incubated at room temperature (25 °C) with constant shaking for 1 hr. Cell lysis was completed by one cycle of freeze-thawing: 1 hr incubation at -80 °C followed by thawing at the room temperature. The plates were centrifuged at 500×g for 30 min at 4 °C. Immediately after centrifugation was done, 30 μL of the supernatant from each well was transferred to a new 96-well plate and mixed with 20 μL of 1×RLB. Then 50 μL of 2× Assay Buffer

containing 1.33 mg/mL O-nitrophenyl-β-D-galactopyranoside was added to each well containing the supernatant in 1×RLB. The enzymatic reaction was done at 37 ^{o}C for 30 min, and the reaction was quenched by adding 150 μL of 1 M Na_2CO_3. The absorbance was measured at 420 nm to determine the β-gal enzymatic activity.

2.2.5 In vitro cytotoxicity assay

5×10^3 cells (MCF-7, U87-MG, or U251-MG) were seeded per well in 96-well plates. The cells were grown at 37 ^{o}C for 24 hr. The culture medium was replaced by the fresh culture medium containing either 5-FC or 5-FU, from 0.1 μM to 3 mM. The cytotoxicity of the drug was quantified by either 3-(4,5-dimethylthiazol-2-yl)-2,5-diphenyl tetrazolium bromide (MTT) or Cell-Titer Blue® Cell Viability Assay (Promega; Madison, WI).

2.2.5.a MTT assay

MTT reagent (3-(4,5-dimethylthiazol-2-yl)-2,5-diphenyl tetrazolium bromide) was purchased from Sigma (St. Louis, MO). MTT solution was made at 5 mg/mL concentration in PBS. The dissolved reagent was filtered through a 0.2 μm membrane. Then 10 μL of MTT was added to 100 μL of culture medium in each well. The reagent was mixed by gently shaking the plate, and the plate was incubated at 37 ^{o}C for 4 hr. After the incubation, the cell culture medium was aspirated, and 100 μL of 2-propanol containing 0.04 N HCl was added to each well to dissolve the dark violet crystal. The absorbance of each well was measured at 570 nm with reference reading at 630 nm. The measure of cell viability was quantified by subtracting $OD_{630\ nm}$ from $OD_{570\ nm}$.

2.2.5.b CellTiter- Blue® assay

At the end of the drug treatments, the cells were washed and 100 μL of fresh culture medium was added to each well. Then 20 μL of CellTiter-Blue® assay reagent containing resazurin was added to each well, and incubated at 37 ^{o}C for 2.5 hr. The fluorescence of resorufin in each well was measured by a microplate fluorometer (excitation wavelength at 544 nm and emission wavelength at 590 nm).

2.2.6 In vitro transfection of MCF-7 with the sCD44::CD::UPRT plasmid

For *in vitro* transient transfection of either the sCD44::CD::UPRT or CD::UPRT fusion gene to MCF-7, 0.5 μg of the plasmid DNA and an equal amount of PEI were mixed together in the RPMI-1640 cell culture medium without the serum. The plasmid/PEI complex was incubated at room temperature for 30 min. The cells were incubated with the plasmid/PEI complex for transient transfection. The duration of transfection was 4 hr at 37^{o}C. The cells were washed with PBS twice, and 200 μL of the culture medium containing 10% FBS was added to each well. Two days after transfection (48 hr), the culture medium was replaced with fresh medium containing serially diluted 5-FC (1 μM to 3 mM). The cells were incubated with 5-FC for 3 days. Cytotoxicity was measured by using CellTiter-Blue® reagent.

2.2.7 Western blot detection for gene expression of sCD44::CD::UPRT

The primary antibody against human CD44 was purchased from Bender Medsystems (Burlingame, CA). The anti-mouse IgG secondary antibody was purchased from Sigma (St. Louis, MO). ECL™ Western Blotting Detection System was purchased from

Amersham Biosciences (Piscataway, NJ). Two days after MCF-7 cells were transfected with the sCD44::CD::UPRT gene, the cell culture medium was pooled by treatment group (i.e. untransfected control or transfected). The transfected MCF-7 cells were washed twice with PBS, and 200 μL of the Cell Lysis Buffer (Cell Signaling Technology) containing 1 mM phenylmethanesulfonylfluoride (PMSF) was added to each well. Then cells were scraped off, and the cell lysate solution in each well was pooled by the treatment group. The collected cell lysates and culture media were loaded on a 10% acrylamide gel (50 μg per lane). SDS-PAGE was done under denaturing conditions. For Western blot analyses, the proteins in the SDS gel were transferred to a PVDF membrane. At the end of transfer, the PVDF membrane was blocked with 5% milk solution in TTBS buffer (1% Tween 20 in 20 mM Tris and 140 mM NaCl) overnight at 4 ^{o}C. The membrane was incubated with 1% milk solution containing the primary antibody against human CD44 (1:500 dilution) at room temperature on an orbital shaker with constant shaking. The antibody solution was removed after 1 hr incubation, and the PVDF membrane was washed with TTBS buffer for 15 min three times. The PVDF membrane was incubated with the secondary antibody solution containing the anti-mouse IgG-horseradish peroxidase conjugate in TTBS buffer (1:5,000 dilution) for 1 hr at room temperature. The membrane was washed with TTBS buffer for 15 min three times. ECL™ Western Blotting Detection Kit reagents were mixed according to the manufacturer instructions and added on to the PVDF membrane. The chemiluminescence of the detected bands on the PVDF membrane was exposed on Kodak film and developed in the darkroom.

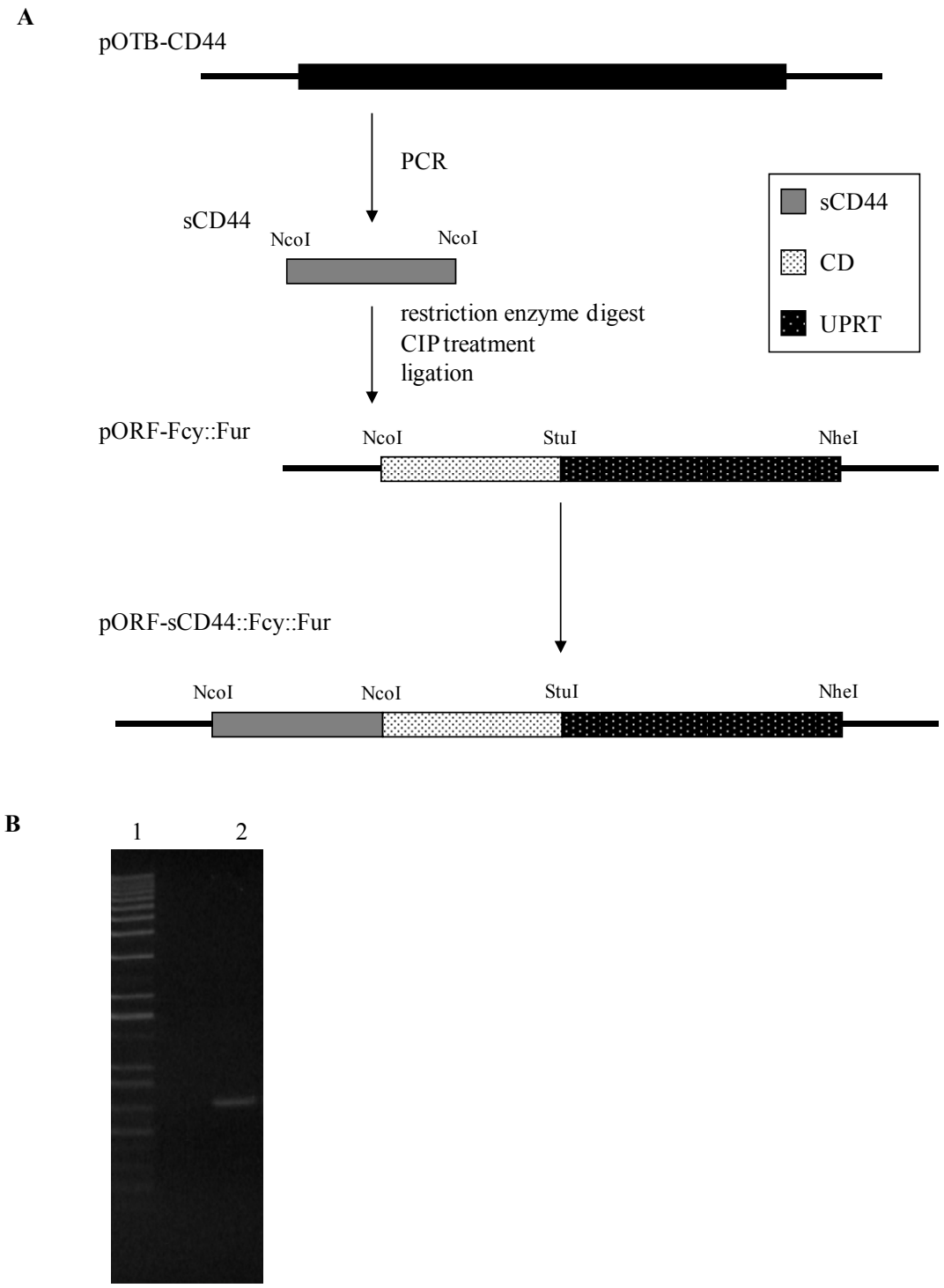

Figure 2-2. Construction of sCD44::CD::UPRT fusion gene in a mammalian expression vector. **A**. The cloning scheme for the construction of pORF-sCD44::CD::UPRT. The sCD44 (exons 1-5 of CD44) was amplified by PCR using a plasmid containing cDNA of human CD44 (pOTB-CD44), and ligated into a mammalian expression vector pORF-CD::UPRT. **B.** Agarose gel image showing the PCR product of sCD44 flanked by the NdeI restriction sites. Lane 1: DNA ladder, Lane 2: PCR product.

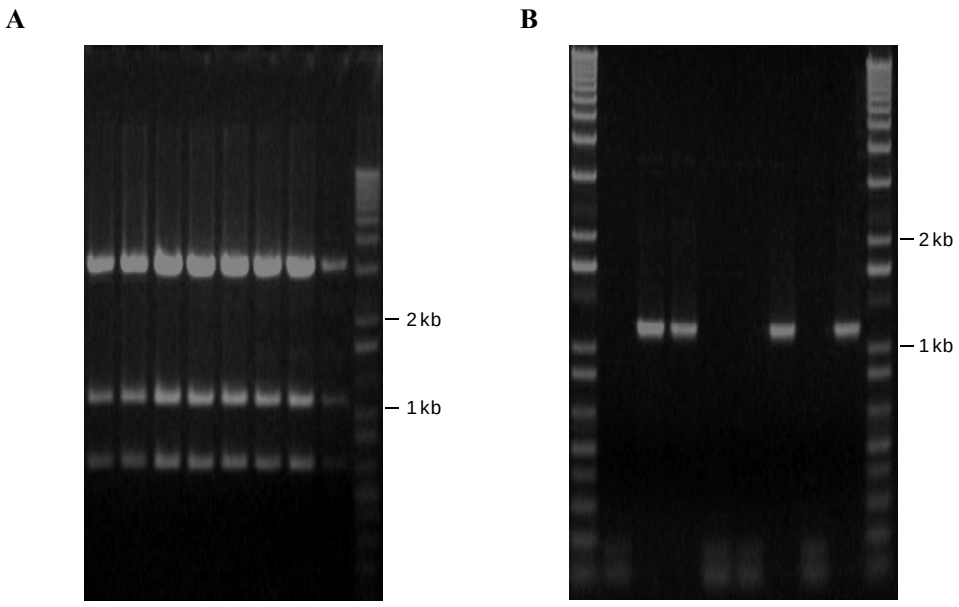

Figure 2-3. Colony screening to identify bacteria cells containing pORF-sCD44::CD::UPRT plasmid. **A**. Restriction enzyme digest screen for the colonies containing pORF-sCD44::CD::UPRT. The top band: empty vector. The second band: CD::UPRT gene. The third band: sCD44 gene. All 8 colonies contained the sCD44::CD::UPRT fusion gene in the plasmid. **B**. PCR-based screen. Only the plasmids containing the sCD44 in the correct orientation with respect to the CD::UPRT reading frame would amplify the sCD44::CD fragment (selected region by the PCR primers), whereas the sCD44 ligated in reverse direction would not be amplified. As shown, 4 out of 8 colonies (lane 2, 3, 6, and 8) amplified sCD44::CD. DNA sequencing confirmed the presence of sCD44.

A

```
ATGGACAAGTTTTGGTGGCACGCAGCCTGGGGACTCTGCCTCGTGCCGCTGAGCCTGGCGCAGATCGATTT
GAATATAACCTGCCGCTTTGCAGGTGTATTCCACGTGGAGAAAAATGGTCGCTACAGCATCTCTCGGACGG
AGGCCGCTGACCTCTGCAAGGCTTTCAATAGCACCTTGCCCACAATGGCCCAGATGGAGAAAGCTCTGAGC
ATCGGATTTGAGACCTGCAGGTATGGGTTCATAGAAGGGCATGTGGTGATTCCCCGGATCCACCCCAACTC
CATCTGTGCAGCAAACAACACAGGGGTGTACATCCTCACATCCAACACCTCCCAGTATGACACATATTGCT
TCAATGCTTCAGCTCCACCTGAAGAAGATTGTACATCAGTCACAGACCTGCCCAATGCCTTTGATGGACCA
ATTACCATAACTATTGTTAACCGTGATGGCACCCGCTATGTCCAGAAAGGAGAATACAGAACGAATCCTGA
AGACATCTACCCCAGCAACCCTACTGATGATGACGTGAGCAGCGGCTCCTCCAGTGAAAGGAGCAGCACTT
CAGGAGGTTACATCTTTTACACCTTTTCTACTGTACACCCCATCCCAGACGAAGACAGTCCCTGGATCACC
GACAGCACAGACAGAATCCCTGCTACCAGTACCATGGTCACAGGAGGCATGGCTTCAAAGTGGGACCAGAA
GGGCATGGACATTGCCTATGAGGAGGCTGCTCTGGGCTACAAGGAGGGAGGGGTCCCAATTGGTGGCTGCC
TCATCAACAACAAGGATGGCAGTGTCCTGGGCAGGGGCCACAACATGAGGTTCCAGAAGGGCAGTGCCACC
CTGCATGGGGAGATCAGCACCCTGGAGAACTGTGGCAGGCTGGAGGGCAAGGTCTACAAGGACACCACTCT
GTACACCACCCTCAGCCCTTGTGACATGTGCACAGGGGCCATCATCATGTATGGCATTCCCAGGTGTGTGG
TGGGAGAGAATGTCAACTTCAAGTCAAAAGGAGAGAAGTACCTCCAGACCAGGGGCCATGAGGTGGTTGTG
GTGGATGATGAGAGGTGCAAGAAGATTATGAAGCAGTTCATTGATGAGAGACCCCAGGACTGGTTTGAGGA
CATTGGGGAGGCCTCTGAGCCCTTCAAGAATGTGTACCTCCTCCCCCAGACCAACCAACTCCTGGGACTCT
ACACCATCATCAGGAACAAGAACACCACCAGGCCAGACTTCATCTTCTACAGTGACAGGATCATCAGGCTC
CTGGTGGAGGAGGGCCTCAACCACCTCCCTGTGCAGAAGCAGATTGTGGAGACTGACACCAATGAGAACTT
TGAGGGAGTGTCTTTCATGGGCAAGATTTGTGGGGTGTCCATTGTGAGGGCTGGGGAGAGCATGGAGCAGG
GCCTGAGGGACTGTTGCAGGAGTGTGAGGATTGGCAAGATCCTGATCCAGAGGGATGAGGAGACTGCCCTG
CCCAAGCTGTTCTATGAGAAGCTCCCTGAAGACATCTCTGAGAGGTATGTCTTCCTCCTGGACCCCATGCT
GGCAACTGGAGGCTCTGCAATCATGGCCACTGAGGTGCTCATCAAGAGGGGAGTCAAGCCTGAGAGGATCT
ACTTCCTCAACCTCATCTGCTCAAAGGAGGGCATTGAGAAGTACCATGCTGCCTTCCCTGAAGTGAGGATT
GTCACTGGGGCTCTGGACAGGGGCCTGGATGAGAACAAGTACCTGGTCCCTGGCCTGGGAGACTTTGGGGA
CAGATACTACTGTGTCTAA
```

B

```
MDKFWWHAAWGLCLVPLSLAQIDLNITCRFAGVFHVEKNGRYSISRTEAADLCKAFNSTLPTMAQMEKALS
IGFETCRYGFIEGHVVIPRIHPNSICAANNTGVYILTSNTSQYDTYCFNASAPPEEDCTSVTDLPNAFDGP
ITITIVNRDGTRYVQKGEYRTNPEDIYPSNPTDDDVSSGSSSERSSTSGGYIFYTFSTVHPIPDEDSPWIT
DSTDRIPATSTMVTGGMASKWDQKGMDIAYEEAALGYKEGGVPIGGCLINNKDGSVLGRGHNMRFQKGSAT
LHGEISTLENCGRLEGKVYKDTTLYTTLSPCDMCTGAIIMYGIPRCVVGENVNFKSKGEKYLQTRGHEVVV
VDDERCKKIMKQFIDERPQDWFEDIGEASEPFKNVYLLPQTNQLLGLYTIIRNKNTTRPDFIFYSDRIIRL
LVEEGLNHLPVQKQIVETDTNENFEGVSFMGKICGVSIVRAGESMEQGLRDCCRSVRIGKILIQRDEETAL
PKLFYEKLPEDISERYVFLLDPMLATGGSAIMATEVLIKRGVKPERIYFLNLICSKEGIEKYHAAFPEVRI
VTGALDRGLDENKYLVPGLGDFGDRYYCV
```

Figure 2-4. **The nucleotide and translated sequences of sCD44::CD::UPRT.** **A**. The nucleotide sequence of the sCD44(yellow)::CD(purple)::UPRT (teal) in pORF5 mammalian expression vector. The restriction enzyme sites between functional proteins are underlined (NcoI between sCD44 and CD, and StuI between CD and UPRT). The total length of the ORF is 1794 bp long. **B**. The translated sequence of the sCD44::CD::UPRT fusion protein.

2.3 Results

2.3.1 Construction of a mammalian expression vector containing the sCD44::CD::UPRT fusion gene

A plasmid vector containing the sCD44::CD::UPRT fusion gene was constructed by inserting the sCD44 gene into pORF-CD::UPRT vector (Figure 2-2). *E.coli* cells were transformed with the ligation product, and 8 colonies were selected for screening. A restriction enzyme digest screening was done with NcoI and XbaI to see if selected colonies contain the sCD44 insert. All 8 colonies contained the sCD44 insert in their plasmids (Figure 2-3A). To examine which of the colonies contained the sCD44 insert in the correct reading frame, a PCR-based screening was performed. One of the two primers used in the PCR reaction annealed to the anti-sense strand of the insert (sCD44), and the other primer annealed to the sense strand of the vector sequence (CD). In this screening strategy, gene amplification by PCR would be shown only if the sCD44 gene is in the same reading frame (i.e., forward direction) as the CD::UPRT fusion gene in the vector sequence. Since there are two possible orientations of the inserted sCD44 gene (forward and reverse), 50% of the colonies were expected to have the sCD44 gene in the forward direction. Indeed, 4 out of the 8 selected colonies showed the amplified gene by the PCR-based screening method (Figure 2-3B). DNA sequencing confirmed that the sCD44::CD::UPRT fusion gene is in the pORF mammalian expression vector (Figure 2-4). The theoretical Mw of the translated sCD::CD::UPRT fusion protein without glycosylation is 63.1 kDa.

2.3.2 Optimization of in vitro gene transfection on mammalian cancer cell lines

The goal of this experiment was to determine the concentration of the plasmid/PEI complex that could transfect cells and express the target protein *in vitro*. Also, I wanted to estimate the threshold concentration of the DNA/PEI that causes a cytotoxic effect. A dose-response for β-gal activity in the transiently transfected U251-MG cells was examined 48 hr after the gene transfection. The β-gal activity was seen in the transfected cells that received 0.3 μg and 1 μg plasmid/PEI dose (Figure 2-5A). However, the cells that were transfected with 0.1 μg plasmid/PEI or lower dose only showed baseline enzyme activity. There was no significant β-gal activity in the cells that were transfected with plasmid alone (Figure 2-5B). Since PEI is known to be toxic to the cells, I also examined a dose-response cytotoxicity of the plasmid/PEI complex by MTT assay (Figure 2-5C). As expected, PEI alone was toxic to the cells whereas the naked DNA was not. The cytotoxicity of DNA/PEI complex was less severe than that of PEI alone. The U251-MG cells that were transfected with 0.3 μg plasmid/PEI complex had greater than 80% survival. Although the cell survival varied at concentrations above 0.3 μg plasmid/PEI complex, the transfection complex seems to be toxic at concentrations above 1 μg plasmid/PEI.

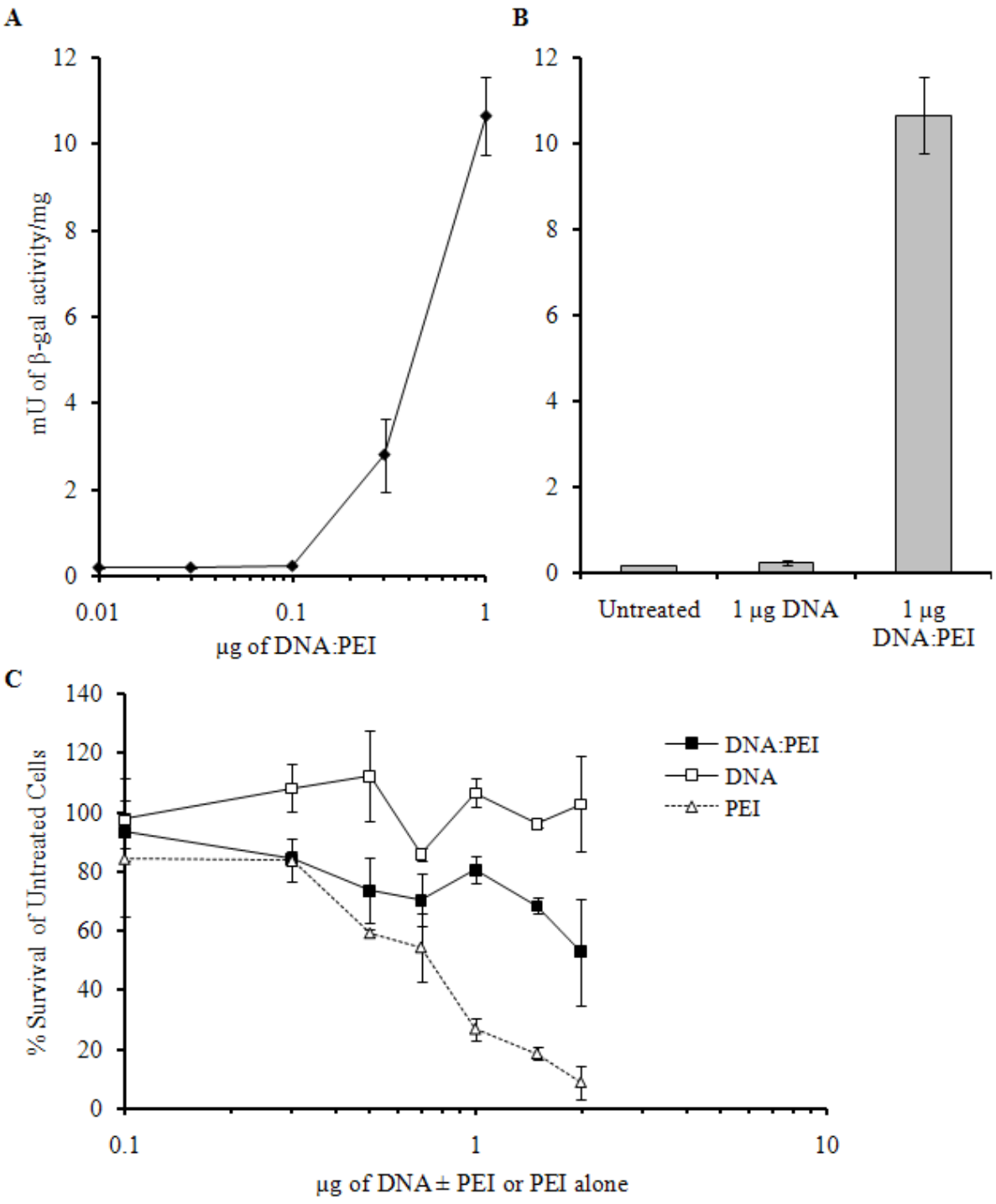

Figure 2-5. *In vitro* reporter gene trasfection of the U251-MG human glioma cell line. **A**. Dose-response for β-gal activity in U251-MG cells transfected with DNA/PEI complex. **B**. β-gal activities in negative controls: U, untreated cell; DNA, 1 µg naked DNA; DNA/PEI, 1 µg DNA/PEI complex. **C**. Dose-response for cytotoxicity of PEI and DNA/PEI complex measured by MTT assay.

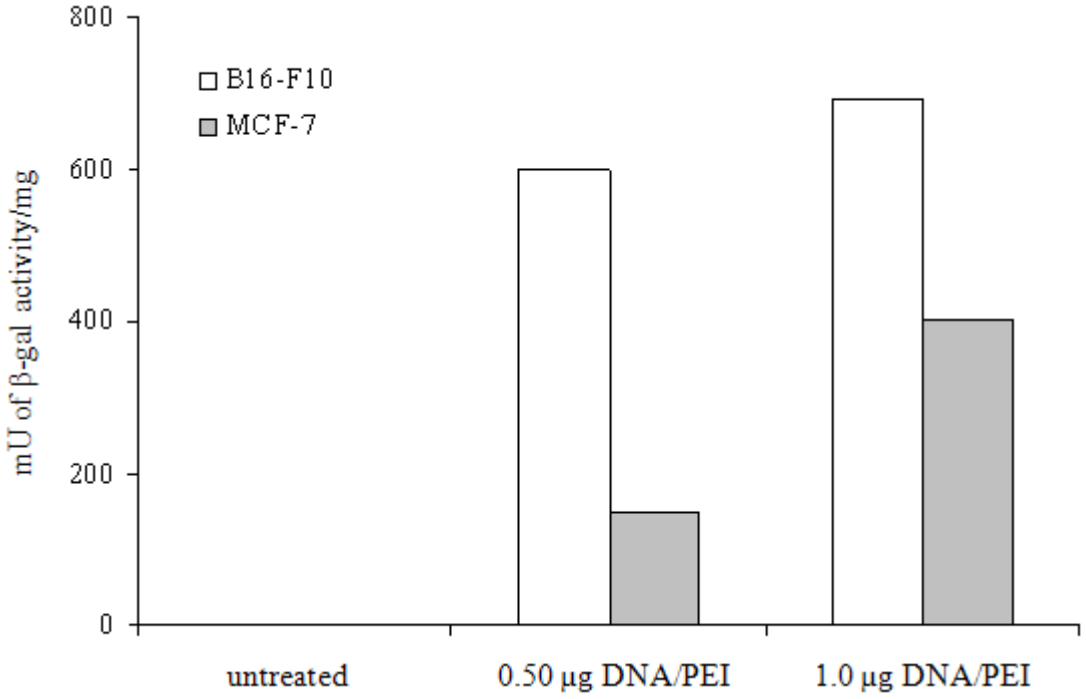

Figure 2-6. **The β-gal activities of MCF-7 and B16-F10 cells that were transiently transfected with β-gal plasmid**. B16-F10 showed 6-fold higher β-gal activity than MCF-7 when both cell types were transfected with 0.5 µg DNA/PEI.

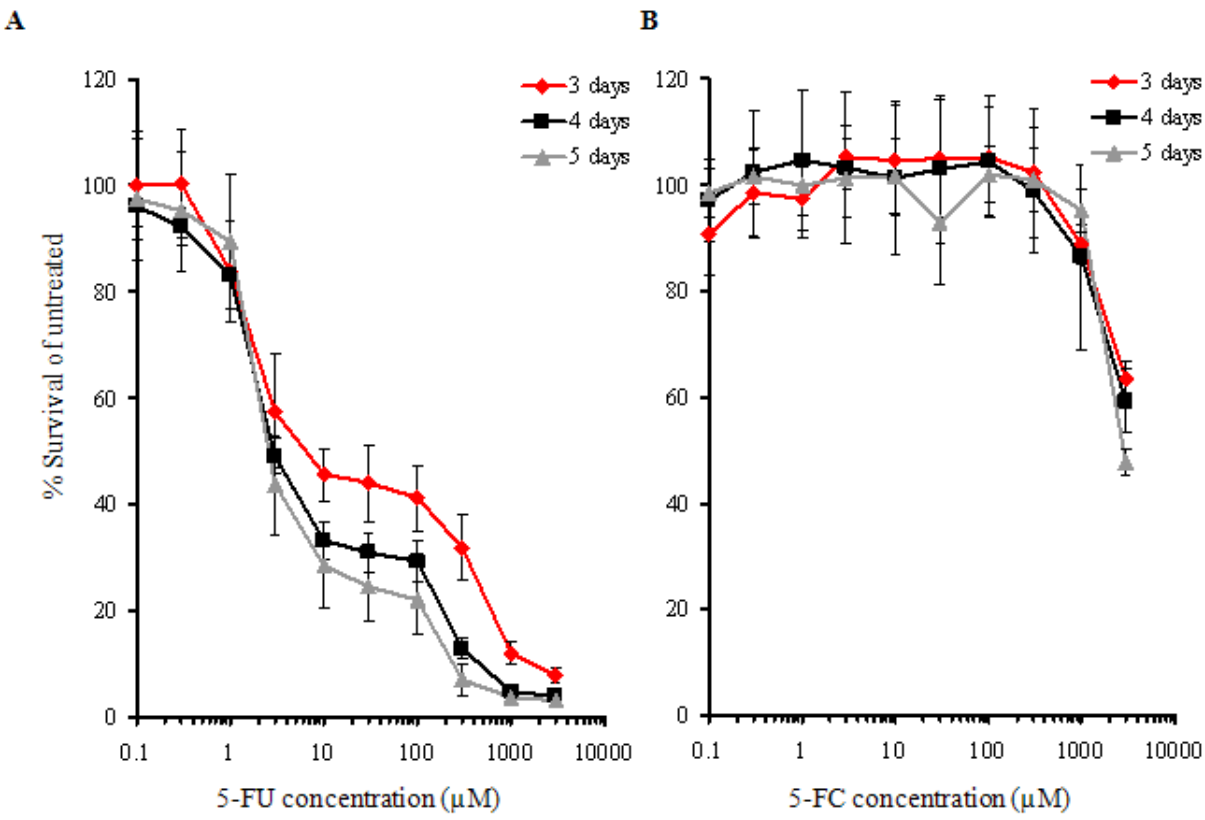

Figure 2-7. Cytotoxicity of 5-FU and 5-FC on MCF-7. *In vitro* dose-response for cytotoxicity of 5-FU (**A**) and 5-FC (**B**) on MCF-7 cell lines were determined after 3 days (red), 4 days (black), and 5 days (gray) of incubation with the drug. The data represents the mean % survival of untreated control ± propagated error. The dose response curve for 5-FU moves downwards with increasing time of incubation. 5-FC is relatively non-toxic up to 1 mM concentration.

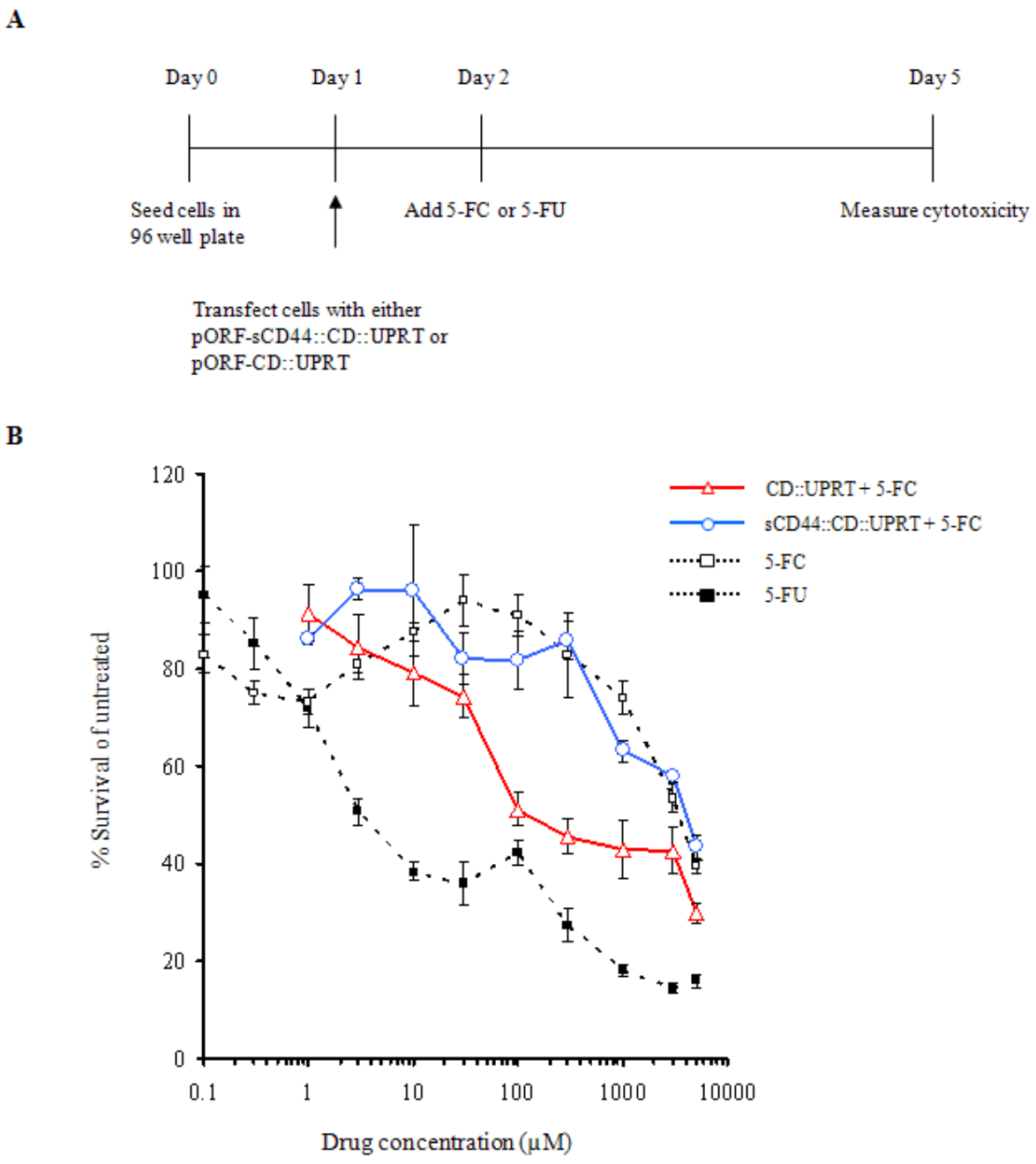

Figure 2-8. Cytotoxicity of 5-FC on MCF-7 cells after transfection with the sCD44::CD::UPRT fusion gene. **A**. *In vitro* gene transfection, drug treatment, and cytotoxicity measurement schedule. **B**. Cytotoxcity of 5-FC on MCF-7 cells transfected with either sCD44::CD::UPRT (blue) or CD::UPRT (red) after 3 days of incubation with the drug. Dotted lines show the cytotoxicity of 5-FU (closed square) and 5-FC (opened square) with an equal amount of transfection agent used for CD::UPRT and CD44::CD::UPRT.

For *in vitro* GDEPT experiment using sCD44::CD::UPRT and 5-FC, I needed the cells to be viable for at least 5 days (2 days for gene expression and 3 days or longer for the drug treatment). I realized that the U251-MG cell line grows too rapidly (< 1 day doubling time) for the GDEPT experiment using sCD44::CD::UPRT and 5-FC. Therefore, I needed to work with a cell line that grows slower than U251-MG. MCF-7 is a human breast cancer cell line that is known to express high levels of hyaluronan (Jojovic et al 2002). The doubling time of MCF-7 cells was approximately 1.5 days. Therefore, MCF-7 was a good alternative cell line to investigate *in vitro* GDEPT experiment using sCD44::CD::UPRT and 5-FC. As shown in Figure 2-6, β-gal activity was observed in MCF-7 cells that were transfected with 0.5 μg plasmid/PEI complex. The gene transfection with 1 μg plasmid/PEI resulted in higher β-gal activity. I decided to transfect MCF-7 cells with the sCD44::CD::UPRT gene with 0.5 μg plasmid/PEI dose since a detectable level of the β-gal activity was observed at this dose of plasmid/PEI. I was also concerned that 1 μg plasmid/PEI would cause some level of cytotoxicity, although I did not carefully examine a dose-response cytotoxicity of plasmid/DNA complex using MCF-7 cells.

2.3.3. Dose-response and time-course cytotoxicity of 5-FC and 5-FU on MCF-7

MCF-7 cells were incubated with either 5-FC or 5-FU for 3, 4, or 5 days of incubation at 37 ^{o}C. To examine the cell viability, CellTiter-Blue® reagent was used. In this assay, the substrate resazurin gets converted to resorufin by intracellular redox enzymes in living cells. 5-FU was able to cause cytotoxicity in MCF-7 cells. The dose-response curve shows that the IC_{50} of 5-FU was less than 10 μM after 3 days of drug treatment

(Figure 2-7). After 4 and 5 days of treatment, IC_{50} decreased to about 3 μM. The measured IC_{50} was about 2-fold higher than the previously reported IC_{50}, which was at 1.6 μM (Chu et al 1991). As expected, 5-FC was relatively non-toxic to the cells up to 1 mM concentration, following 3 to 5 days of incubation with the drug. U87-MG cells were more resistant to 5-FU than MCF-7 with IC_{50} of ~ 60 μM after 5 days of incubation with 5-FU (Supplementary Figure 2-1). The measured IC_{50} of 5-FU on U87-MG was about 6-fold higher than previously reported IC_{50} of 5-FU on U87-MG (Miller et al 2002).

2.3.4. Dose-response cytotoxicity of 5-FC on MCF-7/sCD44::CD::UPRT or MCF-7/CD::UPRT

MCF-7 cells were transiently transfected with either pORF-sCD44::CD::UPRT or pORF-CD::UPRT plasmid using PEI. Two days (48 hr) after gene transfection, the cells were treated with various concentrations of 5-FC for 3 days (Figure 2-8A). As expected, 5-FC caused dose-dependent cytotoxicity to MCF-7 cells that were transfected with CD::UPRT fusion gene. However, there was no cytotoxicity of 5-FC in cells that were transfected with sCD44::CD::UPRT (Figure 2-8B). The dose response curve of 5-FC treatment on MCF-7/sCD44::CD::UPRT cells was similar that of 5-FC treatment alone, which implies the lack of functional sCD44-CD-UPRT fusion protein.

Western blots were done on the MCF-7 cells that were transfected with the sCD44::CD::UPRT gene, and the cell culture medium to see the level of expressed fusion protein. Unfortunately, multiple bands were observed on all Western blots. The detected

bands were coming from the non-specific interaction of the secondary antibody to the cell lysate, and it appears that Western blots failed to detect the fusion protein containing sCD44 (Figure 2-9A and B). The epitope region of the human CD44 antibody is on the N-terminal domain of CD44, although the exact sequence of the epitope is not known (its location is proprietary). Since the sCD44 gene I cloned contained most of the extracellular CD44 domain, it is likely that the epitope region was included in the construct. The failure to detect the CD44 protein is probably due to the lack of the target fusion gene expression in MCF-7 cells, because there was no conversion of 5-FC to 5-FU to cause cytotoxicity. I also transfected B16-F10 cells with pORF-sCD44::CD::UPRT fusion gene to see if the lack of expression was cell line dependent. Although there seem to be a single band near 50 kDa region in both untransfected and transfected cell lysate, Western blot failed to detect expressed sCD44::CD::UPRT in the transfected B16-F10 cells (Figure 2-10C).

2.4 Discussion

One of the major strengths of GDEPT approach for cancer treatment is the ability to generate cytotoxic drug from a subpopulation of tumor cells that are expressing the exogenous enzyme and cause a bystander effect to the neighboring tumor cells. The challenge, however, is safe and effective gene delivery to the tumor cells (discussed in Chapter 1). This study exploited a possibility of demonstrating the MAT strategy with the GDEPT approach by transiently transfecting MCF-7 cells with a mammalian expression plasmid containing the sCD44::CD::UPRT fusion gene, and treating the cells with 5-FC.

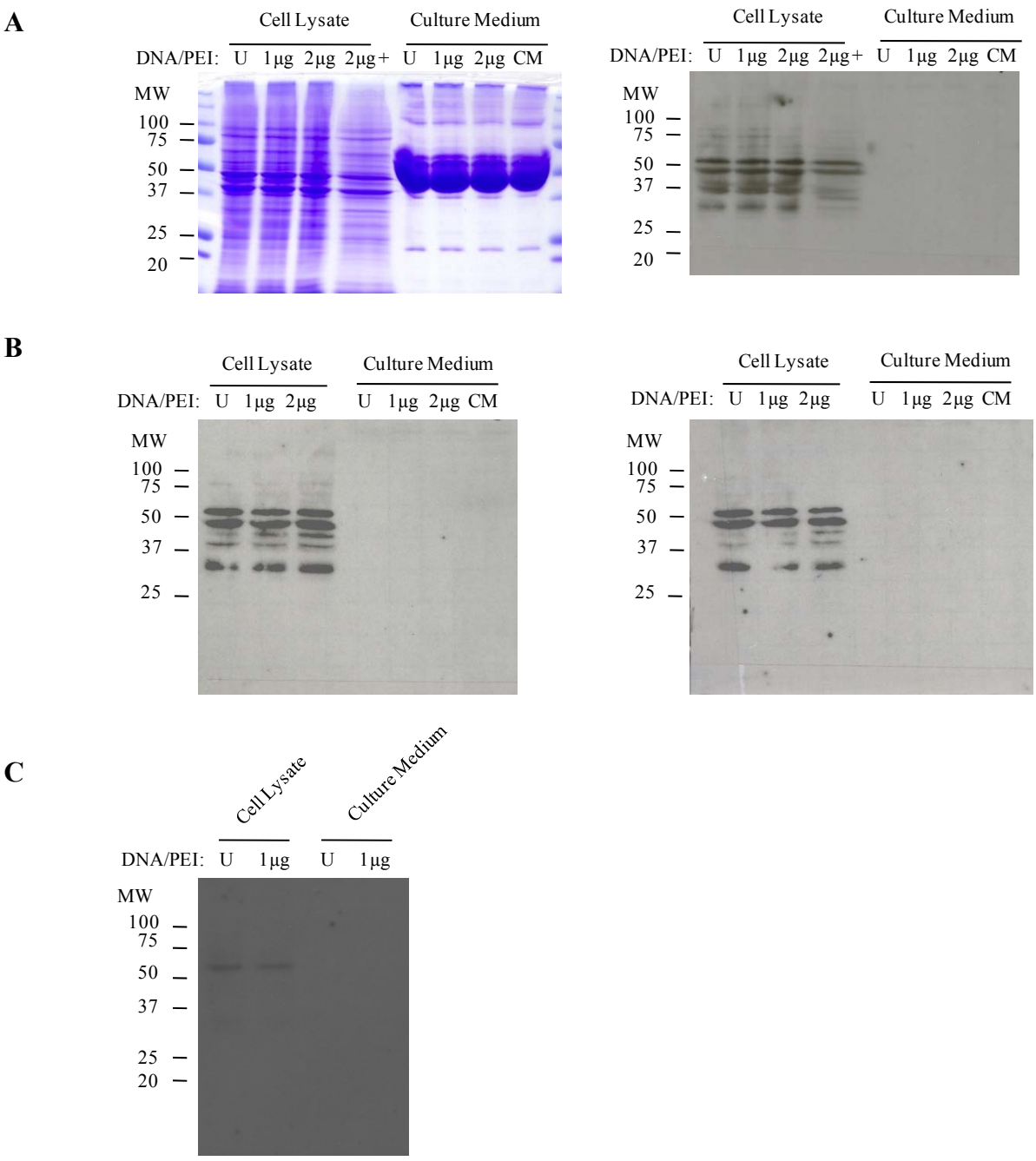

Figure 2-9. Western blots to detect sCD44::CD::UPRT expression. A. SDS-PAGE gel image of collected samples from transfected MCF-7 cells (left), and Western blot detection for sCD44::CD::UPRT using anti-CD44 antibody. U: untreated control, CM: fresh culture medium with 10% FBS **B.** Western blot detection for sCD44::CD::UPRT using anti-CD44 antibody (left) and blotting with anti-mouse IgG. **C.** Western blot detection of sCD44::CD::UPRT on transfected B16-F10 cell line.

MCF-7 cell line was chosen for the *in vitro* transfection studies because the growth rate is slower than the human glioma cell lines U87-MG and U251-MG, which is necessary for 2 days of transfected gene expression followed by 3 days of incubation with 5-FC. Also, MCF-7 seemed to be more sensitive to 5-FU than U87-MG (Figure 2-7 and Supplementary Figure 2-1). 5-FU was cytotoxic to MCF-7 after 3 days of incubation. Interestingly, the morphology of the cells treated with 5-FU seemed to be normal until day 2 under a microscope (results not shown). On day 3, the cells treated with high concentration of 5-FU seemed to be apoptotic since most of them were detached from the plate.

MCF-7 cells transfected with the CD::UPRT fusion gene exhibited dose-dependent cytotoxicity by 5-FC treatment (Figure 2-8). This result was expected since there are reports of successful tumor killing by the combination of CD::UPRT gene transfection and 5-FC treatment (Adachi et al 2000, and Koyama et al 2000). However, 5-FC was not able to cause dose response cytotoxicity to the MCF-7 cells transfected with the sCD44::CD::UPRT fusion gene. In fact, the dose response curve of the sCD44::CD::UPRT + 5-FC treatment group overlaps with the 5-FC treatment group, indicating that there was no enhanced cytotoxicity caused by the sCD44::CD::UPRT fusion gene.

There are some remaining questions that need further investigation. The most important being whether the sCD44::CD::UPRT fusion gene was expressed in MCF-7 cells. The Western blot failed because of the non-specific interaction of the anti-mouse IgG reacting

against MCF-7. It is also possible that the primary antibody failed to detect sCD44. The primary antibody against CD44 was raised from the N-terminal domain of human CD44. Unfortunately, the exact location of the epitope is proprietary information, so it is not clear whether the cloned region of sCD44 contained the epitope region that the antibody can detect. Since there was no sign of cytotoxicity of 5-FC on the cells that were transfected with sCD44::CD::UPRT gene, there was either lack of the fusion gene expression or the translated triple-fusion protein was unstable in the cells and not fully functional.

Human nerve growth factor receptor (NGFR) and vp22 protein from herpes virus simplex-1 are two targeting ligands that were used to create fusion constructs with the CD gene, and demonstrated anti-tumor effect with 5-FC via the GDEPT approach (Ramnaraine et al 2003, and Lee et al 2006). A recent GDEPT study showed that a triple fusion gene containing the human nerve growth factor receptor (NFGR) and CD::UPRT is difficult to expresse in the CEM human leukemia lymphoid cell line (O'Brian et al 2006). In their study, several different arrangements of NGFR, CD, and UPRT genes were created in a retroviral vector to transfect CEM cells to examine the expression of the fusion protein containing NGFR. Since all constructs were designed to express NGFR on the cell surface, flow cytometric analysis was performed to directly compare the expression levels of NGFR among CEM cells that were transfected with different arrangements of the fusion genes. The study showed that the CEM cells transfected with a retroviral vector containing the direct fusion of the NGFR::CD::UPRT genes had ~10-fold lower expression of NGFR than the cells that were transfected with the vector

containing the NGFR::CD fusion gene. Furthermore, the level of 5-FC metabolism correlated with the NFGR fusion protein expression level in CEM cells. Interestingly, when the internal ribosome entry site (IRES) sequence was inserted between the CD and UPRT genes to create a single bicistronic message construct of NGFR::CD::UPRT, the expression level of NGFR was almost equal to the level of NGFR detected from the cells that were transfected with NGFR::CD. The CD and UPRT enzyme activities were confirmed *in vitro*, which confirmed the expression of the NGFR, CD, and UPRT genes. Therefore, it is possible the transient transfection of MCF-7 cells with the sCD44::CD::UPRT fusion gene was not able to express enough fusion protein to catalyze the prodrug 5-FC to cause cytotoxicity. Perhaps the use of a sCD44::CD fusion gene construct would have resulted in a better gene expression in MCF-7 cells and enhance the *in vitro* cytotoxicity of 5-FC on the transfected MCF-7 cells.

Although 5-FC was able to cause cytotoxic effects on MCF-7/CD::UPRT, the resulting cytotoxic effect was not as good as 5-FU treatment on MCF-7 cells (Figure 2-8B). A successful bystander effect caused by transfected cells depends on the sustained expression of the fusion protein containing CD to generate cytotoxic drug 5-FU. It may be possible to enhance the cytotoxic effect *in vitro* by transfecting more cells with higher doses of DNA/PEI complex. However, it would be extremely difficult to target and achieve higher expression of the fusion protein in the tumor cells *in vivo* without causing unwanted toxicities from the gene delivery treatment.

It would be interesting to examine the cytotoxicity of 5-FC on MCF-7 cells that are stably transfected with a multi-cycle replication competent retroviral vector (the same RCR vector used in Tai et al 2005) containing the sCD44::CD::IRES::UPRT fusion gene. Under this strategy, the RCR vector would target and transfect rapidly dividing tumor cells to express the sCD44-CD fusion protein. The expressed sCD44-CD would be secreted from the stably transfected tumor cells and convert 5-FC to 5-FU in the cell culture medium. The UPRT enzyme inside the transfected tumor cells would rapidly catalyze 5-FU to 5-FUMP to make these tumor cells more sensitive to 5-FU. This GDEPT strategy of MAT could be particularly useful for those cell lines that are less sensitive to 5-FU treatment.

There are many missing experiments that I needed to perform in order to make the story of this chapter complete. Instead of optimizing the mammalian expression construct to make the MAT strategy work via GDEPT approach, I shifted my focus to express and purify a recombinant fusion protein containing the hyaluronan binding domain of TSG-6 and the CD enzyme. The following two chapters describe design, cloning, expression, purification, and functional characterization of the LinkCD fusion protein, as well as *in vivo* anti-tumor effect in combination with 5-FC.

2.5 Conclusions

The non-toxic prodrug 5-FC was able to cause a dose-dependent cytotoxicity on the MCF-7 cells transiently transfected with CD::UPRT fusion gene. However, the level of cytotoxicity was not as strong as 5-FU treatment alone. 5-FC was not able to cause cytotoxicity on the MCF-7 cells transfected with sCD44::CD::UPRT fusion gene, presumably because the fusion gene was not expressed well in MCF-7 cells. Thus, this *in vitro* study demonstrates the limitations of GDEPT for killing cancer cells.

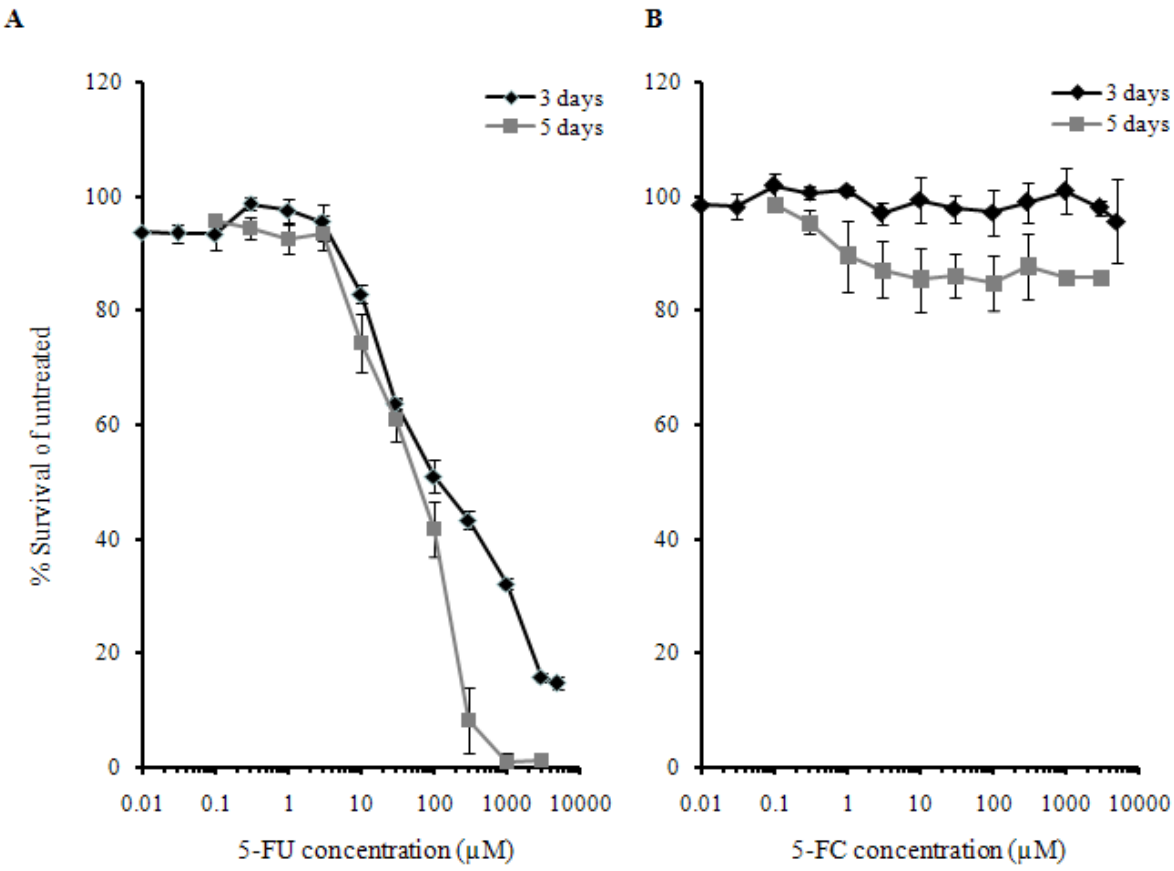

Supplementary Figure 2-1. *In vitro* dose-dependent cytotoxicity of 5-FU (**A**) and 5-FC (**B**) on U87-MG cell lines after 3 days (black) and 5 days (gray) of incubation with the drug. The data represents the mean % survival of untreated control ± propagated error. The dose response curve for 5-FU moves downwards with increasing time of incubation. 5-FC is relatively non-toxic up to 1 mM concentration.

CHAPTER 3

Cloning, Expression, Purification, and Characterization of the LinkCD Fusion Protein for Targeting the Extracellular Matrix of Solid Tumors

3.1 Abstract

Matrix Attachment Therapy (MAT) is an enzyme prodrug strategy that targets hyaluronan in the tumor extracellular matrix to deliver a prodrug converting enzyme near the tumor cells. To test a proof of concept for MAT, a recombinant fusion protein containing the hyaluronan binding domain of TSG-6 (Link) and yeast cytosine deaminase (CD) with an N-terminal His(×6) tag was constructed in bacterial expression vector. LinkCD was expressed in *E.coli* and purified by metal-chelation affinity chromatography. The purified LinkCD fusion protein exhibits a K_m of 0.33 mM and V_{max} of 15 μM/min/μg for the conversion of 5-FC to 5-fluorouracil (5-FU). The duration of the enzyme activity for LinkCD was longer than that of the CD enzyme at 37 ^oC: the fusion protein retained 20% of its initial enzyme activity after 24 hr, and 12% after 48 hr. The LinkCD fusion protein can bind to hyaluronan oligomer (12-mer) at a K_D of 55 μM at pH 7.4 and a K_D of 5.32 μM at pH 6.0 measured using surface plasmon resonance (SPR). His-tagged CD enzyme and Link protein were also expressed in *E.coli*. His-tagged CD enzyme was purified from the soluble fraction of the *E.coli* lysate as a native protein. The functional mutant of the CD enzyme was also created to knock out the enzyme function of LinkCD for an additional control for a subsequent animal study. His-tagged Link protein was expressed as an inclusion body protein, and recovered from the insoluble fraction of the *E.coli* lysate.

3.2 Introduction

A variety of strategies have been proposed to improve the selectivity of chemotherapeutic drugs. Antibody-Directed Enzyme Prodrug Therapy (ADEPT) is a strategy devised to target cancer cells with an antibody-enzyme conjugate (reviewed in Senter and Springer 2001). The antibody targets the enzyme to the cancer cell and the enzyme converts a relatively non-toxic prodrug to a cytotoxic drug. In theory, targeting the enzyme to the cancer results in local production of the cytotoxic drug; the high drug concentration could eradicate the cancer cells in the vicinity of the enzyme. Gene-Directed Enzyme Prodrug Therapy (GDEPT, or VDEPT for Viral-Directed Enzyme Prodrug Therapy) is a variant of ADEPT where the enzyme is expressed in the tumor cells. ADEPT and GDEPT systems exploit the Enhanced Permeability and Retention (EPR) effect of the leaky tumor vasculature to access the cancer while reducing accumulation of the system in normal tissue (O'Conner et al 1984). ADEPT and GDEPT approaches to treat cancer have been investigated since the late 1980's (reviewed in Bagshawe 2006 and Glasgow et al 2006) without clinical success. A major disadvantage for both ADEPT and GDEPT is the lack of a robust target. Tumor specific antigens, which are usually growth factor receptors, are heterogeneous. Moreover, not all patients over-express the same cancer cell marker; for instance, only 25% of breast cancer patients over-express Her-2/neu (Slamon et al 1989). Thus, a single antibody is unable to target all variants. An unresolved challenge to GDEPT is the lack of a safe and effective vector. Inefficient transfer of genetic materials into cancer cells, and the short survival of the genetically modified cells are additional barriers for the GDEPT approach (reviewed in Greco and Dachs 2001).

To overcome several of the obstacles of current enzyme prodrug therapies, the Matrix Attachment Therapy (MAT) strategy was devised to target hyaluronan in the extracellular matrix of cancer cells to localize a prodrug converting enzyme in the tumor. Hyaluronan is a linear polysaccharide (Mw > 10^6 Da) consisting of repeating disaccharides of N-glucosamine and D-glucuronate (Fraser et al 1997). Hyaluronan is implicated in the proliferation, migration, and metastasis of cancer (Itano et al 1999 and Kosaki et al 1999). Although present in normal tissues, hyaluronan is up-regulated in many cancers including: breast, ovarian, colon, lung, and prostate (reviewed in Toole 2004). In particular, breast and ovarian cancers have high levels of hyaluronan where its up-regulation is associated with poor patient survival (Anttila et al 2000 and Auvinen et al 2000).

Using the MAT strategy directed towards hyaluronan has several distinct advantages for targeting cancer: 1) there is no known heterogeneity of hyaluronan; 2) hyaluronan in the tumor matrix can be targeted by the EPR effect. Extravasation into normal tissue is greatly diminished because of their intact endothelial cell barrier. Thus, the hyaluronan content in the tumor does not have to be elevated for MAT to achieve selective tumor targeting; 3) there are many binding sites on hyaluronan; 4) the cytotoxic drug generated in the tumor matrix can also target stromal cancer cell-associated fibroblasts that support tumor metastasis (Olumi et al 1999); and 5) disrupting cell-to-hyaluronan association inhibits tumor progression in some experimental models (Peterson et al 2000, Ahrens et al 2001, Mummert et al 2003, and Xu et al 2003).

CD44, TSG-6 (Tumor necrosis factor alpha-stimulated Gene-6), and RHAMM (Receptor for hyaluronan-mediated mobility) are major hyaluronan binding proteins found in human and other mammals (reviewed in Day and Prestwich 2002). The function and structure of hyaluronan binding domains of CD44 and TSG-6 (also known as the Link domain) are well characterized (Blundell et al 2005, and Banerji et al 2007). The TSG-6 Link domain binds to hyaluronan tighter than does the CD44 Link domain (Lesley et al 2002), so we used the Link domain from TSG-6 as the hyaluronan binding portion of the fusion protein. We selected cytosine deaminase (CD) from yeast to create a chimeric fusion protein, LinkCD, for a proof of concept of the MAT strategy. Cytosine deaminase is found in bacteria and fungi but not mammals, and has been extensively employed for ADEPT and GDEPT to generate cytotoxic 5-fluorouracil (5-FU) from the prodrug 5-fluorocytosine (5-FC). 5-FC is a widely used orally available antimicrobial prodrug with high bioavailability (Cutler et al 1978). In this chapter, I describe the creation and functional characterization of a LinkCD fusion protein. Site-directed mutagenesis was done to make a functional mutant of LinkCD.

3.3 Methods

3.3.1 Chemicals and reagents

All restriction enzymes and T4 ligase used for cloning were purchased from New England Biolabs (Beverly, MA). Primers used for cloning and performing mutagenesis were synthesized by IDT (Coralville, IA) and Invitrogen (Carlsbad, CA). The bacterial expression vectors pET41a and pET15b were purchased from Novagen (San Diego, CA).

All chemicals used in our experiments were purchased from Sigma-Aldrich (St. Louis, MO).

3.3.2 Construction of bacterial expression vectors and site-directed mutagenesis

The sequences of primers used for cloning and mutagenesis are listed in Table 3-1. The restriction enzyme sites used for all constructs were carefully selected by analyzing the restriction enzyme map of each open reading frame (ORF) to avoid unwanted cleavage of the target gene sequence. Thus, only the restriction enzymes that do not cut ORF were chosen for cloning. The web-based sequence analysis software package is available on the UCSF Sequence Analysis and Consulting Service webpage (www.sacs.ucsf.edu/Resources/sequenceweb.html). All plasmid purifications were done using either Qiagen HiSpeed Midi or Qiagen Spin Miniprep Kits (Qiagen; Valencia, CA).

To create a bacterial expression construct for producing the LinkCD fusion protein in *E.coli*, the cloning was performed in two steps. First, GST-tag fusion in pET41a vector was created. Using cDNA of yeast CD (Invivogen; San Diego, CA), the ORF was amplified by the primers [1] and [2] (Table 3-1). The ORF was ligated into SacII and XhoI restriction sites of pET41a vector. Then the ORF of the Link domain of TSG-6 (Link) was amplified from cDNA of TSG-6 (American Type Culture Collection; Manassas, VA) using the primers [3] and [4] (Table 3-1). The Link ORF was inserted into the SacII site of pET41-CD to create pET41-LinkCD.

Table 3-1: List of oligonucleotide primers used for cloning and mutagenesis

Clone	Target amplicon	Direction	Restriction enzyme site	Sequence
pET41-GST-LinkCD	CD	5’	SacII	**[1]** *GCTCGT*CCGCGGGTCTGGTGCCACGCGGTAGTGTCACAGGAGGCATGGC
		3’	XhoI	**[2]** *GCTCGT*CTCGAGTTACTCCCCAATGTCCTCAAAC
	Link	5’	SacII	**[3]** *GCTCGT*CCGCGGGTCTGGTGCCACGCGGTAGTGGTGTGTACCACAGAGAAGCAC
		3’	SacII	**[4]** *GCTCGT*CCGCGGCTTTGCGTGTGGGTTGTAG
pET15-His-LinkCD	CD	5’	NdeI	**[5]** *GCTCGT*CATATGGGTGGTGGTGGTAGCGGTGGTGGTGGTAGCGGTGGTGGTGGTAGCATGGTCACA GGAGGCAT
		3’	BamHI	**[6]** *GCTCGT*GGATCCTTACTCCCCAATGTCCTCAAACCAGT
	Link	5’	NdeI	**[7]** *GCTCGT*CATATGGGTGTGTACCACAGAGAAGCA
		3’	AseI	**[8]** *GCTCGT*ATTAATCTTTGCGTGTGGGTTGTAGC
pET41-His-CD	CD	5’	NdeI	**[9]** *GCTCGT*CATATGCATCATCACCACCATCACCTGGTGCCACGCGGTAGTGTCACAGGAGGCATGGC
		3’	XhoI	**[10]** *GCTCGT*CTCGAGTTACTCCCCAATGTCCTCAAAC
pET41-His-Link	CD	5’	NdeI	**[11]** *GCTCGT*CATATGCATCATCACCACCATCACCTGGTGCCACGCGGTAGTGGTGTGTACCACAGAGAA GCAC
		3’	XhoI	**[12]** *GCTCGT*CTCGAGTTACTTTGCGTGTGGGTTGTAG
pET41-His-mtCD(E68A)	CD	5’	N/A	**[13]** CCCTGCATGGGGCGATCAGCACCCTG
		3’	N/A	**[14]** CAGGGTGCTGATCGCCCCATGCAGGG
pET41-His-mtLink(Y78V)	Link	5’	N/A	**[15]** GGAAAAACTGGCATTATTGATGTGGGAATCCGTCTCAATAGG
		3’	N/A	**[16]** CCTATTGAGACGGATTCCCACATCAATAATGCCAGTTTTTCC

GCTCGT (italicized) was used as non-specific extra nucleotide sequence to facilitate the annealing of the terminal ends of the resulting PCR products. The restriction enzyme site sequences are underlined. The mutagenesis primers for pET41-His-mtCD(E68A) were also used to create pET41-His-Link-mtCD for the expression of a functional mutant of the fusion protein that lacks cytosine deaminase activity.

The bacterial expression vector for producing N-terminal His-tagged LinkCD with a flexible linker between the Link and CD domains was constructed in pET15 vector. Using pET41-GST-LinkCD as a template, the CD gene was amplified using the primers [5] and [6] (Table 3-1). The 5'-primer contained the nucleotide sequence for a $(Gly_4Ser)_3$ flexible linker. The amplicon was inserted into pET15b vector between NdeI and BamHI restriction sites. The ORF of the Link domain was amplified using the primers [7] and [8] (Table 3-1), and it was inserted into the NdeI site of pET15-CD to produce pET15-His-LinkCD (compatible-end ligation was used between ORFs of Link and $(Gly_4Ser)_3$ - CD).

To construct a bacterial expression vector containing His-tagged CD enzyme, the CD gene was amplified from the cDNA of yeast CD by using the primers [9] and [10] (Table 3-1) and ligated into NdeI and XhoI restriction sites of pET41. Thus, the nucleotide sequence for the N-terminal GST-tag in the vector sequence was replaced by the N-terminal His-tag from the 5' primer sequence. A bacterial expression vector for His-tagged Link protein was also constructed in pET41 without a GST-tag. The primers [11] and [12] (Table 3-1) were used to amplify the nucleotide sequence of the Link domain of TSG-6 from the cDNA of TSG-6. The Link amplicon was inserted into NdeI and XhoI restriction sites in pET41 vector.

All final ligation products were transformed into DH-5α *E.coli* cells (Invitrogen; San Diego, CA) for screening, and the nucleotide sequences of all expression vectors were

verified by DNA sequencing reactions (SeqWrite DNA Technology Services; Houston, TX).

A functional mutant of CD that lacks the enzyme activity was created by a single point mutation, resulting in a Glu to Ala change at the residue 64 using the QuikChange® II Site-Directed Mutagenesis Kit (Stratagene; La Jolla, CA) and designed primers for the point mutation ([13] and [14] in Table 3-1). Using pET41-His-CD as a template, the mutagenesis was done with 12 cycles of denaturing (95 ^{o}C), annealing (55 ^{o}C), and extension (68 ^{o}C). After DpnI treatment of the reaction mixture to digest methylated template plasmid, 2 µl of PCR reaction mixture was transformed into DH-5α *E.coli* cells for screening to confirm the mutation sequence. Using the same pair of primers, a functional mutant of the LinkCD fusion protein that lacks the CD enzyme activity was also created by performing site-directed mutagenesis reaction on the pET15-His-LinkCD plasmid.

A functional mutant of the Link protein (mtLink Y78V) that has attenuated hyaluronan binding activity (Mahoney et al 2001) was created. Site-directed mutagenesis was performed by using the primers [15] and [16] (Table 3-1) on pET41-His-Link plasmid. The reaction conditions for PCR amplification of the mutant plasmid and DpnI digestion of the template plasmid were the same as the above conditions for creating functional mutants of CD and LinkCD.

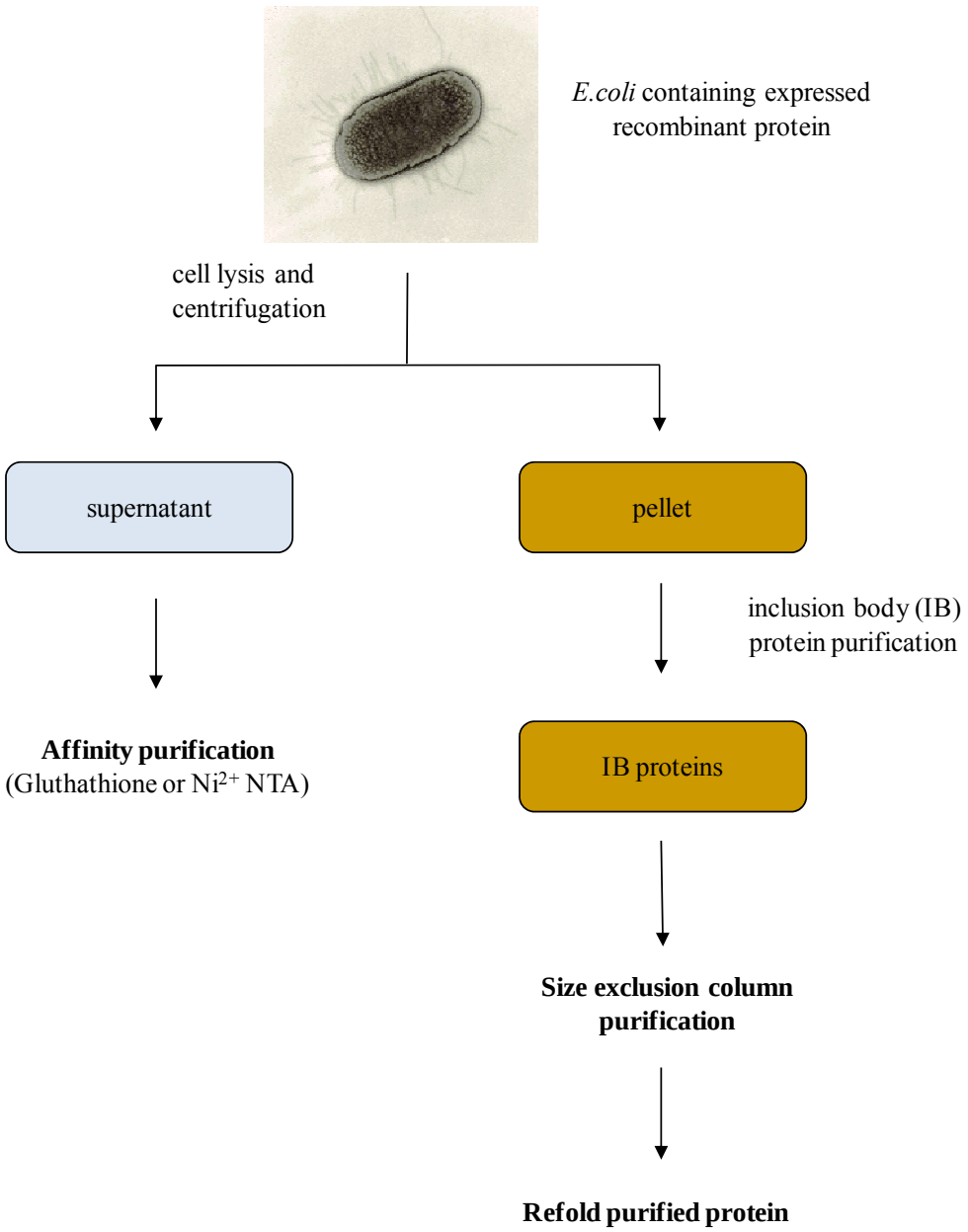

Figure 3-1. Overview of protein purification. GST-tagged or His-tagged LinkCD fusion protein (pET41-GST-LinkCD or pET15-His-LinkCD) and CD enzyme (pET41-His-CD) were purified from the soluble supernatant fraction (left), whereas His-tagged TSG-6 Link protein (pET41-His-Link) was purified from the inclusion body proteins and refolded subsequently (right).

To prepare frozen stocks of plasmid-containing *E.coli*, glycerol was added (15% v/v) to the overnight culture *E.coli* and stored at -80 ^{o}C.

3.3.3 Protein expression and purification in E.coli

All proteins were expressed using *E.coli.* An overview of the protein purification procedures is shown in Figure 3-1. The LinkCD fusion protein and CD enzyme, as well as the functional mutants of these proteins that lack cytosine deaminase activity (Link-mtCD and mtCD), were purified from the soluble fraction. The Link protein was purified from the inclusion body proteins.

3.3.3.a Expression and purification of GST-tagged LinkCD

pET41-GST-LinkCD plasmid was transformed into BL21 (DE3) pLySs *Ecoli* cells (Stratagene; La Jolla, San Diego). This strain of *E.coli* contains lysozyme gene (pLysS), which facilitates the breakdown of the cell wall after protein expression. *E.coli* cells containing pET41-GST-LinkCD plasmid were grown in 1 L LB containing 30 μg/ml of kanamycin at 37 ^{o}C until OD_{600nm} reached between 0.6 and 0.9. The protein expression was induced by adding 0.5 mM isopropyl *β*-D-1-thiogalactopyranoside (IPTG) to the *E.coli* cell culture, and the expression was done at 37 ^{o}C for 4 hr. Bacterial cells were collected by centrifugation at 6,000×g for 30 min at 4 ^{o}C, and resuspended in 20 mL of PBS buffer containing 0.5 mM phenylmethylsulphonyl fluoride (Roche Applied Science; Indianapolis, IN). After one cycle of freeze-thawing, the cells were lysed by lysozyme treatment (1 mg/ml final concentration) on ice for 30 min, followed by sonication (3 × 30 sec, with 1 min pause between each step). The cell lysate was mixed with an equal

volume of 2% Triton X-100. After vigorous shaking to mix the detergent solution and cell lysate evenly, DNase and RNase were added (5 µg/ml final concentration) to digest nucleic acid at 4 ^{o}C with constant shaking for 10 min (or until the cell lysate was no longer viscous). The cell lysate was centrifuged at 3,000×g for 30 min at 4 ^{o}C. The supernatant containing soluble proteins was collected. A 50% slurry of Glutathione Sepharose 4B (0.5 ml) was added to the collected supernant, and was incubated at room temperature with end-over-end rotation. The GS-4B beads were spun-down by centrifugation at 500×g for 5 min at room temperature. The supernatant (flow-through, which contain unbound proteins) was removed, and the GS-4B beads were washed with 10 bed volumes of PBS. Washed beads were spun-down by centrifugation at 500 × g for 5 min at room temperature. The wash step was repeated twice using PBS buffer. The protein bound to GS-4B beads was eluted by resuspending the GS-4B in Elution Buffer containing 50 mM Tris-Cl and 10 mM glutathione at pH 8 at room temperature for 10 min on end-over-end rotor. The elution step was repeated twice.

3.3.3.b Expression and purification of His-tagged LinkCD and CD

For expression of pET15-His-LinkCD, the purified plasmid was transformed into BL21-Codon Plus (DE3)-RIPL *E.coli* cells (Stratagene; La Jolla, CA), which contains tRNAs for rare codons to express mammalian proteins. *E.coli* cells containing pET-LinkCD plasmid were grown in 1 L LB containing 50 µg/mL of carbenicillin at 35 ^{o}C until OD_{600nm} reached between 0.6 and 0.9. The protein expression was induced by adding IPTG (0.5 mM final concentration), and the expression was done at 23 ^{o}C overnight with constant shaking at 200 rpm. Bacterial cells containing the expressed protein were

collected by centrifugation at 6,000×g for 30 min at 4 ^{o}C, and resuspended in 20 mL of Lysis Buffer containing 300 mM NaCl, 20 mM Tris-Cl, 40 mM imidazole, 0.2% Triton X-100, and 0.5 mM PMSF. After one cycle of freeze-thawing, the cells were lysed by combination of lysozyme and sonication treatments in an ice-water bath. The cell lysate was treated with DNase I and RNase A to digest nucleic acid, and centrifuged at 10,000×g for 45 min at 4 ^{o}C. The supernatant containing soluble proteins was collected, and 10 mM β-mercaptoethanol was added to the supernatant fraction and filtered through a 0.4 μm membrane. The filtered supernatant fraction was applied on a HisTrap™ FF affinity column (Amersham Biosciences; Piscataway, NJ) that was pre-equilibrated with binding buffer containing 300 mM NaCl, 20 mM Tris-Cl, and 40 mM imidazole, pH 8. After the entire soluble fraction was passed through the column, the column was washed with 20 column volumes of the binding buffer, followed by 10 column volumes of 2 M NaCl, 20 mM Tris-Cl, and 40 mM imidazole, pH 8. The bound protein was eluted using elution buffer containing 300 mM NaCl, 20 mM Tris-Cl, and 500 mM imidazole, pH 8. The eluates were pooled and applied onto an Econo-Pac® 10DG desalting column (Bio-Rad; Hercules, CA) to remove imidazole and to exchange buffer to PBS. The purified protein was concentrated using Amicon® Ultra Centrifugal Filter Unit (Millipore; Billerica, MA). For expression of the Link-mtCD fusion protein, pET15-Link-mtCD was transformed into BL21-Codon Plus (DE3)-RIPL *E.coli* cells. Link-mtCD was expressed and purified using the same procedure that was used for LinkCD. The average yield for LinkCD and Link-mtCD was 0.5 mg per liter culture.

For expression of the CD enzyme, pET41-His-CD plasmid was transformed into BL21-Codon Plus (DE3)-RIPL *E.coli* cells. The expression and purification procedure for the CD enzyme were also done using the same methods described above for the LinkCD fusion protein using HisTrap™ FF affinity column (Amersham Biosciences). The pooled eluates containing the CD enzyme were immediately loaded on a HiPrep Sephacryl™ S-100 HR 16/60 column (Amersham Biosciences) that was pre-equilibrated with 50 mM NaCl, 25 mM Tris-Cl pH 8.0 at 4 ^{o}C. The column was operated at the flow rate of 0.5 mL/min, and 2 mL was collected for each fraction. The fractions containing the CD enzyme were measured by OD_{280nm} and pooled together. The average yield for CD enzyme was 30 mg per liter culture.

3.3.3.c Expression and purification of His-tagged Link protein

1% Glucose was added to all culture medium for pET41-His-Link/*E.coli* to inhibit the basal level expression of the Link protein, because the expression of the Link protein in *E.coli* was reported to be toxic to the host cells (Day et al 1996). The pET41a-His-Link plasmid was transformed into BL21 Codon Plus (DE3)-RIPL *E.coli* cells. Overnight-culture of the *E.coli* cells containing pET-LinkCD plasmid were grown in 1 L LB containing 1% glucose and 50 μg/mL of carbenicillin at 35 ^{o}C until OD_{600nm} reached between 0.6 and 0.9. Then protein expression was induced by adding 0.5 mM IPTG (final concentration) to the culture medium. The protein expression was done at 35 ^{o}C for 4 hr with constant shaking at 200 rpm. Bacterial cells containing the expressed protein were collected by centrifugation at 6,000×g for 30 min at 4 ^{o}C. The cells were resuspended in 20 ml PBS with 0.5 mM PMSF. After one cycle of freeze-thawing, the

cells were lysed by combination of lysozyme and sonication treatments in an ice-water bath. An equal volume of PBS was added to the cell lysate and mixed with 5 μg/ml of DNase I and RNase A, and 0.2% Triton X-100. The cell lysate containing nucleases were incubated at 4 ^{o}C for 10 min (or until the lysate solution was non-viscous). The cell lysate was centrifuged at 12,000×g for 30 min at 4 ^{o}C to collect the pellet containing insoluble (inclusion body) proteins. After centrifugation, the supernatant was removed and the pellet was resuspended in 400 mL of ice-cold dH_2O containing 0.1% Triton X-100 and 0.1 mM PMSF. The resuspended pellet was centrifuged at 10,500×g for 45 min at 4 ^{o}C. The pellet was resuspended in 400 mL of ice-cold dH_2O with 0.1 mM PMSF, and centrifuged again at 10,500×g for 45 min at 4 ^{o}C. The pellet was resuspended in 5 mL of 8 M guanidine-HCl, 50 mM Tris-Cl, pH 8, and 100 mM DTT. The solution was incubated at 37 ^{o}C for 1 hr. Then the insoluble material was removed by centrifugation at 12,000×g for 5 min at 4 ^{o}C. The supernatant containing denatured inclusion body protein was filtered through 0.4 μm membrane, and loaded on to HiLoad Superdex 2000 size exclusion column equilibrated with 6 M guanidine-HCl and 20 mM Tris-Cl, pH 8. After sample loading, the running buffer (6 M guanidine-HCl and 20 mM Tris-Cl, pH 8) ran through the column at the constant flow of 0.5 mL/min using Bio-Rad Econo Pump (Bio-Rad; Hercules, CA). The entire column volume (120 mL) was collected using a fraction collector, with each fraction containing 2 mL volume.

The refolding procedure for the Link protein was adopted from the protocol described in Kahmann et al (1997). To refold the Link protein, a C4 column (Vydac; Deerfield, IL) was pre-equilibrated with 95% Solvent A (0.1% trifluoroacetic acid) and 5% Solvent B

(80% acetonitrile and 0.09% trifluoroacetic acid) with a flow rate of 3 mL/min for 10 min using Dionex HPLC. The denatured Link protein was injected to the pre-equilibrated C4 column. The linear gradient of Solvent B was set up as follows: 5% Solvent B (the initial condition) from 0 min to 10 min after the sample loading, 5 – 40% Solvent B from 10 min to 20 min, and 40 – 60% of Solvent B from 20 min to 40 min. The protein peak eluted during the last gradient time point was collected. Acetonitrile in the protein solution was evaporated using a rotor evaporator at room temperature, and the protein was lyophilized in a 15-ml conical tube. The lyophilized protein was resuspended in 50 mM ammonium acetate buffer at pH 6 to a final concentration of 0.5 mg/mL (40 μM). Then 100-fold molar excess β-mercaptoethanol (4 mM) was added to the protein solution. The protein solution was incubated at room temperature for 2 days without stirring, in a 15-mL conical tube with holes in the lid for air oxidation. The average yield for Link protein was 10 mg per Liter culture.

3.3.4 Determination of the molecular weights of LinkCD and CD by size exclusion column

To determine the native molecular weights of LinkCD and CD, a Sephacryl™ S-100HR (Amersham Biosciences) size exclusion column was used. The column was calibrated using a Low Molecular Weight Gel Filtration Calibration Kit (Amersham Biosciences; Piscataway, NJ) containing blue dextran 2000 (for the void volume measurement), albumin (67 kDa), ovalbumin (43 kDa), chymotrypsinogen A (25 kDa), and ribonuclease A (13.7 kDa). The column was operated on Dionex HPLC, with a constant flow-rate of 0.5 mL/min using PBS buffer. The chromatograms containing the retention time of the

protein standards, LinkCD, and CD were recorded by the UV absorbance at 280 nm. The gel-phase distribution coefficient (K_{av}) for protein standards, LinkCD, and CD were calculated and a calibration standard curve plotted. The standard curve of K_{av} versus MW was used to estimate the molecular weights of LinkCD and CD.

3.3.5 Enzyme assay and kinetics measurements

Enzyme assays for measuring cytosine deaminase activity were performed at 37 ^{o}C in PBS. A 1-mL reaction mixture containing 5 mM of 5-FC and 5 μg of LinkCD fusion protein was incubated in a 37 ^{o}C water bath, and 20 μL of aliquots were taken out at various time points (10–30 min) and quenched in 980 μL PBS containing 0.1 N HCl. The concentrations of 5-FU in quenched solutions were calculated by measuring absorbance at 255 nm and 290 nm, as described by Senter and coworkers (Senter et al 1991):

$$\text{mM 5-FU} = 0.185\ \text{Abs}_{255\text{nm}} - 0.049\ \text{Abs}_{290\text{nm}}$$

$$\text{mM 5-FC} = 0.119\ \text{Abs}_{290\text{nm}} - 0.025\text{Abs}_{255\text{nm}}$$

These equations were validated by measuring the molar extinction coefficients of 5-FC and 5-FU at 255 nm and 290 nm in PBS containing 0.1 N HCl ($\varepsilon_{255\text{nm, 5-FC}}$ 2.069 $mM^{-1}cm^{-1}$, $\varepsilon_{290\text{nm, 5-FC}}$ 8.815 $mM^{-1}cm^{-1}$, $\varepsilon_{255\text{nm, 5-FU}}$ 5.831 $mM^{-1}cm^{-1}$, and $\varepsilon_{290\text{nm, 5-FU}}$ 1.528 $mM^{-1}cm^{-1}$). For enzyme kinetics measurement, 5 μg of LinkCD was added to a pre-warmed 1-mL reaction volume with various concentrations of 5-FC. A 20 μL aliquot was removed from the reaction mixture every 90 sec for 12 min and quenched in 980 μL PBS containing 0.1 N HCl. The K_m and V_{max} parameters were calculated from double-reciprocal plots.

To determine the stability of the enzyme activity at 37 ^{o}C, 50 μg of LinkCD or CD was stored in 1-mL volume of PBS at 37^{o}C. After various periods of incubation at 37 °C (1–124 hr), the enzyme activity was measured using the method described above, and activity was normalized as the percent of enzyme activity at time zero.

3.3.6 Circular dichroism and differential scanning calorimetry

Jasco J-715 spectropolarimeter with a Peltier temperature controller was used to measure the circular dichroism spectra on CD and LinkCD. All protein samples were prepared in PBS for circular dichroism studies. Circular dichroism spectrum measurements were done using wavelength scans from 270 nm to 200 nm using a 0.1-cm path length cuvette at 25 ^{o}C. To determine thermal denaturation of LinkCD, circular dichroism at a fixed wavelength (222 nm or 223 nm) was monitored in a 1-cm path length cuvette as a function of increasing temperature starting at 20 ^{o}C. EXAM software (Kirchhoff 1993) was used to fit the melting temperature curves and calculate T_m for each protein sample. Multi-Cell Differential Scanning Calorimeter (Calorimetry Sciences Corporation) was used to measure the melting temperature of CD enzyme. The purified CD enzyme sample in PBS and PBS were inserted into two different chambers. The instrument software measured and calculated the heat capacity of the protein sample using PBS as the reference as a function of increasing temperature.

3.3.7 Hyaluronan binding affinity measurement

Biacore T100 surface plasmon resonance (SPR) machine was used to measure the binding affinity of hyaluronan oligomer toward LinkCD. The surface of CM5 chip was

modified with tri-nitrilotriacetic acid (tri-NTA) by the following protocol: 1) Activate the CM5 chip by flowing the mixture of EDC (0.4 M)/NHS (0.1 M) at 10 μL/min for 7 minutes. 2) Flow the solution of amino tri-NTA (10 mM) in 50 mM pH 8.5 borate buffer at 10 μL/min in 2 minutes pulses for 15 cycles. 3) Block the remaining activated dextran with 1 M pH 8 ethanolamine (two 4 minutes cycles). 4) Wash the chip with 0.25% SDS and 0.35 M EDTA alternatively until a stable baseline is reached. The tri-NTA chip was then loaded with 5 mM $NiCl_2$, and LinkCD was immobilized on the surface through His-tag. The kinetics data were measured by flowing the hyaluronan oligomers (12-mer or 8-mer) through the LinkCD loaded chip at pH 7.4 and pH 6.0 respectively. Data were processed and analyzed with the Biacore T100 Evaluation software. Hyaluronan oligomers were digested from crude hyaluronan and purified by the published method (Ruhela et al 2006).

3.3.8 Matrix-assisted laser desorption (MALDI) and electro spray ionization mass spectrometry (ESI-MS)

To determine the molecular weight of purified Link protein, the protein sample was submitted to the Mass Spectrometry Facility at UCSF. The sample was prepared in sinapinic acid matrix. Also, to confirm the point mutation on the CD enzyme (E64A), purified samples of CD enzyme and mtCD(E64A) were submitted to the Biomolecular Resource Center at UCSF for ESI-MS analysis.

3.4 RESULTS

3.4.1 Characterization of the CD enzyme and Link protein

The pET41-His-CD expression vector was constructed to express the CD enzyme with an N-terminal His-tag and purified from *E.coli* to serve as a control protein for the LinkCD fusion protein characterizations (Figure 3-2). On average, about 30 mg of highly pure CD enzyme was purified per liter culture of *E.coli*. The activity of the CD enzyme was measured using 5-FC and cytosine (Figure 3-3). As shown in Figure 3-3C, even though K_m values match closely to the reported values (0.78 mM vs. 0.8 mM for 5-FC, and 4.9 mM vs. 3.9 mM; Kievit et al 1999), V_{max} for both 5-FC and cytosine were significantly higher in my experiments (0.14 μM/min/μg vs 0.067 μM/min/μg for 5-FC, and 0.57 μM/min/μg vs. 0.18 μM/min/μg for cytosine). The cause of this difference is not understood, but it may be due to the N-terminal His-tag.

The E64A functional mutant of the CD enzyme was created before the Link-mtCD. The yield of the mtCD enzyme was almost the same as that for the CD enzyme (~ 30 mg per liter culture of *E.coli*). DNA sequencing confirmed the mutation site on the pET41-His-mtCD plasmid (data not shown). Furthermore, the molecular weights of the purified CD and mtCD (E64A) were analyzed by electro-spray ionization mass spectrometry (ESI-MS) to confirm E64A mutation. ESI-MS analysis on the whole proteins were able to detect the difference in the molecular weights between CD and mtCD (Figure 3-4). For both CD and mtCD, there was a difference of 1.5 Da between the theoretical and observed molecular weights. A bacterial expression vector containing the ORF for Link-mtCD was constructed using the same pair of primers used for creating mtCD (primers [13] and [14] in Table 3-1), with pET15-His-LinkCD plasmid as the template.

The Link protein was also expressed and purified from *E.coli* containing pET41-His-Link plasmid (Figure 3-5A). Since the Link protein is known to be toxic to the host *E.coli* cells, the protein was purified from the inclusion body proteins. The denatured inclusion body proteins were separated on a HiLoad Superdex 200 size exclusion column (Figure 3-5B). There were two distinct peaks obtained from the size exclusion column. SDS-PAGE analysis shows that the most of the Link protein is found in the second peak, whereas the first peak contained higher molecular weight inclusion body proteins (Figure 3-5C). The molecular weight of the purified protein was confirmed by MALDI using sinapinic acid as the matrix (Figure 3-5D). The absolute m/z ratio did not match exactly to the theoretical mass of the Link protein (12578.5 observed vs. 12490 calculated), presumably due to the poor calibration of the instrument in this molecular weight range. The purified Link protein was refolded by the method described by Kahmann et al (1997). Using the C4 column, the Link protein was first solubilized in acetonitrile/ddH_2O mixture (Figure 3-6A). The refolding procedure continued with air-oxidation in the presence of excess β-mercapthoethanol in 50 mM ammonium acetate at pH 6.0 at room temperature. The circular dichroism scan suggests that the Link protein has secondary structure, though there is a strong interference signal below 210 nm, presumably due to the trace amount of β-mercapthoethanol (Figure 3-6B).

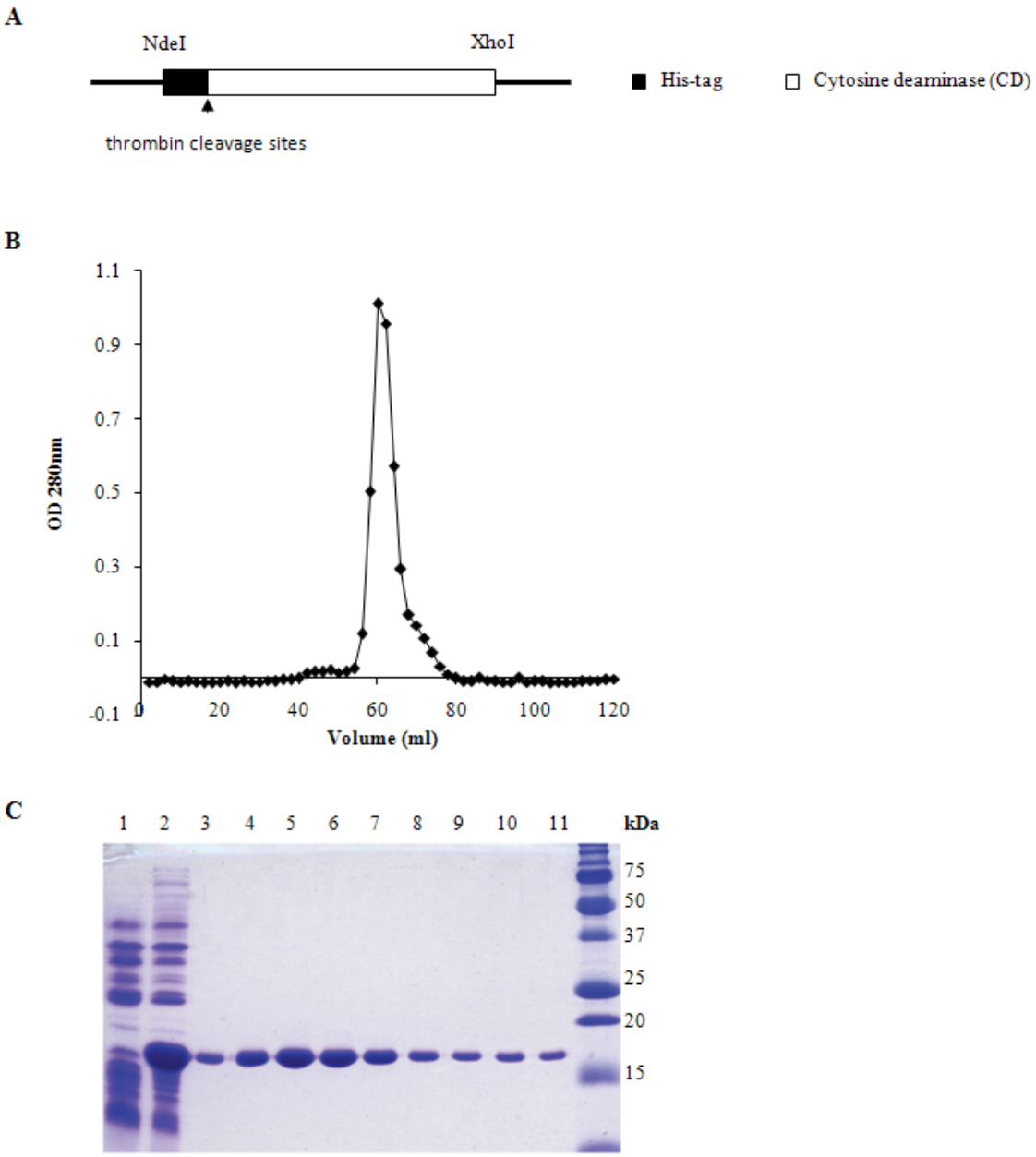

Figure 3-2. Purification of the His-tagged CD enzyme. A. pET41 vector containing the ORF of His-tagged CD (pET41-His-CD). The N-terminal GST-tag sequence in the expression vector was replaced by an N-terminal His-tag. **B.** Size exclusion column purification of CD enzyme. **C.** SDS-PAGE shows the purified CD enzyme from the size exclusion column. Cell lysates before (lane 1) and after (lane 2) IPTG induction. Lanes 3 – 11 show fractions collected from the size exclusion column. Fractions 5 – 7 were pooled together (the peak fractions) to be used for liposome conjugation.

A

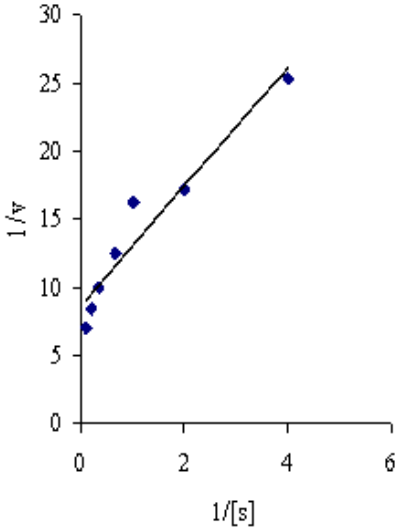

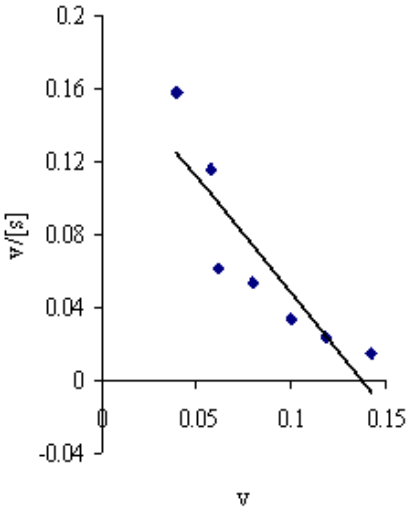

B

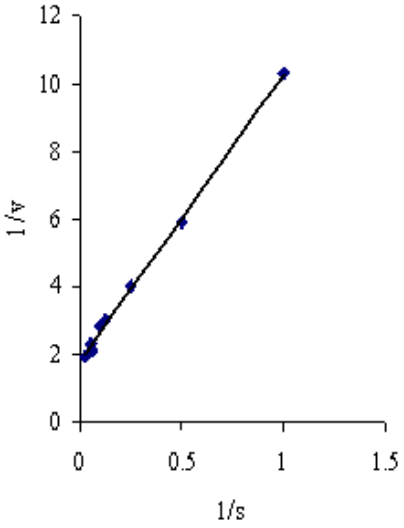

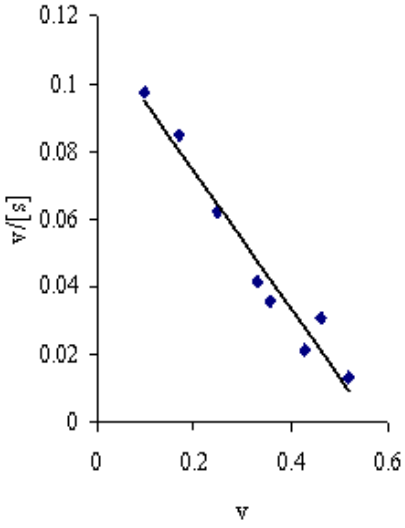

C

	5-FC	Cytosine
K_m (mM)	0.78 (0.8)	4.9 (3.9)
V_{max} (µM/min/µg)	0.14 (0.067)	0.57 (0.18)

Figure 3-3. Analyses of enzyme activity of the CD enzyme. The enzyme activity of the CD enzyme was measured with 5-FC (**A**) and cytosine (**B**) (v: mM 5-FU or uracil/min/µg, s: mM). **C**. The summary of the kinetics measurement. The numbers in the parenthesis are the literature values from Kievit et al (1999).

A

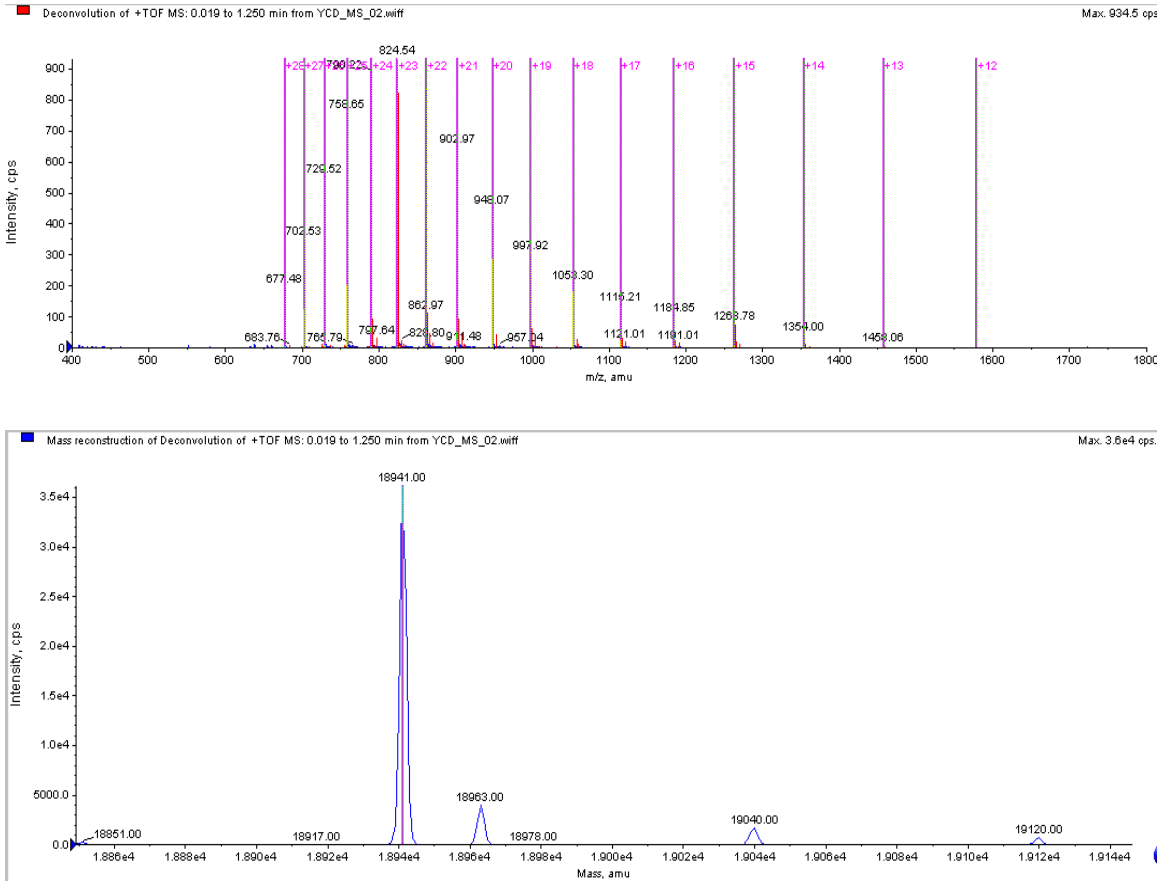

Figure 3-4. Determination of the molecular weights of CD and mtCD enzymes by ESI-MS. A. ESI-MS of the CD enzyme. The raw data showing the number of charges on the protein peak (top). The molecular weight of the CD enzyme was determined to be 18941.0 Da (bottom). The theoretical mass is 18939.5 Da.

B

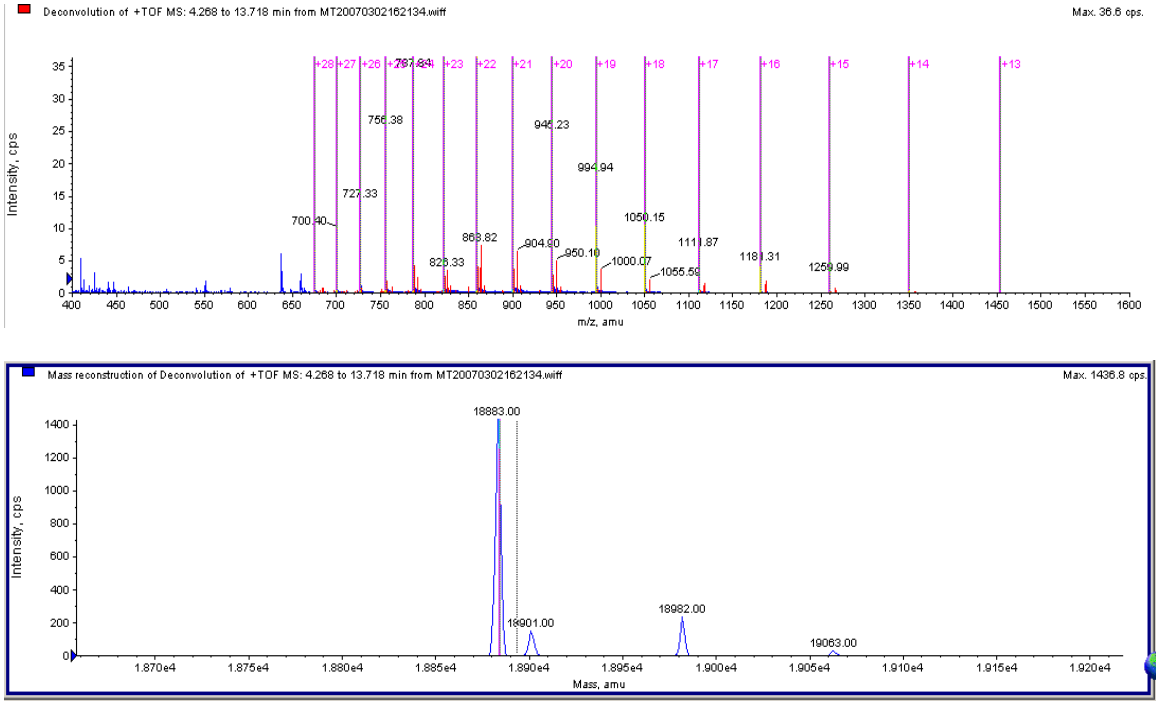

Figure 3-4. Determination of the molecular weights of the CD and mtCD enzymes by ESI-MS. B. ESI-MS of the mtCD (E64A) enzyme. The raw data showing the number of charges on the protein peak (top). The molecular weight of the functional mutant of CD enzyme with E64A mutation was determined to be 18883.0 Da (bottom). The theoretical mass is 18881.5 Da.

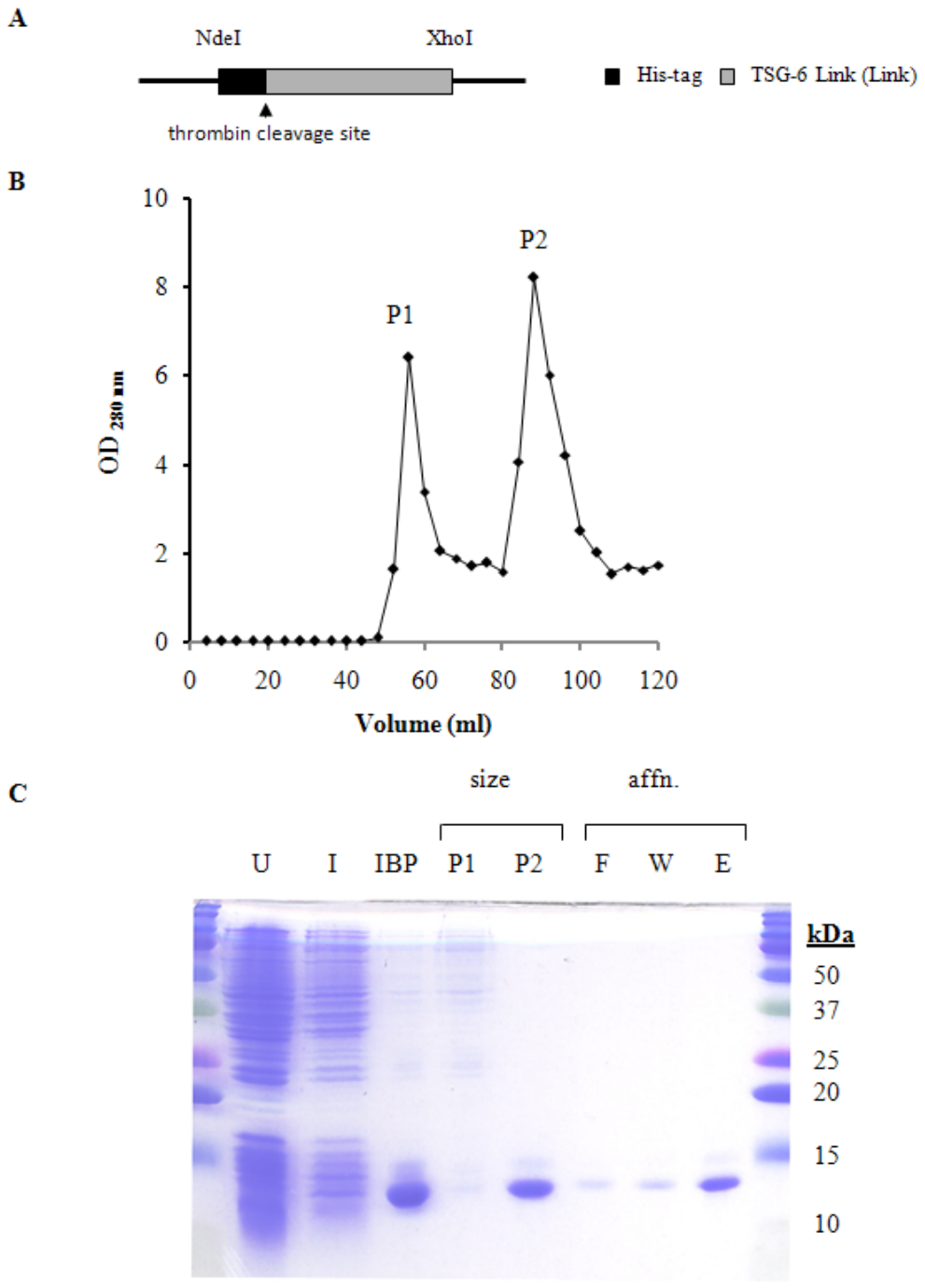

Figure 3-5. Purification of the His-tagged Link protein. A. pET41 vector containing the ORF of His-tagged Link (pET41-His-Link). The N-terminal GST-tag sequence in the expression vector was replaced by an N-terminal His-tag. **B.** The chormatogram shows the separation of the isolated inclusion body proteins on a Superdex 200 size exclusion column. Peak 1 (P1) and peak 2 (P2) were collected. **C**. SDS-PAGE analysis of purified Link protein. Abbreviations: U (uninduced), I (IPTG induced), IBP (inclusion body proteins), P1(peak 1), P2 (peak 2), F (flowthrough), W (wash), and E (eluate).

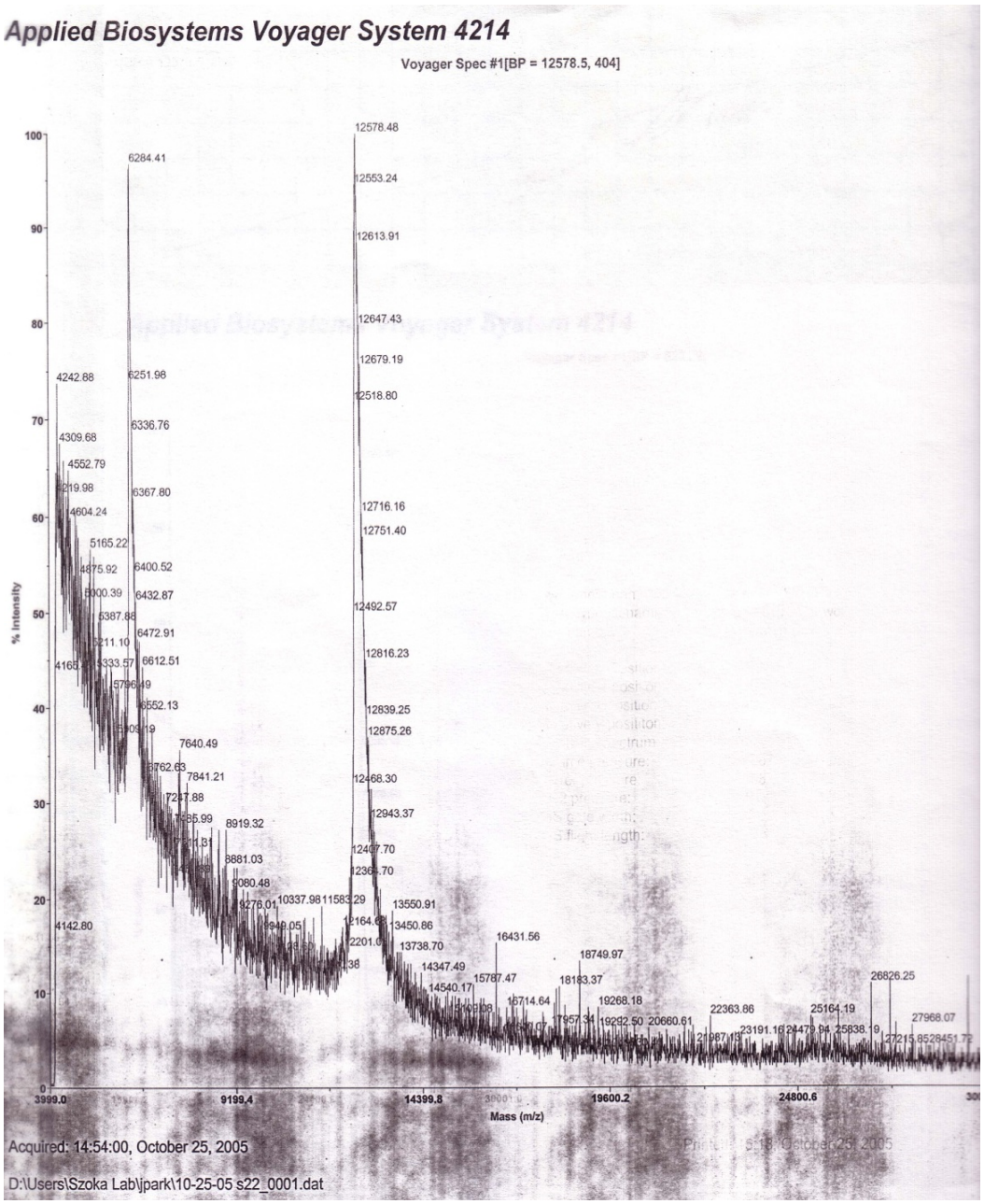

Figure 3-5 Purification of His-tagged Link (continued from the previous page). D. MALDI shows that the molecular weight of the purified Link protein is 12578.5 kDa. The theoretical mass of the Link protein is 12490.3 Da The peak at 6284.4 appears to be the double charged protein.

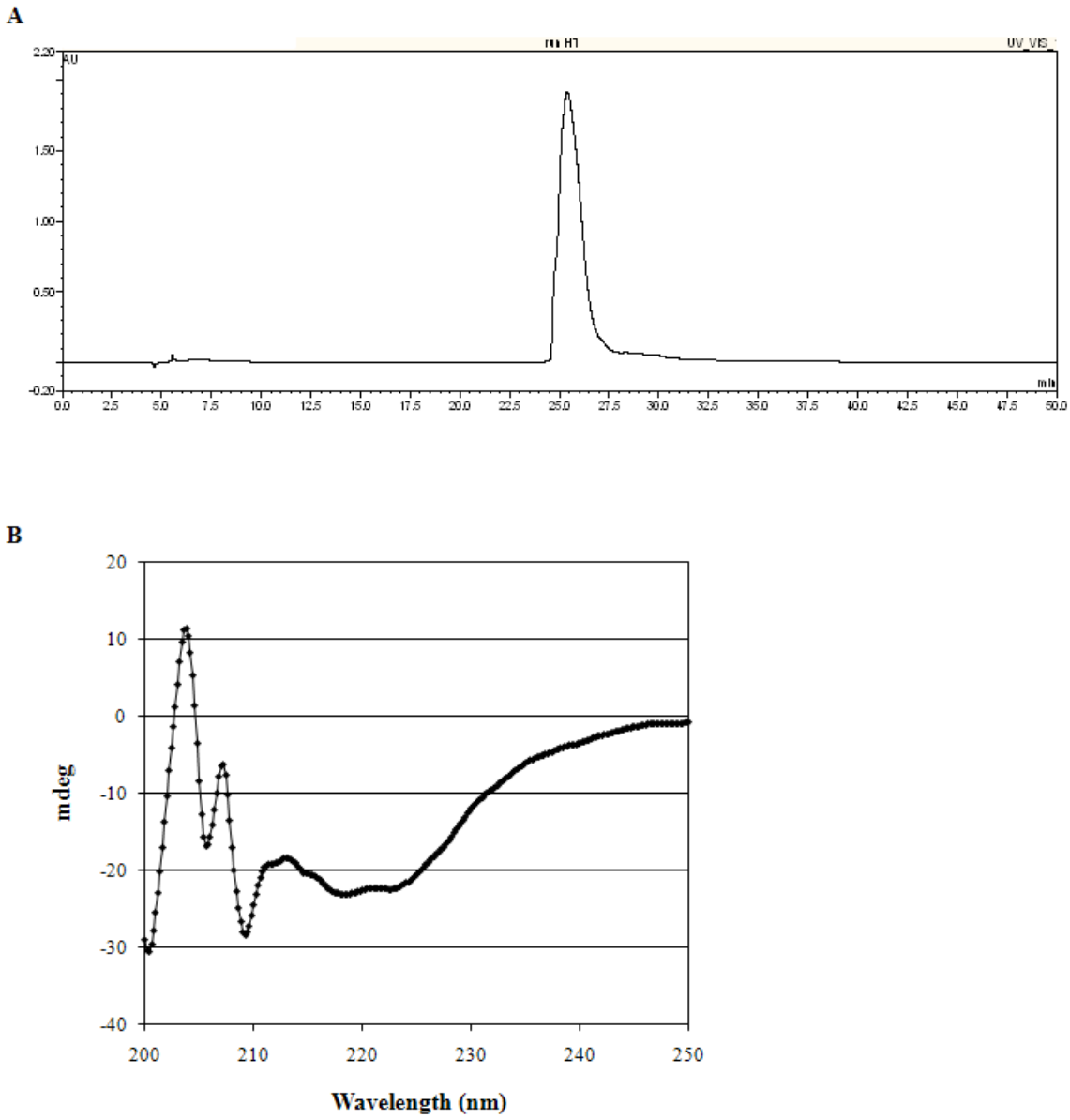

Figure 3-6. Refolding the denatured Link protein. **A**. Denatured Link protein in 6 M guanidine HCl, 100 mM Tris-Cl at pH 8.0, and 100 mM DTT buffer was applied on a prep-grade C4 column using HPLC for initial refolding of the Link protein in acetonitrile/water mixture. The protein was subsequently lyophilized and reconstituted at 0.5 mg/ml concentration in 50 mM ammonium acetate buffer at 6.0 containing 100-fold molar excess β-mercaptoethanol. **B.** Circular dichroism spectrum of the refolded Link protein (0.1 mg/ml concentration) in PBS buffer.

A

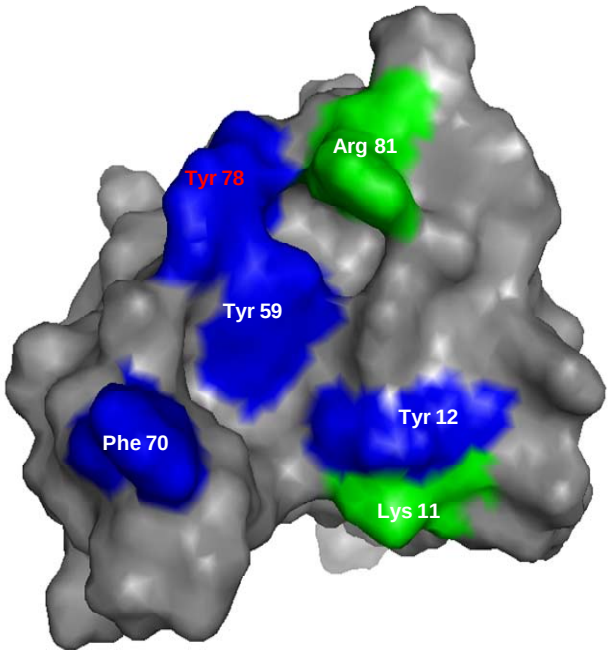

B

```
mtLink          GGATTTGGAAAAACTGGCATTATTGATGTGGGAATCCGTCTCAATAGGAGTGAAAGATGG
Link            GGATTTGGAAAAACTGGCATTATTGATTATGGAATCCGTCTCAATAGGAGTGAAAGATGG
                ***************************   ******************************
```

Figure 3-7. Site-directed mutagenesis on the Link domain to create a functional mutant. **A**. The structure of TSG-6 Link domain with the key binding residues determined by site-directed mutagenesis (Blundell et al). **B.** The Y78V mutagenesis on the Link domain was confirmed.

A functional mutant of the Link protein (Y78V) was created by site-directed mutagenesis (Figure 3-7). This mutation knocked-down hyaluronan binding kinetic (K_b) to 6% of the wild-type, which was determined by isothermal titration calorimetry (Mahoney et al 2001). However, this mutant protein was not expressed for further characterization studies.

3.4.2 Expression and Purification of LinkCD

The ORF of LinkCD was first constructed in pET41a containing an N-terminal GST-tag (Figure 3-8). This construct also contains a His-tag between the GST and Link domains, followed by a thrombin cleave site. The GST-tag was used to increase the yield of the LinkCD fusion protein from the soluble fraction of the *E.coli* cells (Smith and Johnson 1988). The GST-tagged LinkCD fusion protein was expressed in *E.coli* (Figure 3-9A). Although the yield of the purified protein was greater than 2 mg per liter culture of *E.coli*, most of the expressed protein was in the pellet fraction. Also, there was significant level of contaminant proteins that eluted together with the GST-tagged LinkCD fusion protein (Figure 3-9B). Thus, I was unable to obtain the fusion protein with reasonable purity using a GST-tag.

To see if I could obtain the LinkCD fusion protein with a purity greater than 70% by removing the GST-tag, the ORF of LinkCD was moved into pET15b, which contained only an N-terminal His(×6) tag followed by a thrombin cleavage site (Figure 3-10). Also, a $(Gly_4Ser)_3$ linker was added to provide a 15-residue long space between the two functional groups (Asai et al 2005). BL21-Codon Plus® (DE3)-RIPL *E.coli* cells were

used as a host to express the fusion protein. Most of the expressed proteins aggregated in the inclusion bodies (Figure 3-11A), in spite of efforts to increase accumulation of the soluble protein by lowering post-induction temperature while increasing the incubation time. The LinkCD fusion protein in the soluble fraction was purified using a HisTrap™ FF, a Ni^{2+}-NTA column.

3.4.3 Secondary structure of LinkCD

Circular dichroism scan of LinkCD was performed to examine if the purified fusion protein from the soluble fraction contains secondary structure. The spectrum of LinkCD in the far-UV range showed a significant alpha-helix signal between 210 nm and 222 nm, which confirmed that the purified protein is folded, and contains secondary structure (Figure 3-11B).

3.4.4 Measurement of the native Mw by size exclusion chromatography

To examine if the soluble LinkCD is a monomer, dimer, or aggregate, the purified protein was applied on a Sephacryl™ S-100HR size exclusion column (Figure 3-12A). The theoretical monomer sizes of LinkCD and CD are 32 kDa and 19 kDa, respectively. A calibration standard curve (Figure 3-12B) was used to calculate the apparent molecular weights of LinkCD and CD. LinkCD eluted at the retention volume corresponding to 45 kDa, which is between the sizes of monomer and dimer (32 and 64 kDa, respectively). The CD enzyme, which has been shown to form a dimer (Ireton et al 2003, and Ko et al 2003), eluted at the retention volume corresponding to 29 kDa. The apparent molecular weight of the CD enzyme is also between the sizes of its monomer and dimer (19 and 38

kDa, respectively), and it is close to the reported mass of native CD (31.4 kDa, with a His-tag) determined by size exclusion chromatography using a Superose™ column (Xiong and Kwon 2005).

3.4.5 Enzymatic activity of LinkCD

Using 5-FC as a substrate, the enzyme kinetics parameters for the conversion of 5-FC to 5-FU by LinkCD were measured at 37 ^{o}C. As shown in Figure 3-13, K_m and V_{max} values were 0.33 mM and 15 μM/min/μg, respectively, for the LinkCD fusion protein. These values were significantly different from the reported kinetics parameters for CD enzyme (Kievit et al 1999). The ratio of V_{max}/K_m, which is a good indicator for the efficiency of catalytic activity, was 53% of that ratio observed in CD. We also created Link-mtCD, a functional mutant that lacks cytosine deaminase activity. In the proposed catalytic scheme of CD enzyme described by Ko et al (2003), the negatively charged Glu 64 is a key residue in the active site of the enzyme to initiate the conversion of cytosine or 5-FC to uracil or 5-FU, respectively. Therefore, site-directed mutagenesis was performed to replace the Glu 64 residue with an Ala. The Link-mtCD fusion protein lacked enzyme activity as shown in Figure 3-14. The purified Link-mtCD fusion protein was used as a negative control in the *in vivo* anti-tumor experiment (Chapter 4).

3.4.6 Stability of LinkCD enzymatic activity

As the stability of CD is known to be limited at 37 ^{o}C (Kievit et al 1999, Xiong and Kwon 2005, Korkegian et al 2005), I thought it would be interesting to see if the Link moiety could increase the stability of the enzymatic activity of LinkCD. The LinkCD

fusion protein lost almost 45% of its enzymatic activity within the first hour of incubation (Figure 3-15A). However, the rate of activity loss after the first hour decreased, and after 24 hr incubation at 37 ^{o}C it LinkCD retained more than 20% of the initial activity. At 48 hr and 124 hr time points, the enzymatic activity of LinkCD decreased to about 12% and 6% respectively of its time zero activity (124 hr time point data is not shown on Figure 3-15A). In contrast, the activity of CD decreased rapidly at 37 ^{o}C, and retained only about 5% of initial activity after 24 hr. In the presence of hyaluronan (0.1 mg/mL) in PBS containing Ca^{2+} and Mg^{2+} after 24 hr incubation at 37 ^{o}C, LinkCD activity remained slightly higher than in the absence of hyaluronan (Figure 3-15B).

The thermal denaturation of the protein was examined by measuring circular dichroism at 222 nm as a function of increasing temperature (Figure 3-16A). The melting curve for LinkCD was shifted to the right of the CD enzyme melting curve: using the EXAM curve fitting software (Kirchhoff 1993), T_m for LinkCD fusion protein was calculated to be at 48 ^{o}C, whereas the T_m for the CD enzyme was 42 ^{o}C. Therefore, the LinkCD fusion protein is both functionally and structurally more thermostable than the CD enzyme. However, because there was significant deviation of the T_m for the CD enzyme from the reported T_m value (Korkegian et al 2005), I measured the T_m of the CD enzyme using differential scanning calorimetry (Figure 3-16B). The results show that the T_m of the CD enzyme is 52 ^{o}C, which agrees with the literature value reported in Korkegian et al (2005).

A

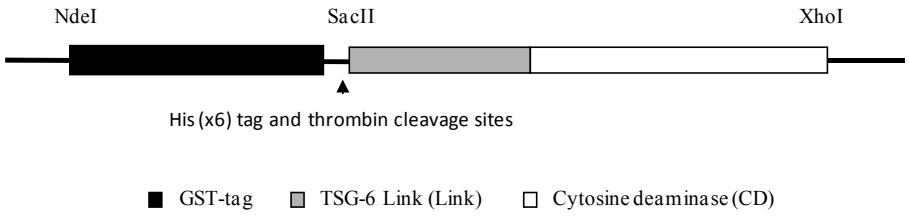

B

```
MSPILGYWKIKGLVQPTRLLLEYLEEKYEEHLYERDEGDKWRNKKFELGLEFPNLPYYIDGDVKLTQSMAIIRYIADKHNMLGG
CPKERAEISMLEGAVLDIRYGVSRIAYSKDFETLKVDFLSKLPEMLKMFEDRLCHKTYLNGDHVTHPDFMLYDALDVVLYMDPM
CLDAFPKLVCFKKRIEAIPQIDKYLKSSKYIAWPLQGWQATFGGGDHPPKSDGSTSGSGHHHHHHSAGLVPRGSGVYHREARSG
KYKLTYAEAKAVCEFEGGHLATYKQLEAARKIGFHVCAAGWMAKGRVGYPIVKPGPNCGFGKTGIIDYGIRLNRSERWDAYCYN
PHAKSSMVTGGMASKWDQKGMDIAYEEAALGYKEGGVPIGGCLINNKDGSVLGRGHNMRFQKGSATLHGEISTLENCGRLEGKV
YKDTTLYTTLSPCDMCTGAIIMYGIPRCVVGENVNFKSKGEKYLQTRGHEVVVVDDERCKKIMKQFIDERPQDWFEDIGE
```

Figure 3-8. pET41a bacterial expression vector containing GST-tagged LinkCD. A. The ORF region containing a N-terminal GST-tag followed by a thrombin cleavage site, the Link domain (gray), and CD enzyme (white). **B**. Translated protein sequence of the GST-LinkCD fusion protein from the ORF region.

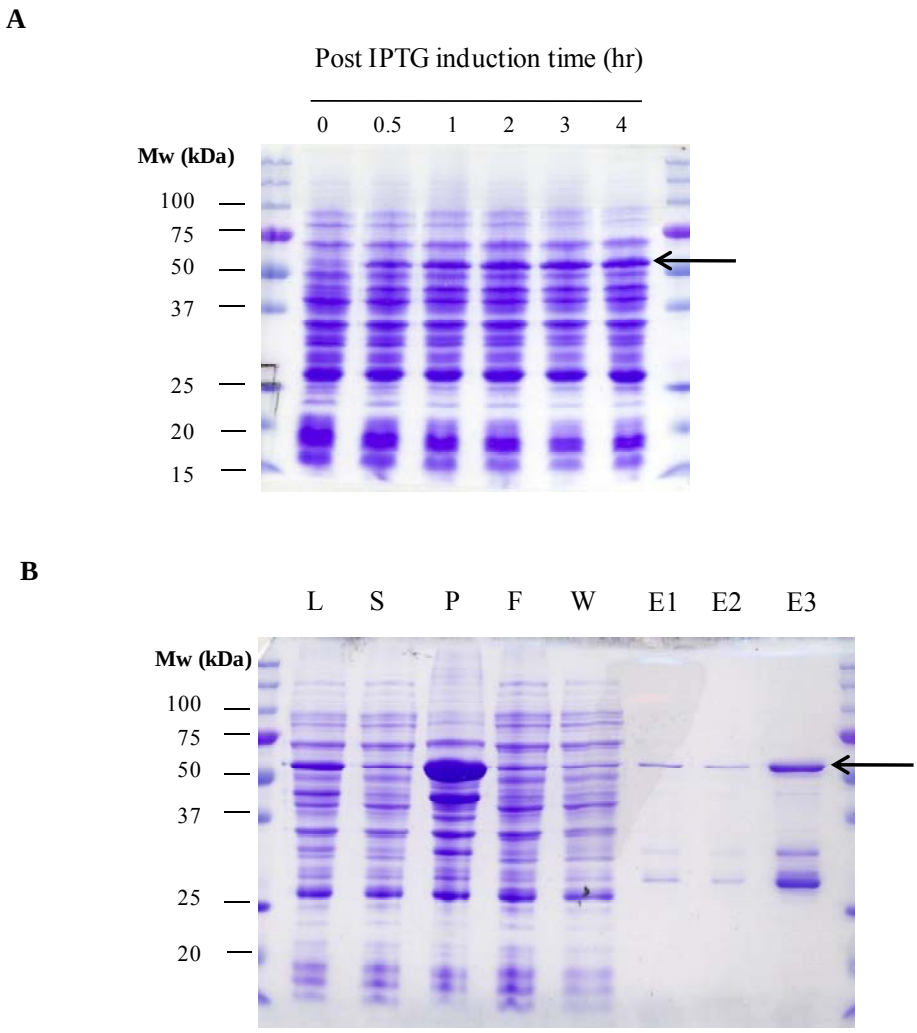

Figure 3-9. SDS-PAGE analysis of the GST-tagged LinkCD fusion protein (56 kDa) expression and purification. **A.** Expression of GST-tagged LinkCD in BL21-(DE3)-pLsS *E.coli* containing pET41-GST-LinkCD plasmid during IPTG induction at 37 ^{o}C. The expression of GST-LinkCD (indicated by the arrow) increases with the induction time. **B.** All fractions containing GST-LinkCD were collected. L: cell lysate, S: supernatant (soluble fraction after high-speed centrifugation), P: pellet (insoluble fraction containing the inclusion body proteins after high-speed centrifugation), F: flow-through from the affinity column, W: wash fraction, E: eluates (followed by the fraction number). Purified protein in E1 – E3 contained significant amount of contaminants.

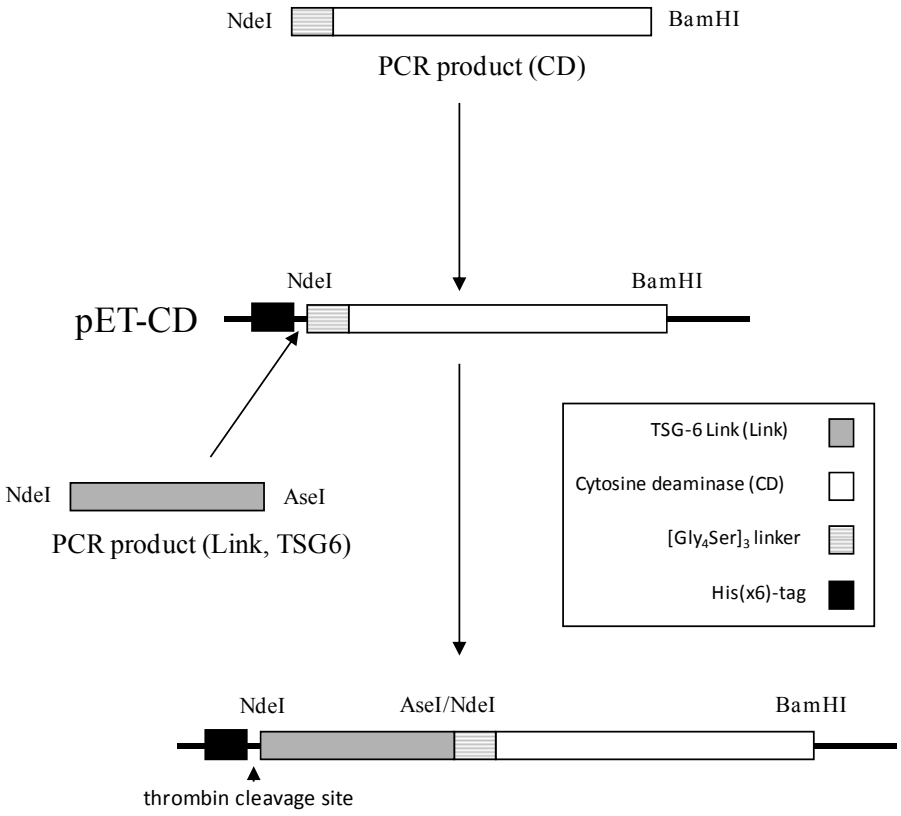

Figure 3-10. Construction of pET15-His-LinkCD. The ORF of LinkCD was inserted into pET15 vector containing the nucleotide sequence for an N-terminal His-tag followed by a thrombin cleavage site (LVPRGS) for the expression of protein in E.coli. Also, a flexible linker $[G_4S]_3$ was inserted between the Link domain and CD enzyme.

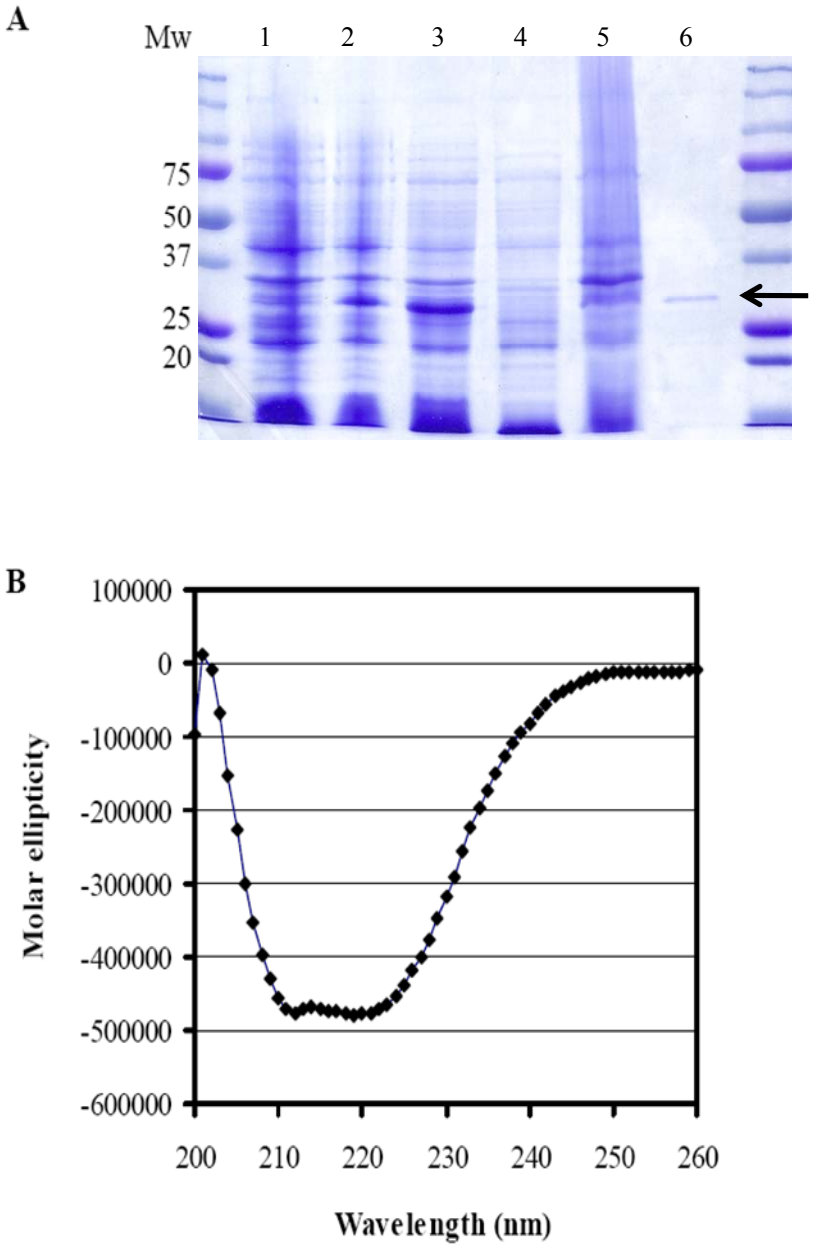

Figure 3-11. Purification of the LinkCD fusion protein. A. SDS-PAGE showing purified LinkCD from the soluble fraction. The expected mass of LinkCD under denatured condition is at 32 kDa. Cell lysate before (lane 1) and after (lane 2) IPTG induction. Lanes 3-6 were collected during protein purification steps: lane 3) cell lysate, 4) soluble fraction, 5) insoluble fraction, and 6) purified LinkCD (indicated by the arrow). **B**. Circular dichroism spectrum of purified LinkCD showing the secondary structure of the protein (Molar ellipticity: deg cm^2/dmol).

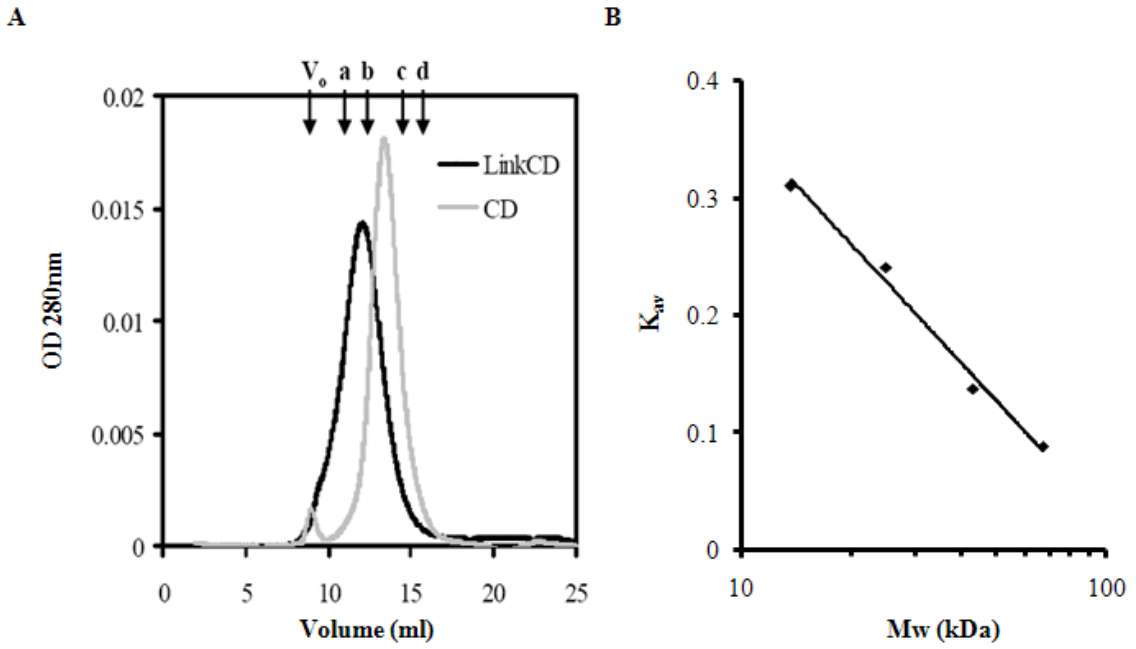

Figure 3-12 Determination of molecular weight of LinkCD. A. The chromatogram of LinkCD (black) and CD (gray) on Sephacryl S-100HR size exclusion column (100 kDa cut-off). The left shift of the retention volume suggests that LinkCD forms a dimer. The arrows indicate the void volume of the colume (V_o) and retention volumes of protein standards: a) albumin (67 kDa), b) ovalbumin (43 kDa), chymotrypsinogen A (25 kDa), and d) ribonuclease A (13.7 kDa) **B**. The calibration curve used to determine the molecular weights of LinkCD and CD enzyme. K_{av} is the gel-phase distribution coefficient. Mw is in log-scale.

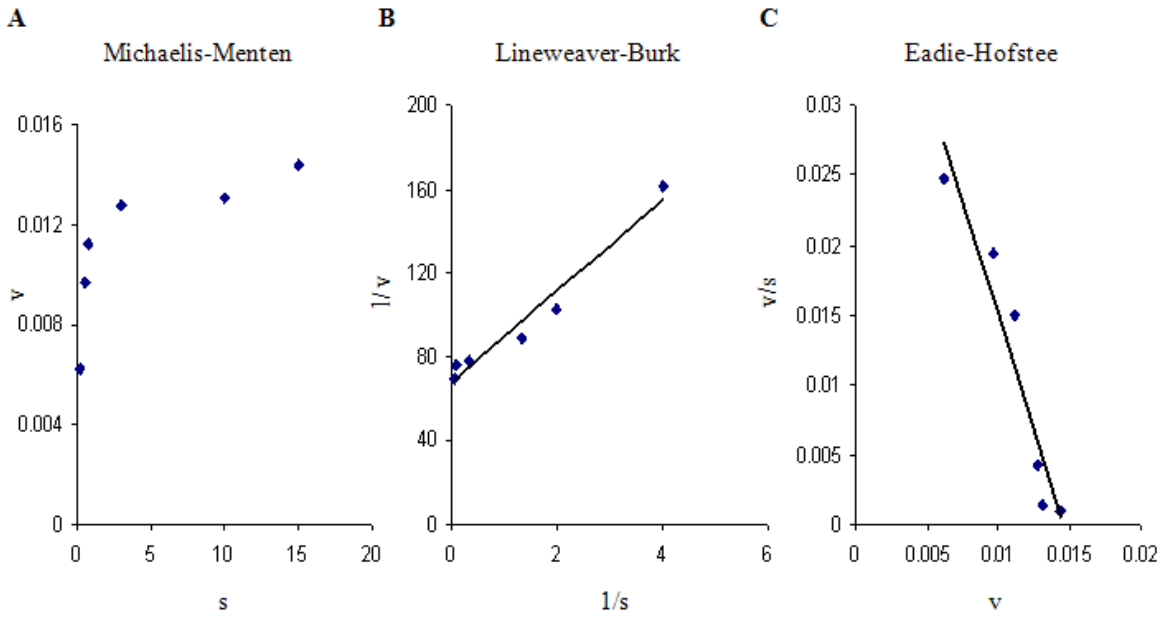

D

	LinkCD	CD*	CD**
K_m (mM)	0.33 ± 0.04	0.8 ± 0.2	0.78
V_{max} (μM/min/μg)	15 ± 1	67 ± 10	0.14

Figure 3-13. Enzyme activity of LinkCD. A. The Michelis-Menton plot shows the rate of 5-FC to 5-FU conversion by LinkCD with increasing 5-FC concentration (v: mM 5-FU/min/μg, s: mM). The analysis of enzyme kinetics by double-reciprocal plot (**B**) and Edie-Hoffstee plot (**C**). **D**. Summary table of the enzyme kinetic parameters for LinkCD (mean ± S.D) obtained from three independent experiments. * Reported kinetic parameters for CD enzyme (Kievit et al 1999). **The enzyme kinetics parameters that I determined for the CD enzyme (from Figure 3-3).

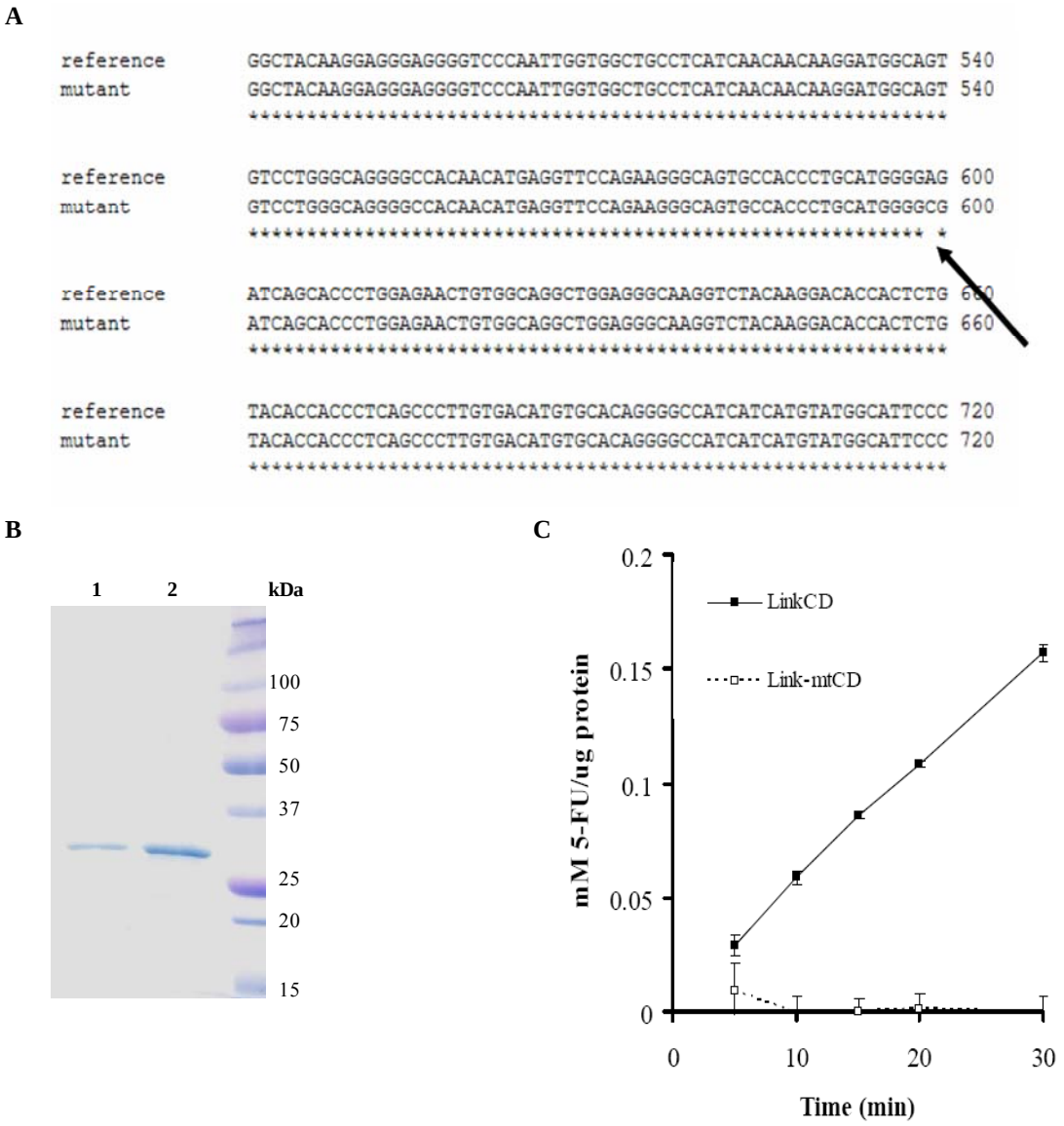

Figure 3-14. A functional mutant Link-mtCD lacks cytosine deaminase activity. A. Site-directed mutagenesis was performed to create a functional mutant of LinkCD that lacks enzymatic activity (E64A mutation on cytosine deaminase). The arrow indicates the point mutation. **B.** Purified LinkCD (lane 1) and Link-mtCD (lane 2) on SDS-PAGE, showing similar Mw. **C**. Enzyme assay shows that Link-mtCD (dotted line, open square) is unable to convert 5-FC to 5-FU.

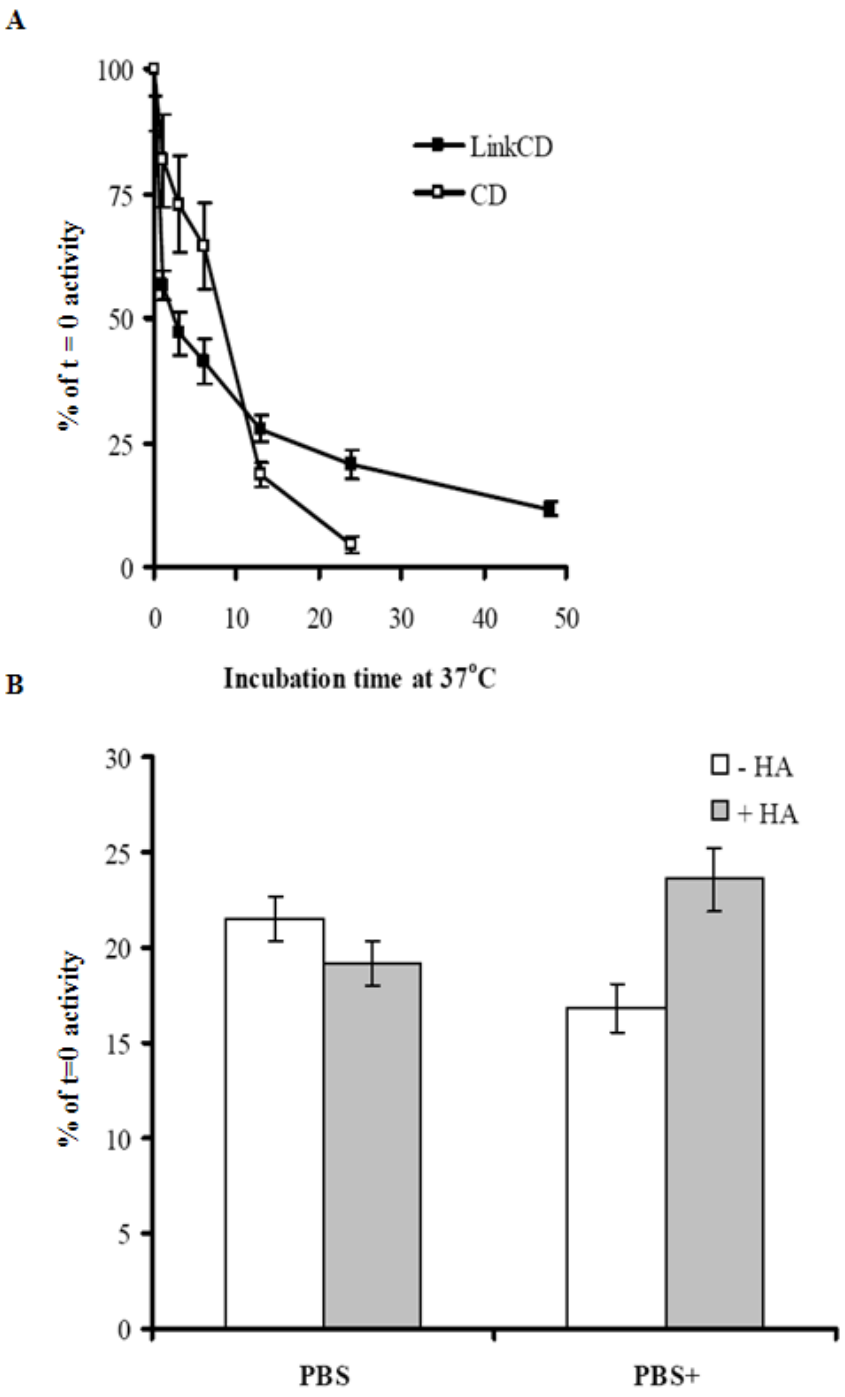

Figure 3-15. Stability of enzymatic activity at 37 °C. A. Enzyme activity as a function of time at 37 °C. An aliquot of 50 µg of purified protein in 1 ml of PBS was incubated at 37 °C for each time point. The enzymatic activities for all time points were normalized to the enzyme activity at the zero hr time point (mean ± propagated erro). **B.** Effect of hyaluronan and divalent cations (Ca^{2+} and Mg^{2+}) on the enzymatic function of LinkCD at 37 °C. Enzyme activity of LinkCD in the presence of 0.1 mg hyaluronan (HA). PBS+ contained Ca^{2+} and Mg^{2+} whereas PBS did not contain these divalent cations.

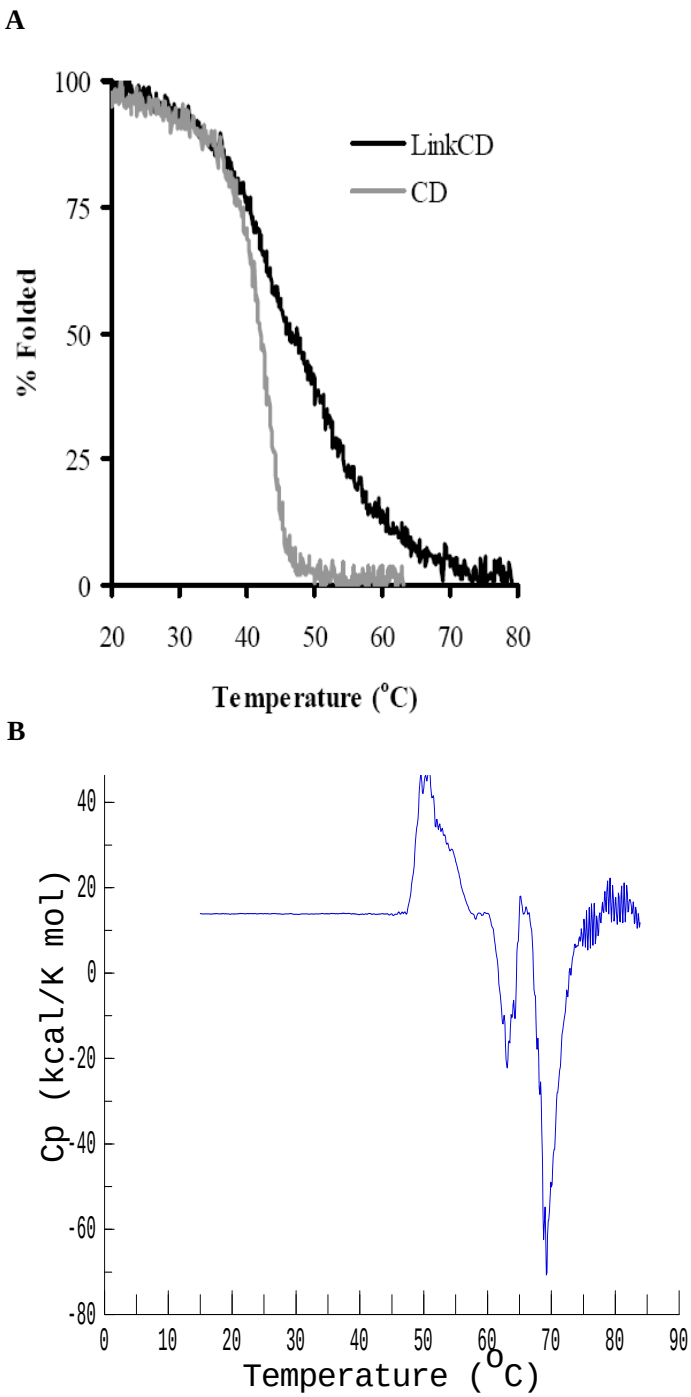

Figure 3-16. Determination of the melting temperature (T_m) of the LinkCD and CD enzyme. A. The melting curves of LinkCD and CD measured by circular dichroism at 222 nm. B. The melting temperature of the CD enzyme measured by differential scanning calorimetry (DSC). The maximum C_p (the heat capacity) was determined to be 52 °C.

3.4.7 Hyaluronan binding activity

The binding affinity of hyaluronan oligomers toward CD44 and TSG6 have been previously measured by either isothermal titration calorimetry (ITC) or surface plasmon resonance (SPR). The equilibrium binding constant (K_D) of the interaction between TSG6 Link and 12-mer hyaluronan was determined to be at 0.32 μM by ITC (Kahmann et al 2000). The K_D of the interaction between CD44 Link and 10-mer hyaluronan was determined to be at 50 μM by SPR (Banerji et al 2007). Both of these measurements were done at pH 6, which is the optimum pH for the interaction between the Link domain and hyaluronan. Since the ITC method generally requires milligrams of protein to detect binding kinetics (reviewed in Jelesarov and Bosshard 1999), I wanted to use the SPR method to measure the binding kinetics since it requires significantly less amount of the protein (micrograms or an order of magnitude more depending on the sensitivity of detection). In order to determine the affinity between hyaluronan and LinkCD by the SPR method, we needed to immobilize either hyaluronan or LinkCD on the surface of the SPR chip. A common strategy is to immobilize a biotinylated ligand or protein on a streptavidin chip. Streptavidin showed strong nonspecific interaction with both hyaluronan and LinkCD which interfered with the measurement of binding between hyaluronan and LinkCD (data not shown). To circumvent this problem, our laboratory developed a tri-NTA chip by modifying the commercially available CM5 chip with our recently reported tri-NTA reagent that has a much higher affinity toward His-tag than mono-NTA (Huang et al 2006). LinkCD can be reversibly immobilized on the tri-NTA chip through the His-tag without obvious dissociation when stabilized. The binding kinetics of 12-mer hyaluronan toward LinkCD at both pH 7.4 and 6.0 are shown in

Figure 3-17. The equilibrium affinity constant K_D at pH 6.0 is 5.32 μM which is about 10 times stronger than the K_D at pH 7.4 (55 μM). There was no detectable interaction between 8-mer hyaluronan and LinkCD at pH 7.4 though others have reported that a 6-mer hyaluronan can bind to TSG6 Link (Kahmann et al 2000). The summary of the binding kinetics between LinkCD and 12-mer hyaluronan is shown in Figure 3-17C.

3.5 Discussion

To provide material to test the MAT concept, a recombinant fusion protein LinkCD was constructed. The LinkCD fusion protein was designed to target hyaluronan in the extracellular matrix and convert 5-FC to 5-FU surrounding tumor cells. The rate of catalysis of 5-FC to 5-FU by LinkCD was significantly slower than the recombinant CD (Figure 3-13). Although we do not know the reason for the decrease in V_{max}, it is possible that the Link domain has a subtle influence on the mobility of the catalytic domains in CD; since the active site of CD is completely occluded by the C-terminal helix, the enzyme must relax to open the active site for a substrate to bind and its product to be released after enzymatic reaction (Ireton et al 2003, and Ko et al 2003). The K_m of 5-FC for LinkCD was lower than the K_m of 5-FC for CD (0.33 mM vs. 0.8 mM): this provides an advantage for LinkCD to generate 5-FU at lower concentrations of 5-FC. The enzymatic activity is retained at 37 °C for the LinkCD fusion protein longer than for CD, which is consistent with the observation that the secondary structure of LinkCD is more thermostable than CD.

A

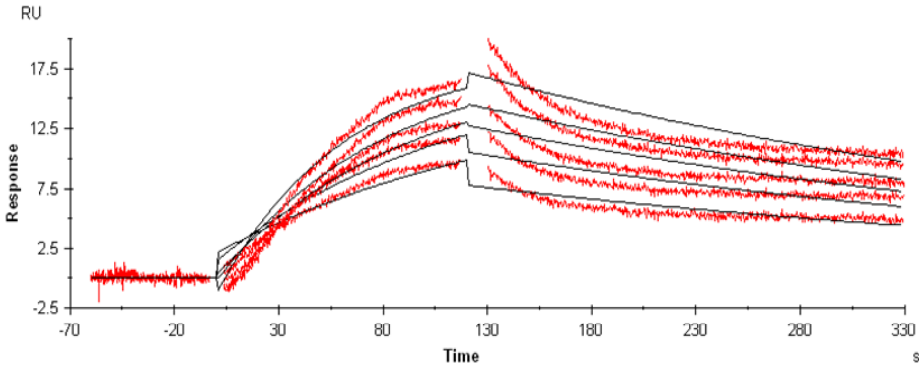

B

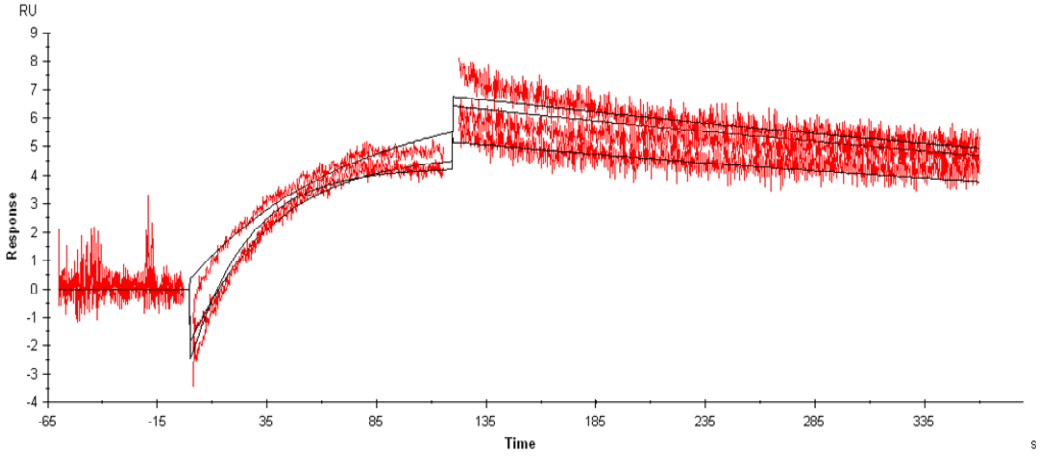

C

pH	k_a ($M^{-1}S^{-1}$)	k_d (s^{-1})	K_D (M)	Chi^2
6.0	246.06	0.0013	5.32E-6	0.168
7.4	49.35	0.0027	5.50E-5	0.705

Figure 3-17. **The binding kinetics between LinkCD and hyaluronan (12-mer) measured by SPR.** **A**. The detection of ligand binding and dissociation at pH 7.4. LinkCD was coated on the surface of a tri-NTA chip. The kinetic measurements were done by flowing 12-mer hyaluronan to interact with LinkCD. **B**. The detection of ligand binding and dissociation at pH 6.0 with 12-mer hyaluronan. **C**. Summary table shows the association constant (k_a) , dissociation constant (k_d), and overall binding constant (K_D). Chi^2 values represent the deviation of experimental values from fitted curve.

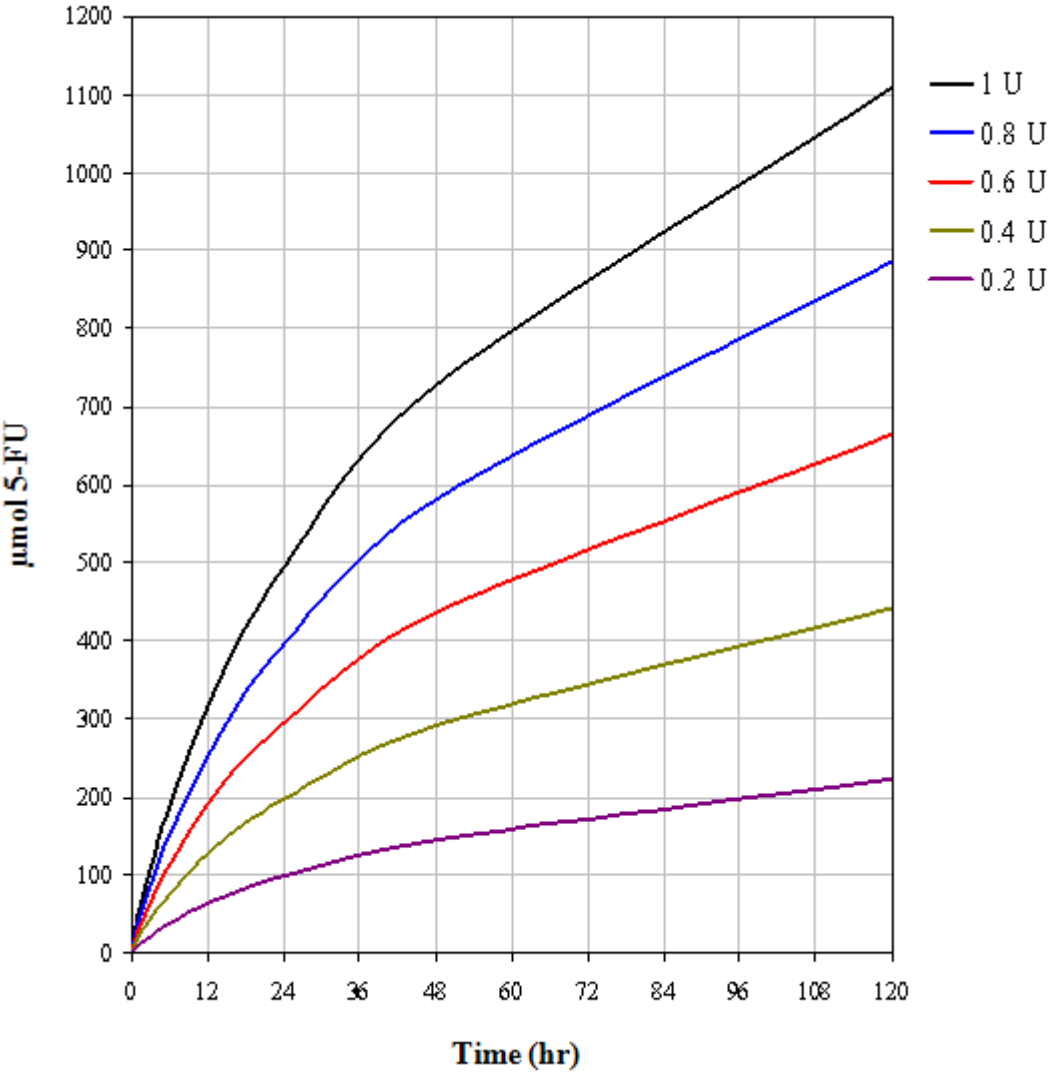

Figure 3-18. **Simulated time-course of production of 5-FU by LinkCD at 37 °C.** This model represents theoretical amount of 5-FU generation by LinkCD in the tumor in the presence of 5-FC prodrug, assuming that 1) the steady-state concentration of 5-FC is unchanged, 2) there is no product inhibition, 3) there is no other mechanism of protein degradation *in vivo*, and 4) 5-FU accumulates in the tumor without elimination. The calculations were based on the enzyme activity data of LinkCD at 37 °C. This plot can serve as a starting point for optimizing dosing schedules for LinkCD/5-FC combination treatment. 1 U (unit) is defined as the amount of protein that can generate 1 µmol of 5-FU in 1 min.

Based on the stability of enzyme activity of the LinkCD fusion protein at 37 °C, a model representing a time-dependent production of 5-FU *in vivo* was plotted using the following assumptions: 1) 5-FC is at a steady-state concentration, 2) there is no significant level of product inhibition, 3) there is no other mechanism for deactivating the enzyme function, 4) and 5-FU is not eliminated from the site. The AUC of the stability curve (Figure 3-15A) was used to calculate the accumulation amount of 5-FU by LinkCD (Figure 3-18). Although the actual amount of 5-FU generated *in vivo* could be significantly less than the calculated amount, this model could serve as a rough estimate of the amount of 5-FU generated.

The LinkCD protein retained the ability to bind hyaluronan. The affinity for a hyaluronan oligomer (12-mer) at pH 6.0 was 5.32 μM. The affinity of the LinkCD for 12-mer hyaluronan at pH 7.4 was an order of magnitude weaker (55 μM). This is an advantage for delivery of the LinkCD via the circulation since hyaluronan affinity at pH 7.4 will be low but will increase at the lower pH values found in tumors (reviewed by Gerweck 1998). This low binding affinity of LinkCD for hyaluronan at pH 7.4 will reduce the likelihood that plasma hyaluronan will occupy the Link domain during the delivery phase to obstruct LinkCD binding to the tumor matrix, or to cause LinkCD to be rapidly eliminated via hyaluronan receptor for endocytosis (HARE) in the liver.

The size exclusion chromatography results show that the LinkCD elutes between where the monomer and dimer would elute. This has previously been found to be the case for the CD enzyme, which also elutes from a sizing column between the expected monomer

and dimer masses (Xiong and Kwon 2005). It may be that the dimeric protein is more compact than the proteins used to calibrate the column so it would elute in a larger volume than expected.

One of the factors impeding the development of ADEPT is the low production levels of therapeutic proteins containing antibody fragments originating from mammalian cells using bacterial expression system (Deckert et al 2003, and Asai et al 2004). The low yield of the soluble LinkCD fusion protein from *E.coli* was also a significant challenge for this study. Yeast CD enzyme is readily expressed as soluble protein in *E.coli* with a yield of least 30 mg per liter of culture (Ireton et al 2003, and Ko et al 2003, and Huang et al 2006). However, the Link domain of human TSG-6 was found to be toxic to the host *E.coli* cells and could only be expressed as an inclusion body protein (Day et al 1997). The Link domains from both TSG-6 and CD44 were recovered from the inclusion bodies after denaturation and refolding steps with yields of 10–20 mg per liter culture medium (Day et al 1996, Kahman et al 1997, and Banerji et al 1998). A TSG-6Link-luciferase fusion protein was expressed and purified from the inclusion bodies with a yield of 75 mg per liter culture medium (Chang et al 2003).

I observed that the majority of LinkCD was in the inclusion bodies, but a sufficient quantity of the functional LinkCD was recovered from the soluble fraction to avoid a refolding step in purification. Recovery of the LinkCD might have been aided by the soluble nature of the CD enzyme.

A

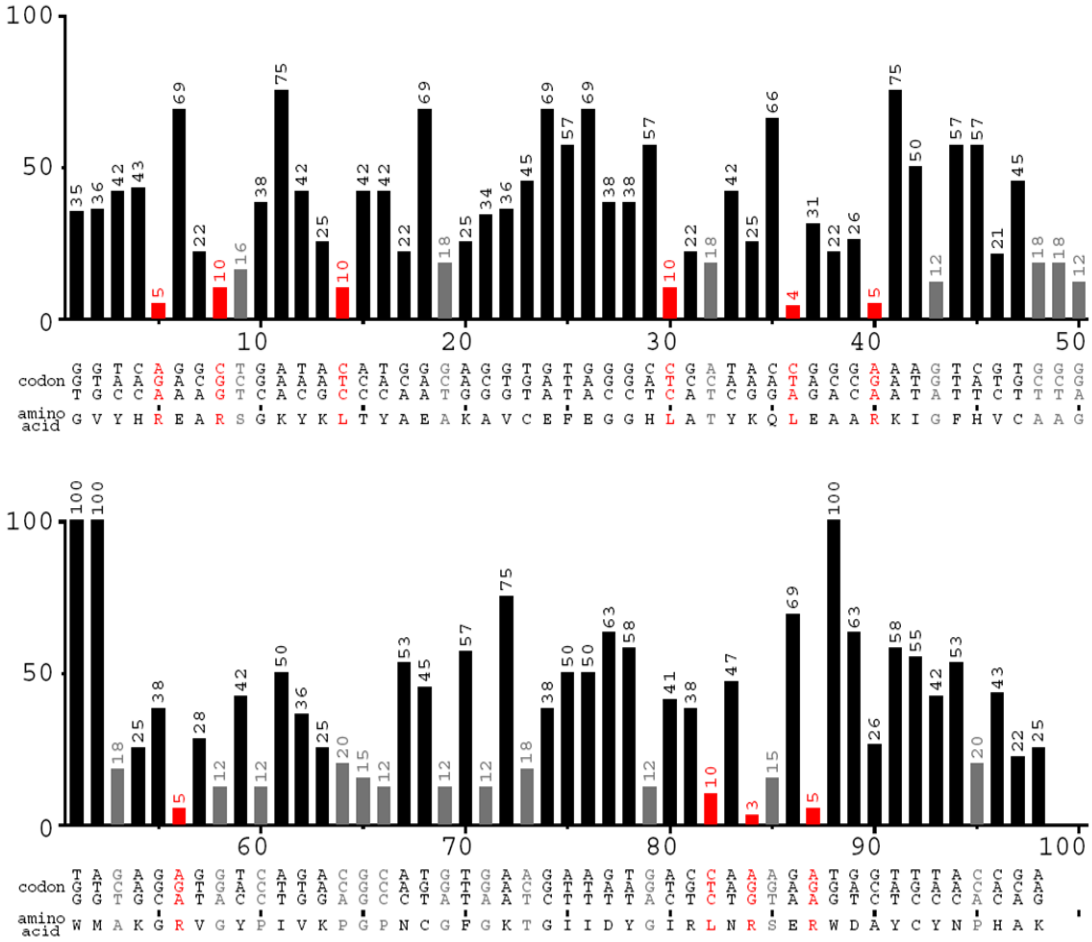

Figure 3-19. Statistical analysis of the codon usage in *E.coli* to identify rare codons in the nucleotide sequence of the ORF of TSG-6 Link and CD. A. The ORF of TSG-6 Link. 10 codons were found to be at or below 10% of usage (indicated by red). 19 additional codons were between 10 to 20% of usage (indicated by gray). **B.** The analysis of the ORF for the CD enzyme (next page). 11 codons were at or below 10% of usage, and 22 codons were semi-rare codons between 10 to 20% of usage. The analysis was performed using Graphical Codon Usage Analyzer version 2.0 (http://gcua.schoedl.de/)

B

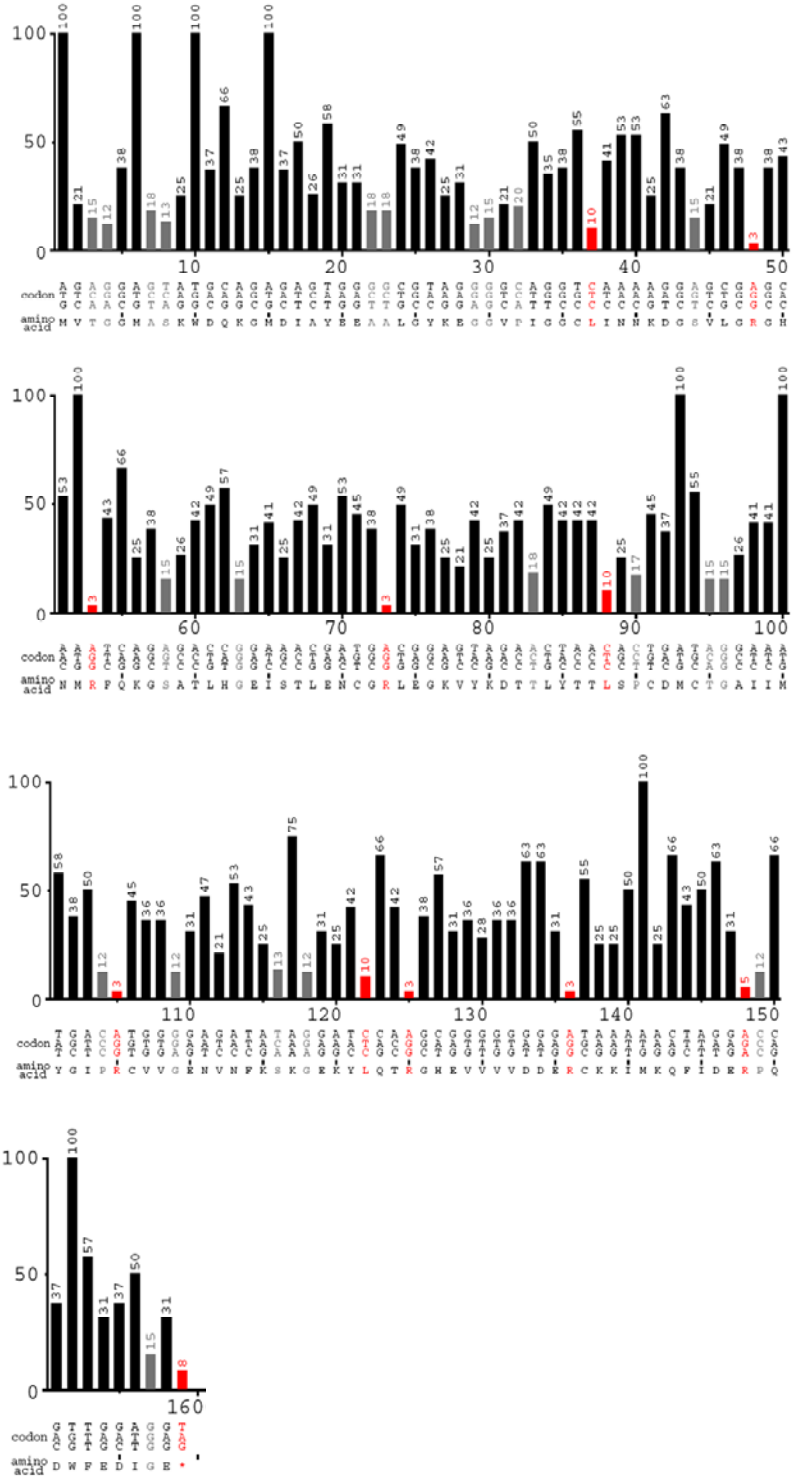

The nucleotide sequences of the Link and CD enzyme were analyzed to see how many rare codons are present in each ORF based on the codon usage of *E.coli* (Figure 3-19). The ORF of Link contained 10 rare codons (out of 98 total), which represent the codons that are used less than or equal to 10% of usage. Moreover, 22 codons were semi-rare codons, which fall between 10 to 20% of usage. Thus, one in three codons in the ORF of Link protein was either rare or semi-rare codons. For CD enzyme, there were 11 rare codons and 22 semi-rare codons. Although I was able to obtain sufficient amounts of Link protein and CD enzyme separately, it may be worthwhile to optimize the codons in the ORF of LinkCD and see whether such modification could improve the expression and yield of the LinkCD fusion protein.

3.6 Conclusions

The LinkCD fusion protein was designed to target hyaluronan and convert 5-FC to 5-FU. I characterized the enzymatic and hyaluronan binding activities of the LinkCD fusion protein. The enzyme activity of LinkCD was retained longer than that of CD at 37 ^{o}C in PBS. The affinity of LinkCD for hyaluronan was significantly greater at pH 6 than at pH 7.4, which is consistent with the affinity of the Link domain of TSG-6 for hyaluronan reported in the literature. Thus, an expression plasmid containing the LinkCD gene was constructed, and LinkCD protein was successfully expressed, purified and characterized.

3.7 Credits

1. SPR measurement of the interaction between LinkCD and hyaluronan was obtained by Dr. Zhaohua Huang. He also synthesized tri-NTA.
2. Hyaluronan oligomers were purified by Virginia M. Platt.
3. The site-directed mutagenesis primers for mtCD and Link-mtCD (primers [13] and [14]) were designed by Jennifer S. Yokoyama.

CHAPTER 4

Anti-Tumor Effect of LinkCD/5-FC Combination Therapy on C26 Murine Colon Adenocarcinoma Tumor Bearing Balb/c Mice

4.1 Abstract

To evaluate the anti-tumor effect of LinkCD/5-FC combination therapy *in vivo*, mice received intratumoral injections of LinkCD on days 11 and 14 after C26 tumor implantation and given drinking water that contained 10 mg/mL of 5-FC starting on day 11. To examine if the Link domain by itself was able to reduce tumor growth, treatment groups that received LinkCD without 5-FC and Link-mtCD (a functional mutant that lacks cytosine deaminase activity) with 5-FC were included. Animals that received LinkCD/5-FC treatment showed significant tumor size reduction and increased survival compared to the CD/5-FC treatment group. Treatment groups that were unable to produce 5-FU had no effect on the tumor growth despite receiving the fusion protein that contained the Link domain. A treatment group that received an intravenous administration of LinkCD with 5-FC resulted in no anti-tumor effect on the tumor growth. The results strongly suggest that a treatment regime consisting of a fusion protein containing the Link domain, the active CD enzyme, and the prodrug 5-FC are required to produce an anti-tumor effect.

4.2 Introduction

Antibody-directed and gene-directed enzyme prodrug therapies have not been yet successful in the clinic for cancer treatments, in spite of many promising preclinical animal studies of ADEPT and GDEPT over the past two decades using a variety of enzyme-prodrug combinations (Chapter 1). The matrix-attachment therapy (MAT) strategy was conceived to overcome major impediments of ADEPT and GDEPT that limit the application of enzyme-prodrug strategy for cancer therapy. To test a proof-of-concept of MAT, the LinkCD fusion protein was designed to target the extracellular matrix of solid tumors and convert a non-toxic prodrug 5-fluorocytosine (5-FC) into 5-fluorouracil (5-FU) in the vicinity of the tumor cells (Chapter 3). The LinkCD fusion protein contains the hyaluronan binding domain of TSG-6 (Link) and yeast cytosine deaminase (CD). The bi-functional recombinant fusion protein was expressed in *E.coli* and purified from the soluble fraction as a native protein. The purified LinkCD fusion protein was able to convert 5-FC to 5-FU, with K_m at 0.33 mM and V_{max} at 15 μM/min/μg (Figure 3-7). The hyaluronan binding activity of LinkCD was also confirmed by surface plasmon resonance (SPR) at both pH 7.4 and pH 6 (Figure 3-11). Thus, the functions of purified LinkCD fusion protein were well characterized *in vitro*.

In this chapter, *in vivo* efficacy of LinkCD/5-FC was examined using C26 murine colon adenocarcinoma model in Balb/c mice. Purified proteins were injected directly into the tumors, and the prodrug 5-FC was given in the drinking water (Figure 4-1).

4.3 Methods

4.3.1 Protein preparation for intratumoral injections

The enzyme activity of either LinkCD or CD was measured one day prior to the first intratumoral injection on day 11 to determine the amount of protein to be used for each animal. Enzyme assays were performed as described in Chapter 3 with 5 mM 5-FC and 5 μg of LinkCD or 1 μg of CD. Since the yield of LinkCD was relatively low, the enzyme activities of different batches were measured separately to make sure that only the active LinkCD was used for the animal studies. The concentration of 5-FU in the reaction mixture was measured at 10, 20, and 30 min time points to determine the specific activity. The batches that exhibited greater than or equal to 10 μM 5-FU/min/μg were pooled together and concentrated using 10-kDa cutoff Amicon® Ultra Centrifugal Filter Unit (Millipore; Billerica, MA). Then the enzyme activity of the concentrated protein was measured again. One unit was defined as the amount of protein that can generate 1 μmol of 5-FU in 1-mL reaction solution containing 5 mM 5-FC. All proteins used for animal studies were chromatographed on Detoxi™ Gel polymixin B column (Pierce; Rockford, IL) to remove endotoxin prior to injections. The removal of endotoxin was confirmed by measurement of endotoxin level using Limulus Amebocyte Lysate Kit (Cambrex Bio Science; Walkersville, MD). All proteins chromatographed on the polymixin B column contained less than 1 endotoxin unit per mg protein.

4.3.2 In vivo anti-tumor experiment using C26 tumor model

The C26 murine adenocarcinoma model in female Balb/c mice was used for anti-tumor studies. Six to eight week old female Balb/c mice were purchased from Charles River

Laboratories (Wilmington, MA). All animals were housed in the UCSF Animal Facility under strict protocols recommended by the National Institute of Health Guide for the Care and Use of Laboratory Animals, and approved by the UCSF Institutional Animal Care and Use Committee. C26 cells were obtained from UCSF Cell Culture Facility, and were cultured in RPMI-1640 medium containing 10% FBS. To implant tumors in mice, 3×10^5 cells in 50 µl volume were injected subcutaneously on the shaved right flank of each mouse. On day 11 after tumor implantation, each mouse received 0.2 units of either purified LinkCD or CD via intratumoral injection. On the same day, drinking water was replaced with water containing 10 mg/mL 5-FC until day 30. 5-FC water was replaced every two days. Also, the amount of 5-FC intake was monitored by weighing the water bottles every two days. Three days after the first dose, the animals were given a second dose of the protein, 0.6 units per mouse (day 14). The tumor sizes and body weights were measured every 2–3 days. Tumor volume (cm^3) was calculated by 0.5 × height (cm) × width (cm) × length (cm).

4.3.3 Statistics

Statistical analysis was performed using MedCalc Software version 9.1.0.1 (Belgium). To find statistically significant tumor size reduction, one-way ANOVA and Student-Newman-Keuls pairwise comparisons were performed using tumor volume data from all treatment groups. Survival data was analyzed by the log rank test and a p value < 0.05 was considered significant.

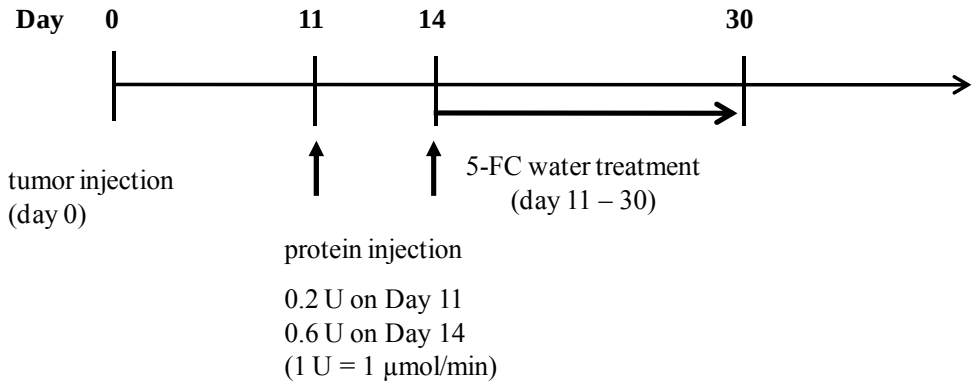

Figure 4-1. Overview of treatment plan for anti-tumor experiment using C26 tumor bearing mice. C26 tumor cells were implanted on day 0. On day 11 0.2 units (U) of either LinkCD or CD was injected into the tumor. Drinking water containing 10 mg/mL of 5-FC was given starting on day 11 until day 30. On day 14, a second dose of either LinkCD or CD (0.6 U) was injected into the tumor. For PBS control, the same volume of PBS was injected into the tumor.

4.4 Results

4.4.1 Anti-tumor effect of LinkCD/5FC on C26 tumor bearing mice

Under the hypothesis of MAT, the LinkCD fusion protein should be retained in the extracellular matrix of tumor because it can bind to hyaluronan, and in the presence of 5-FC, generate 5-FU to kill surrounding tumor cells. To test this hypothesis I examined if the LinkCD induced a better therapeutic effect than CD when injected into the C26 murine colon adenocarcinoma in female Balb/c mice. Two intratumoral injections of LinkCD, CD, or PBS were given: the first injection on day 11 and the second on day 14. 5-FC was administered in the drinking water starting on day 11 for 30 days.

The LinkCD/5-FC treatment was able to reduce tumor growth for 3 out of 5 mice (Figure 4-2A). One of the mice in this group that had low tumor volume was sacrificed due to severe weight loss (Figure 4-2B). However, in the CD/5-FC and PBS/5-FC treatment groups there was no noticeable effect on tumor progression. The mean tumor volume of the mice treated with LinkCD/5-FC was significantly lower than CD/5-FC and PBS/5-FC controls ($p < 0.05$ on days 20–24, Figure 4-3A). The absence of an effect of CD enzyme is most likely due to a rapid elimination of CD from the tumor site; CD lacks a matrix binding domain and was probably not retained in the vicinity of the tumor. As shown in Figure 4-4B, the survival of LinkCD/5-FC treatment group animals was significantly better than the groups that received either CD/5-FC or PBS/5-FC ($p < 0.025$ for both comparisons by log rank test). The median survival time for LinkCD/5-FC group was 45 days with 40% long-term survivors, whereas those of CD and PBS control groups were 28 and 26 days, respectively.

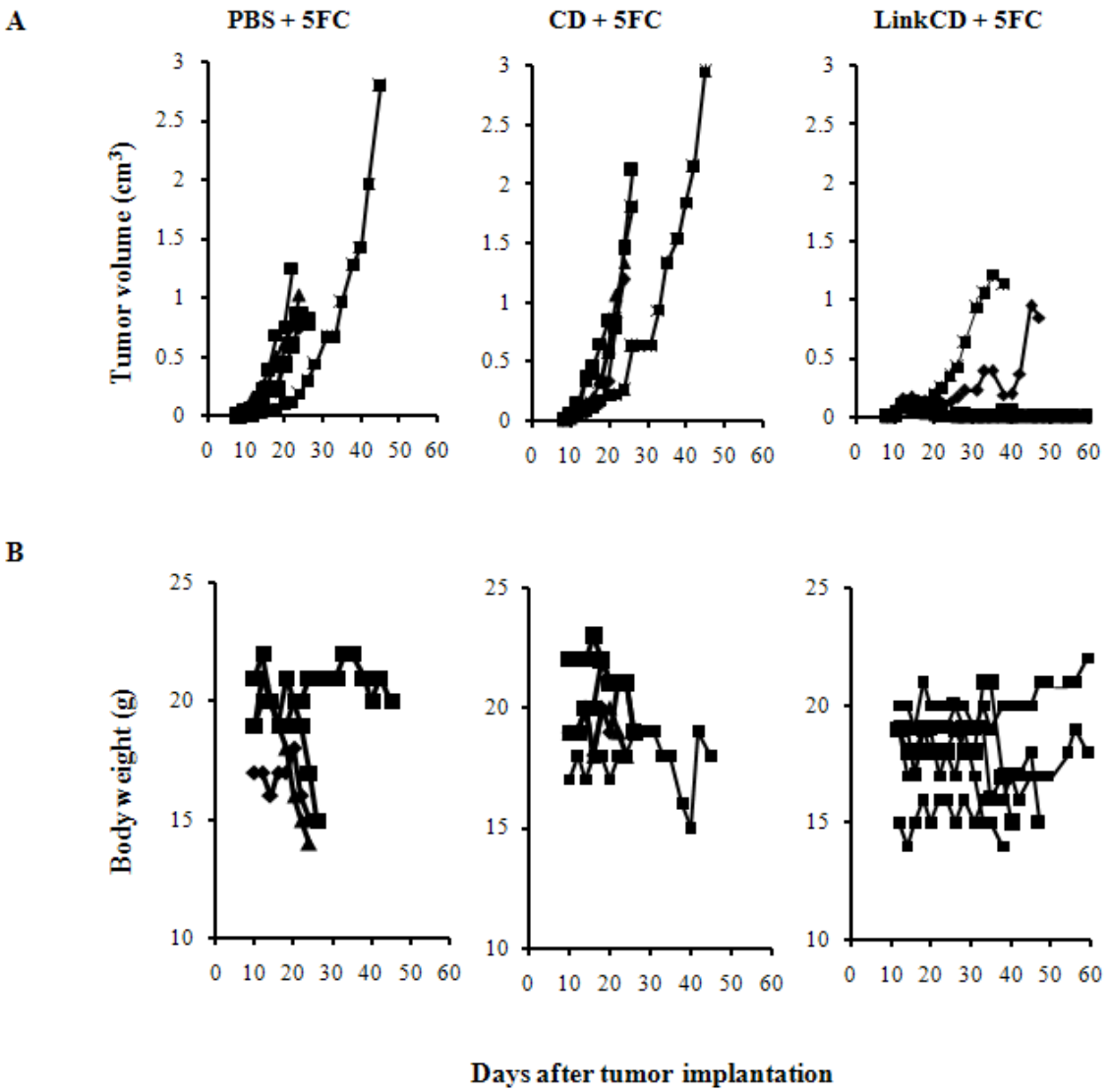

Figure 4-2. Individual tumor growth and bodyweight measurements of C26 tumor bearing mice. A. Tumor growth curves show that LinkCD was able to reduce tumor growth in the presence of 5-FC, whereas CD and PBS with 5-FC did not show anti-tumor effect. **B**. The body weights of individual mice show that most of the mice lost weight with increasing tumor volume.

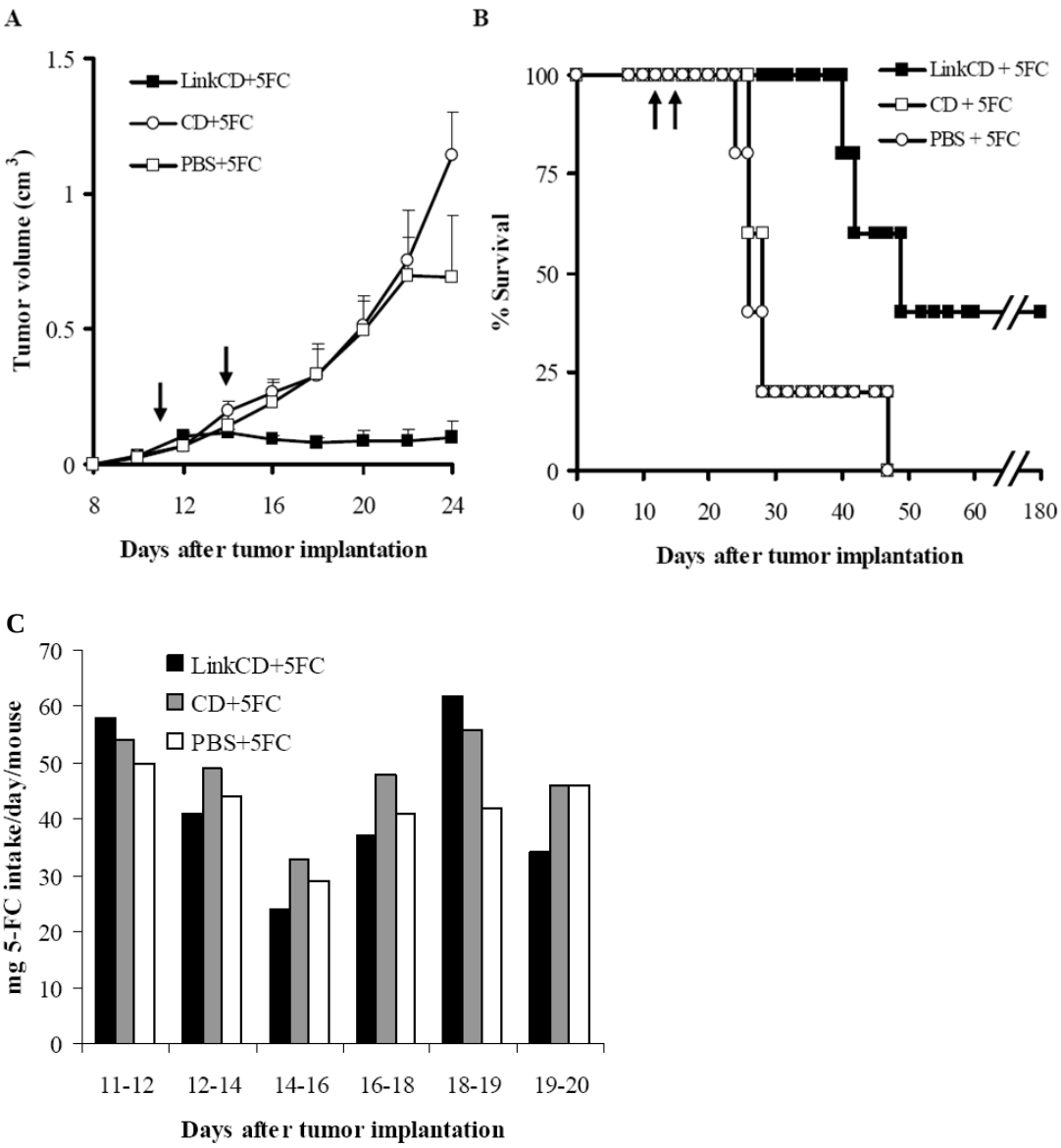

Figure 4-3. Anti-tumor effect of LinkCD/5-FC treatment on C26 tumor bearing mice. **A**. Average tumor volumes (n ≥3 mean ± SEM). Tumor volumes were significantly reduced by LinkCD/5-FC treatment (p <0.05, days 20 – 24). **B**. Survival curve for LinkCD, CD, and PBS groups that received 5-FC in drinking water. The survival of the animals in the LinkCD/5-5FC treatment was statistically significant over that of the other treatment groups (p < 0.025) with 40% long-term survivors. The arrows indicate the injection time points (day 11 and day 14). **C**. The amount of 5-FC consumption was estimated by weighing 5-FC containing water bottles (10 mg/mL).

Several groups have published that the disruption of the extracellular matrix-tumor cell interaction through competition between cell surface CD44 and soluble CD44 or hyaluronan binding peptides for the hyaluronan in the matrix, inhibits tumor growth (Peterson et al 2000, Ahrens et al 2001, Mummert et al 2003, and Xu et al 2003). These observations raised the possibility that the Link domain could be responsible for the anti-tumor effect. To examine whether the Link domain contributed to the anti-tumor effect, the *in vivo* experiment was repeated with two treatment groups that contained the Link domain but could not generate 5-FU: 1) LinkCD with no 5-FC in drinking water and 2) Link-mtCD with 5-FC in the drinking water. Link-mtCD fusion protein is a functional mutant that lacks cytosine deaminase activity (Figure 3-8). There was no tumor growth reduction observed in any groups that were unable to generate 5-FU (Figure 4-4A). There was also no tumor growth inhibition in animals that received LinkCD via the intravenous route and 5-FC in the drinking water. Three of the five mice in the LinkCD/5FC treatment group had severe weight loss despite having relatively small tumor volumes at the time of deaths (Figure 4-4B), possibly due to treatment-related toxicity or dehydration. Nonetheless, the animals treated with LinkCD/5-FC treatment had a significantly reduced tumor progression ($p < 0.05$ for days 16–20, and 24–32) and 40% long-term survivors (Figures 4-5A), which demonstrated that the anti-tumor effect of LinkCD/5-FC is reproducible. The median survival time for the LinkCD/5-FC group in the repeat experiment was 36 days, which did not reach the $p < 0.05$ significance level for survival when compared to all other treatment groups. However the survival data, when combined from the two experiments for the LinkCD/5-FC treatment groups (n=10), is highly significant when compared to the survival data combined from the LinkCD and

Link-mtCD/5-FC treatment groups that could not generate 5-FU ($p < 0.002$, with n=10). The consistency of the results in the two experiments strongly suggests that the tumor regression is only observed when three conditions are present: 1) the Link, a hyaluronan binding protein, 2) active CD enzyme that converts prodrug 5-FC to cytotoxic 5-FU, and 3) the prodrug 5-FC. Absence of any one of these conditions did not result in a tumor reduction or lead to long-term survival for C26 tumor bearing mice.

4.5 Discussion

MAT for cancer is based on the hypothesis that the generation of cytotoxic drug in the extracellular matrix of a tumor can effectively eradicate nearby cancerous cells. This strategy is fundamentally different from ADEPT: 1) there is no heterogeneity in the target site; 2) the level of hyaluronan in the tumor does not need to be significantly higher than hyaluronan in normal tissue because the fusion protein is either administered into the tumor site or reaches the site via the enhanced permeability and retention phenomenon, an effect that is not present in normal tissues; 3) hyaluronan, the target for MAT is more accessible than the tumor-specific antigen on the cell surfaces of tumors; 4) there are more binding sites available on the hyaluronan matrix than for most, if not all, tumor antigens; 5) the tumor is unlikely to down regulate or shed the matrix. MAT for cancer has the potential to overcome many of the limitations of ADEPT, which are the heterogeneity of the cancer specific antigen that may compromise the binding of the designed antibody, the limited number of available binding sites on the cancer cell surface, and the internalization of the antibody-enzyme conjugate into the tumor cells.

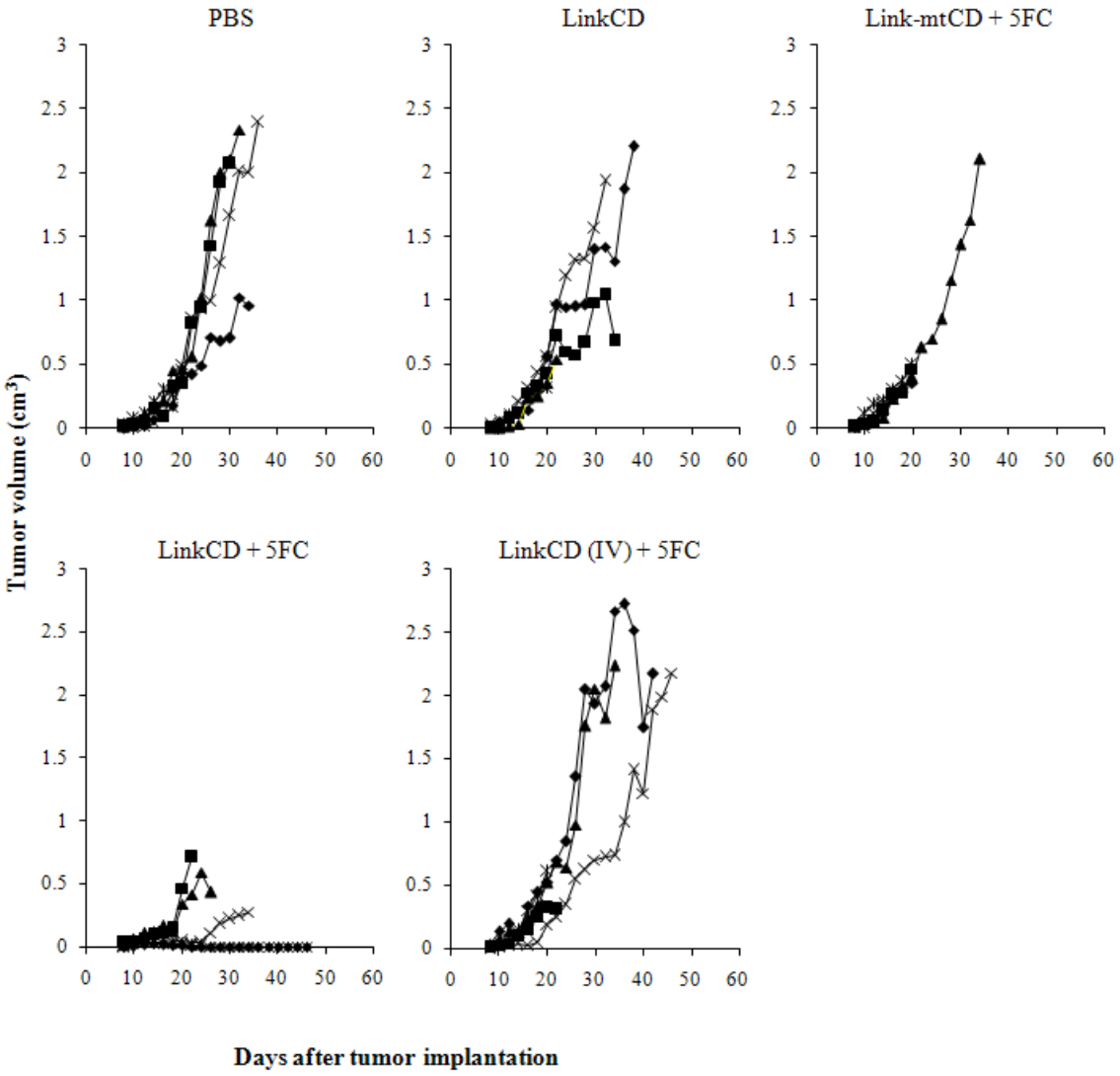

Figure 4-4. Individual tumor growth and bodyweight measurements of C26 tumor bearing mice. A. Tumor growth curves show that the treatment groups that were unable to produce 5-FU did not have anti-tumor effect. The anti-tumor effect of LinkCD/5-FC was reproducible. **B**. The body weights of individual mice show that most of the mice lost weight with increasing tumor volume (next page). The three mice in the LinkCD/5-FC treatment group died due to severe weight loss, despite having relatively small tumor volumes.

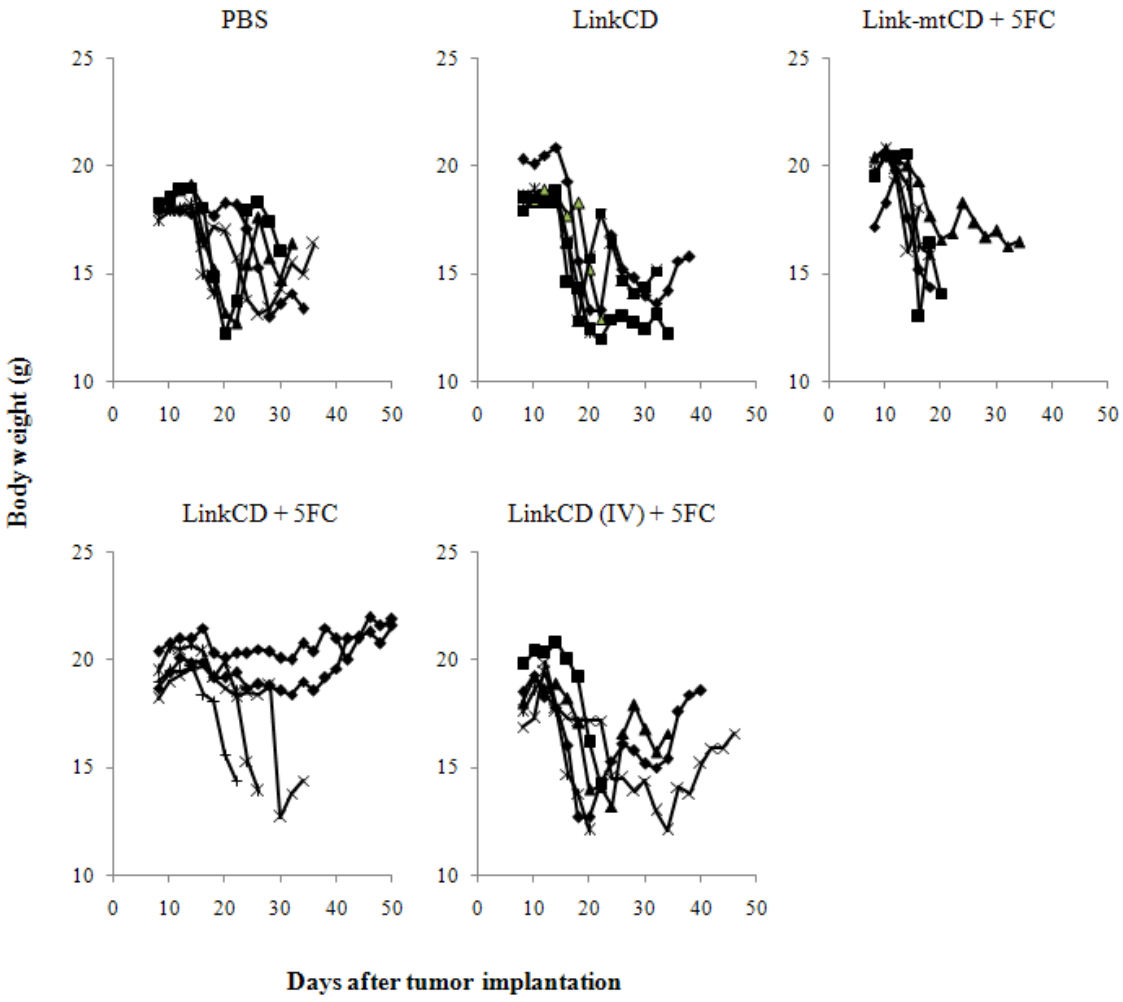
PBS
LinkCD
Link-mtCD + 5FC
LinkCD + 5FC
LinkCD (IV) + 5FC
Body weight (g)
Days after tumor implantation

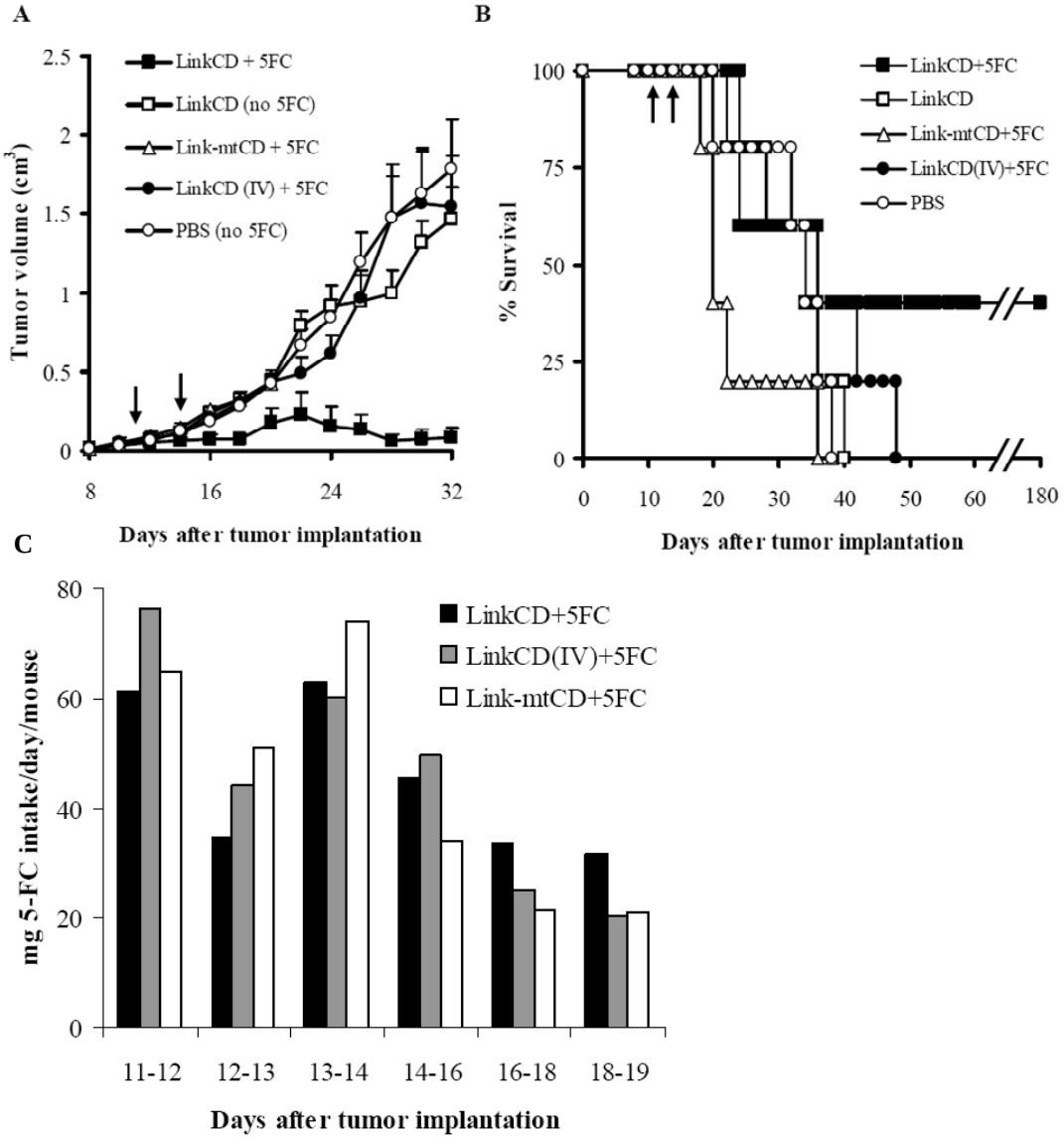

Figure 4-5. Anti-tumor effect of LinkCD requires the Link domain and conversion of 5-FC to 5-FU. **A**. Tumor growth curves (n ≥3 mean ± sem) show that the mean tumor volume of the LinkCD/5-FC treatment group was significantly smaller than that of the other groups ($p < 0.05$ for days 16 – 20, and 24-32). **B**. Survival curves for all treatment groups in the study (next page). LinkCD/5-FC treatment group has 40% long-term survivors. The arrows indicate the injection time points (day 11 and day 14). **C**. Estimated amount of 5-FC intake among the treatment groups that received 5-FC in the drinking water.

In this study, two intratumoral injections of the LinkCD fusion protein were able to inhibit the tumor growth significantly with the prodrug 5-FC, and 4 out of the 10 treated mice from the *in vivo* experiments are tumor-free and remain healthy beyond 180 days post treatment. There was no anti-tumor effect by LinkCD/5-FC treatment when the same amount of the LinkCD fusion protein was injected intravenously. For this treatment group, the dosing amount of LinkCD was probably too small for intravenous administrations, and the injected protein was possibly rapidly eliminated from the systemic circulation. In the study design used in *in vivo* experiments reported here, we did not include a 5-FU treatment as a control group. The reason for this is that 5-FU treatment (from 25 mg/kg to 100 mg/kg) in the C26 tumor models have delayed tumor growth, but no animals in the 5-FU treatment groups survived longer than 50 days when 5-FU treatment started on day 7 (Evrard et al 1999) and day 10 (Bourquin et al 2006) after tumor implantation. This is presumably due to the toxicity of 5-FU. The results herein demonstrate superior efficacy of LinkCD/5-FC treatment over published protocols using 5-FU drug treatment alone.

In most ADEPT and GDEPT experiments that used CD enzyme, the major route of 5-FC administration was daily i.p. injections (400–500 mg/kg) for up to 2 weeks (Wallace et al 1994, Kievit et al 1999, Miller et al 2002, Tai et al 2005, and Alderson et al 2006). Because the oral bioavailability of 5-FC is relatively high (Cutler et al 1978), the prodrug was administered in the drinking water at a concentration of 10 mg/mL. Oral administration of 5-FC from the drinking water (10 mg/mL) was previously done for targeting CD-expressing tumor cells in rats (Gavelli et al 2004) and in antifungal

combination therapy experiments in mice (Larsen et al 1996). 5-FC administration via drinking water is less likely to stress the animals compared to multiple day regimes of intraperitoneal administration. The daily ingestion of 5-FC per mouse ranged from 20 mg to 75 mg (Figures 4-3C and 4-5C). Since the amount of the prodrug consumed by individual animals was not monitored, I do not know whether the cured mice in the LinkCD/5-FC treatment group had consumed a significantly different amount of 5-FC than the mice that did not survive in the same treatment group. Animals that were sacrificed in the LinkCD/5-FC treatment group had relatively small tumor volumes at the times of deaths compared to animals sacrificed in the other treatment groups. The deaths in the LinkCD/ 5-FU treatment group might have been due to systemic toxicity of 5-FU generated from 5-FC in these animals. The blood and tumor levels of 5-FC and 5-FU are a subject for future studies that will enable a rationale dosing strategy (Stegman et al 1999).

The disruption of the hyaluronan-cell interaction by over-expression of soluble CD44 demonstrated tumor growth inhibition in mammary carcinoma and melanoma models, although long-term survival of animals in these studies was not reported (Peterson et al 2000 and Ahrens et al 2001). Synthetic hyaluronan-binding peptides also reduce tumor progression (Mummert et al 2003 and Xu et al 2003). These studies were done using stably transfected tumor cell lines that secreted soluble CD44 or hyaluronan-binding peptide (Peterson et al 2000, Ahrens et al 2001, and Xu et al 2003), or by co-injection of a hyaluronan-binding peptide with tumor cells *in vivo* at the time of tumor implantation (Mummert et al 2003). A direct effect of the Link domain on tumor progression does not

appear to be operative in established tumors since neither the LinkCD without 5-FC treatment group nor the Link-mtCD with 5-FC treatment group reduced C26 tumor growth (Figure 5A) or resulted in long-term survivors (Figure 5B). It is possible that the dose of the protein injected into the tumor in our studies was insufficient to disrupt the cell-to-matrix interaction, or the growth of C26 tumor cells may be independent of their interaction with hyaluronan. Nonetheless, in the absence of long-term survival data from the earlier studies, the therapeutic benefit of using just a hyaluronan-binding protein, or peptide, for anti-tumor treatment does not appear promising.

An antibody-CD enzyme conjugate was created and employed for ADEPT approach for cancer in the early 1990's, and was successful in targeting tumor and generating 5-FU both *in vitro* and *in vivo* in H3719 human colon carcinoma model in nude mice (Senter et al 1991 and Wallace 1994). However, because of the extended circulation time of antibody-CD conjugate, which potentially could cause systemic toxicity by 5-FU generation in the blood, a secondary antibody specific for the CD enzyme was used to clear the antibody-CD conjugate *in vivo* (Kerr et al 1993). To reduce the circulation time of antibody-enzyme conjugate, a recombinant fusion protein containing single chain variable fragment of antibody (scFv) and the CD enzyme was characterized *in vitro* (Deckert et al 2003 and Coelho et al 2007). However, the therapeutic efficacy of antibody-CD conjugates *in vivo* remains to be tested. Recently, Schellenberger and coworkers have characterized and shown an *in vivo* anti-tumor effect of a recombinant fusion protein containing scFv and β-lactamase conjugate in combination with a prodrug GM-Mel up to day 36 (Alderson et al 2006). Significant drug toxicity was reported with

their treatment regime; thus, unwanted toxicity from the conversion of active drug remains a challenge for ADEPT.

The MAT strategy would also appear to be better than the GDEPT approach to treat cancer, with the ability to deliver higher amount of prodrug converting enzyme at the tumor site with local delivery. Based on the enzyme stability test at 37 ^{o}C in PBS (Figure 3A), 0.2 units of LinkCD can generate 9.4 μmole of 5-FU after 60 min, with assumptions that the enzyme activity does not change *in vivo* and 5-FC concentration is at steady state. Since the expression level of CD enzyme in stably transduced cells that express CD has not been quantified in the GDEPT approach, the amount of the expressed CD enzyme can only be estimated from the intratumoral 5-FU concentration after 5-FC administration. Using stably transfected HT29 colon carcinoma model in mice, Stegman et al (1999) reported that 60 min after 1 g/kg of 5-FC administration, the peak level of 5-FU in the ~250 mm^3 tumor was measured to be 3.4 mM or 0.85 μmole. Assuming saturation kinetics from time zero, about 1 μg of CD enzyme is needed to produce 3.4 mM 5-FU in the tumor after 60 min. This is much less than the amount of 5-FU that can be generated by 0.2 units of LinkCD. The amount of CD enzyme expressed in the subpopulation of transfected tumor cells as a result of vector-mediated gene delivery to the tumor is expected to be much less than that in above example of the stably transduced flank tumor.

Thus, the limited amount of 5-FU generation is yet another challenge for GDEPT. As a consequence, there are few reports of long-term survivors (> 100 days) in GDEPT studies where the CD enzyme/5-FC combination was employed for therapy. One GDEPT study

where the U-87 glioma was transduced by replication-competent retrovirus vector in athymic mice 7 days after tumor implantation, resulted in 90% long-term survivors up to 110 days (Tai et al 2005). A combined therapy using the 5-FC, CD-uracil phosphoribosyltransferase genes delivered in an adenoviral vector at 4 days post tumor implantation and radiation treatment in 9L brain tumor in rats produced 80% long-term survivors at 90 days (Kambara et al 2002). In both of these studies, the viral vector was inoculated into the tumor site soon after tumor implantation; the tumor volume at the time of treatment (7 or 4 days after tumor implantation) is expected to be smaller than the tumor volume in the studies reported here. It will be of interest to learn if a local delivery of LinkCD into the brain via convection enhanced delivery (CED) (Bobo et al 1994, Voges et al 2002, Voges et al 2003, and MacKay et al 2005) can provide a similar therapeutic effect to that observed in these GDEPT studies (Kambra et al 2002 and Tai et al 2005).

The MAT strategy is not limited to the use of recombinant proteins—matrix targeting ligands and prodrug converting enzymes can be conjugated to other widely used drug delivery vehicles, such as liposomes and biocompatible polymers. There is an additional advantage for the combined formulation of recombinant proteins and vehicles for drug delivery: the properties of the delivery vehicles can be modified to optimize the blood circulation time for systemic delivery or CED for local administrations for brain tumor therapy (Gillies et al 2005 and MacKay et al 2005). In this regard CD has been PEGylated to increase the circulation time (Xiong and Kwon 2005). Although CD enzyme activity seemed to be relatively stable with 2 PEG chains, attachment of 3 or

more PEG chains on CD reduced the thermal stability of the enzyme at 37 ^{o}C with a half-life to less than 2 hr (Xiong and Kwon 2005). In spite of the reduced stability, this general approach of PEGylating enzymes seems promising, and may be applied to LinkCD developed here.

The anti-tumor activity of the LinkCD fusion protein provides a proof-of-concept for the MAT approach to cancer therapy. Using a recombinant fusion protein containing the hyaluronan binding domain of TSG-6 and the CD enzyme from yeast, we show that the minimal elements for successful MAT against C26 tumor are 1) a matrix binding domain, 2) a prodrug-converting enzyme, and 3) the prodrug. MAT is a versatile prodrug activation strategy that complements ADEPT and GDEPT, and has the potential to target neoplastic and inflammatory diseases where components of the matrix such as hyaluronan are an accessible target.

4.6 Conclusions

The anti-tumor effect of LinkCD/5-FC treatment was successfully demonstrated in the animal studies using C26 tumor model in mice. There was no anti-tumor effect caused by CD/5-FC treatment on C26 tumor bearing mice. In addition, other control treatment groups (LinkCD without 5-FC and Link-mtCD/5-FC) that were unable to produce 5-FU did not exhibit anti-tumor effect.

4.7 Credits

Animals were handled and monitored by Edward Dy or Nichole Macaraeg.

CHAPTER 5

Rational Design of CD44 Link Chimeras to Optimize Hyaluronan Binding Affinity

5.1 Introduction

The intratumoral injections of LinkCD and 5-FC administration in the drinking water successfully demonstrated a proof-of-concept for MAT strategy for anti-tumor therapy in mice (Chapter 4). However, the preliminary results of the pharmacokinetics experiment suggest that the LinkCD fusion protein may have a very short circulation time in the blood when the protein is injected intravenously (see Appendix Chapter). This is a major limitation for systemic delivery of the LinkCD fusion protein to target tumor. For targeted therapy using macromolecules such as monoclonal antibodies, liposomes, and drug conjugated polymers, long circulation time in the blood is an important factor for significant accumulation of macromolecules at the tumor site by the EPR effect (reviewed in Allen and Cullis 2004). Therefore, the LinkCD fusion protein must be modified to increase the circulation time for effective tumor targeting via systemic delivery.

Since circulating soluble CD44 (the extracellular matrix domain of CD44) is detected in the blood in humans and rodents (Katoh et al 1994, van Hal et al 1999, Molica et al 2001, Komura et al 2002, and Sjoberg et al 2005), it is possible that CD44 Link has better pharmacokinetics property than TSG-6 Link. This is a reasonable assumption, because CD44 Link is heavily glycosylated. The glycosylated form of CD44 Link could have longer circulation time in the blood than the un-glycosylated form, since the apparent

molecular weight of the glycosylated form is much higher (Katoh et al 1994). The tradeoff, however, is that the affinity of CD44 Link towards hyaluronan is weaker than that of TSG-6 Link (Lesley et al 2002). Moreover, eukaryotic expression system must be employed for protein production, because bacterial expression system cannot glycosylate expressed target proteins. Thus, in order to utilize glycosylated CD44 Link or other variants of the LinkCD fusion protein, CD44 Link should be engineered to increase its affinity towards hyaluronan, and employ mammalian cell expression system.

In this chapter, I propose a strategy to engineer the hyaluronan binding surface of the Link domain of CD44 for enhanced hyaluronan binding by a rational protein design approach. Bioinformatics tools were employed to perform sequence and structure alignments between the CD44 and TSG-6 Link domains. I hope that the results in this chapter could be used as the starting point for future experiments on creating a functional chimeric CD44 Link domain based on the binding residues of the TSG-6 Link domains. It would be interesting to see whether the chimeric CD44 Link could improve the pharmacokinetics and biodistribution of the LinkCD fusion protein *in vivo*. Thus, protein engineering work on the CD44 Link domain could be expanded further to design the next generation of the LinkCD fusion protein for systemic targeting of solid tumors.

5.2 Soluble CD44 found in the circulating blood in humans

The Link domain of TSG-6 was chosen for construction of the LinkCD fusion protein because its affinity to hyaluronan is thought to be better than that of CD44 (Lesley et al 2002). However, since TSG-6 is expressed locally when induced by pro-inflammatory

cytokines and there are no reports of circulating TSG-6 detected in the blood, it could be assumed that the blood circulation time may not be long enough for the Link domain of TSG-6.

There are reports of circulating soluble CD44 (sCD44) in humans. Elevated levels of sCD44, which contains the extracellular domain of the full-length protein (including the Link domain), is found in the serum of patients who are suffering from early B-cell lymphocytic leukemia (Molica et al 2001), non-Hodgkin's lymphoma (Ristamaki et al 1998), head and neck squamous carcinoma (van Hal et al 1999), and systemic sclerosis (Komura et al 2002). Early B-cell chronic lymphocytic leukemia patients who have elevated level of sCD44 in the serum (greater than 645 ng/mL) have significantly worse survival, which makes sCD44 a marker for high risk of disease progression (Mollca et al 2001). The level of sCD44 in normal adults ranges from 350 ng/mL to 450 ng/mL (Sjoberg et al 2005). These observations suggest that sCD44 containing the Link domain could stay in the blood circulation, although the precise half-life in the circulation is still unknown.

The biological function of sCD44 in the circulating blood was confirmed by Katoh and coworkers using a murine squamous cell carcinoma model (1994). The serum containing sCD44 from the KLN tumor-bearing mice was able to competitively inhibit the interaction between FITC-labeled hyaluronan and hybridoma cells, whereas the serum from the normal mice could not inhibit the interaction. This finding suggests that the sCD44 in the blood retains its ability to interact with hyaluronan.

The majority, if not all, of sCD44 found in the blood comes from two sources: 1) truncated CD44 formed as a result of early termination before the transmembrane domain, 2) and CD44 shed from the tumor cell surface where matrix metalloproteinase activity is relatively high in the extracellular matrix (Kajita et al 2001). Although the presence of circulating sCD44 in humans and rodents has been reported in the literature, the elimination rate of sCD44 has not been measured. CD44 is a glycoprotein—the extracellular matrix domain of CD44 becomes extensively glycosylated during the post-translational modification in mammalian cells, which increases the apparent molecular weight of the mature protein. There are four possible *N*-linked glycosylation sites on the Link domain alone. It is possible that glycosylated sCD44 would be eliminated slower than the unglycosylated form. Thus, it could be beneficial to use CD44 Link (or the entire extracellular matrix domain of CD44) for the next generation of the LinkCD fusion protein to increase its circulation time.

In order to produce glycosylated CD44 Link, the bacterial expression system can no longer be used because bacteria lack the ability to glycosylate expressed target protein. Eukaryotic expression system must be employed to produce a glycosylated LinkCD fusion protein. Unfortunately, the hyaluronan binding affinity for CD44LinkCD could potentially be weaker than that for TSG-6LinkCD, and this is a possible negative outcome for using the CD44 Link domain. Therefore, this problem became the impetus for me to engineer the hyaluronan binding surface of CD44 Link to resemble that of TSG-6 Link by employing bioinformatics tools.

5.3 Rational design of CD44 Link chimeras to optimize the affinity towards hyaluronan by incorporating the key residues of TSG-6 Link for hyaluronan binding

The structures of the Link domains of CD44 and TSG-6 are available from the Protein Data Bank at www.pdb.org (Table 5-1). These structures could serve as the basis for creating chimeras of the CD44 Link domain with higher affinity for hyaluronan than the wild-type CD44 Link. Ultimately, the engineered CD44 Link could potentially improve the blood circulation time of the LinkCD fusion protein by replacing the TSG-6 Link domain with glycosylated CD44 Link using the mammalian expression system.

The hyaluronan binding site of TSG-6 Link was determined by site-directed mutagenesis (Mahoney et al 2001). More recently, high resolution structures of the Link domains from TSG-6 and CD44 have been solved by NMR and X-ray crystallography methods (Teriete et al 2004, Blundell et al 2005, Takeda et al 2006, Banerji et al 2007, and Higman et al 2007). These structural studies have become the basis for elucidating the functions of the Link domain of TSG-6 (Blundell et al 2007), including the interaction of TSG-6 Link with other glycosamino glycans such as chondroitin sulfate and heparin (Mahoney et al 2005 and Wisniewsky et al 2005).

Table 5-1. Structures of CD44 Link and TSG-6 Link

Protein	PDB ID	Species	HA Ligand	Reference
CD44 Link	1UUH	Human	No	Teriet et al 2004
	2I83	Human	Yes	Takeda et al 2006
	2JCP	Mouse	No	Banerji et al 2007
	2JCR	Mouse	Yes	Banerji et al 2007
	2JCQ	Mouse	Yes	Banerji et al 2007
TSG-6 Link	1O7B	Human	No	Blundell et al 2005
	1O7C	Human	Yes	Blundell et al 2005
	2PF5	Human	No	Higman et al 2007

For structure comparisons between CD44 Link and TSG-6 Link, the hyaluronan bound forms were chosen (2JCR and 1O7B for CD44 Link and TSG-6 Link, respectively). 1UUH, 2I83, 1O7B, and 1O7C were determined by NMR and 2JCP, 2JCR, and 2PF5 were determined by X-ray crystallography.

There are significant differences between TSG-6 Link and CD44 in the ways that these Link domains interact with hyaluronan. The interaction between hyaluronan and TSG-6 Link is dominated by CH-π stacking with the tyrosine residues and ionic interactions with lysine and arginine residues in the binding groove, whereas the interaction between hyaluronan and CD44 Link is dominated by hydrogen bonding (Blundell et al 2005 and Banerji et al 2007). Therefore, it would be very interesting to see whether the affinity between the CD44 Link domain and hyaluronan could be increased by introducing hydrophobic pockets and ionic interactions for ligand binding. This can be done by identifying the key residues of the TSG-6 Link domain for hyaluronan binding and modifying appropriate residues on the CD44 Link domain. However, this approach could work only if there is structural similarity between CD44 Link and TSG-6 Link.

Using available bioinformatics tools, the Link domains of CD44 and TSG-6 were directly compared at both sequence and structure levels. In addition, a global sequence analysis of the Link domain was done to see if there are key residues in the Link domain that are shared commonly among these proteins.

5.3.1 Bioinformatics tools used for sequence and structure analyses

All protein structures were obtained from Protein Data Bank database (http://www.pdb.org). These structure identifications from the PDB database are listed in Table 5-1. The structure viewing, alignments, and RMSD (root mean square deviation) calculations were performed by PyMol software version 0.99rc6 (http://www.pymol.org). ClustalW2 program was used (http://www.ebi.ac.uk/Tools/clustalw/index.html) for

multiple sequence alignments of the Link domains. Protein sequences were obtained from the PubMed database (http://pubmed.gov). Proteins that contain one or more Link domains were found by Position-specific iterative basic local alignment search tool (PSI-BLAST) program (http://www.ncbi.nlm.nih.gov/blast/Blast.cgi), using the mouse CD44 Link domain as the query sequence. The theoretical molecular weights and pI of the proposed CD44 chimeras were calculated by ExPASy server tool called Compute pI/Mw (http://ca.expasy.org/tools/).

5.3.2 Sequence and structure comparisons between CD44 Link and TSG-6 Link

When mouse CD44 Link was co-crystalized with hyaluronan, two distinct structures were found (Banerji et al 2007). These structures were separately determined as Type A binding (PDB ID: 2JCQ) and Type B binding (PDB ID: 2JCR) to hyaluronan. The Type B form represents tighter binding of CD44 Link to hyaluronan, so this form was chosen for comparison with the hyaluronan bound form of TSG-6 Link.

For structure comparison between CD44 Link and TSG-6 Link, the mouse CD44 Link domain was used because the hyaluronan-bound human CD44 Link structure is not yet available. Despite the species difference, there is greater than 84% sequence identity between the mouse CD44 Link and human CD44 (Figure 5-1A). The unbound structures of the mouse and human CD44 Link domains align very well (Figure 5-1B). Thus, the hyaluronan-bound form of the mouse CD44 Link structure was used to subsequently engineer human CD44 Link (shown in Figure 5-3).

A

```
human           AQIDLNITCRFAGVFHVEKNGRYSISRTEAADLCKAFNSTLPTMAQMEKALSIGFETCRY
mouse           QQIDLNVTCRYAGVFHVEKNGRYSISRTEAADLCQAFNSTLPTMDQMKLALSKGFETCRY
                 *****:***:**********************:********* **: *** *******

human           GFIEGHVVIPRIHPNSICAANNTGVYILT-SNTSQYDTYCFNASAPPEEDCTSVTDLPNA
mouse           GFIEGNVVIPRIHPNAICAANHTGVYILVTSNTSHYDTYCFNASAPPEEDCTSVTDLPNS
                *****:*********:*****:******. ****:************************:

human           FDGPITITIVNRDGTRYVQKGEYRTNPEDIY
mouse           FDGPVTITIVNRDGTRYSKKGEYRTHQEDID
                ****:************ :******: ***
```

B

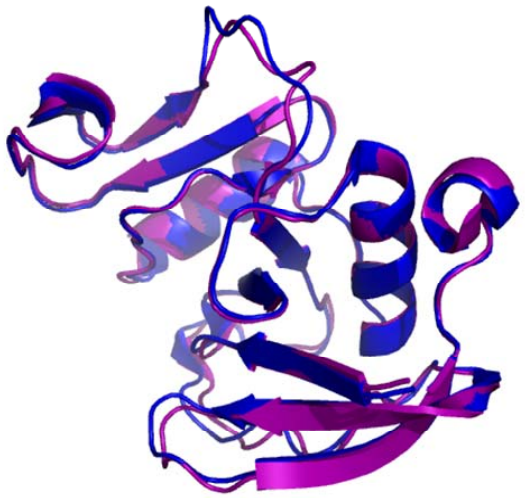

Figure 5-1. Comparison between mouse CD44 Link and human CD44 Link. A. Primary sequence alignment between mouse CD44 Link and human CD44 Link (* identical match, : conserved substitution, . semi-conserved substitution). **B.** Structural alignment between mouse CD44 Link (PDB ID: 2JCP, blue) and human CD44 Link (PDB ID: 1UUH, purple). Both structures were determined without hyaluronan. The mouse CD44 Link is very similar to the human CD44 Link (RMSD value is at 0.662 Å).

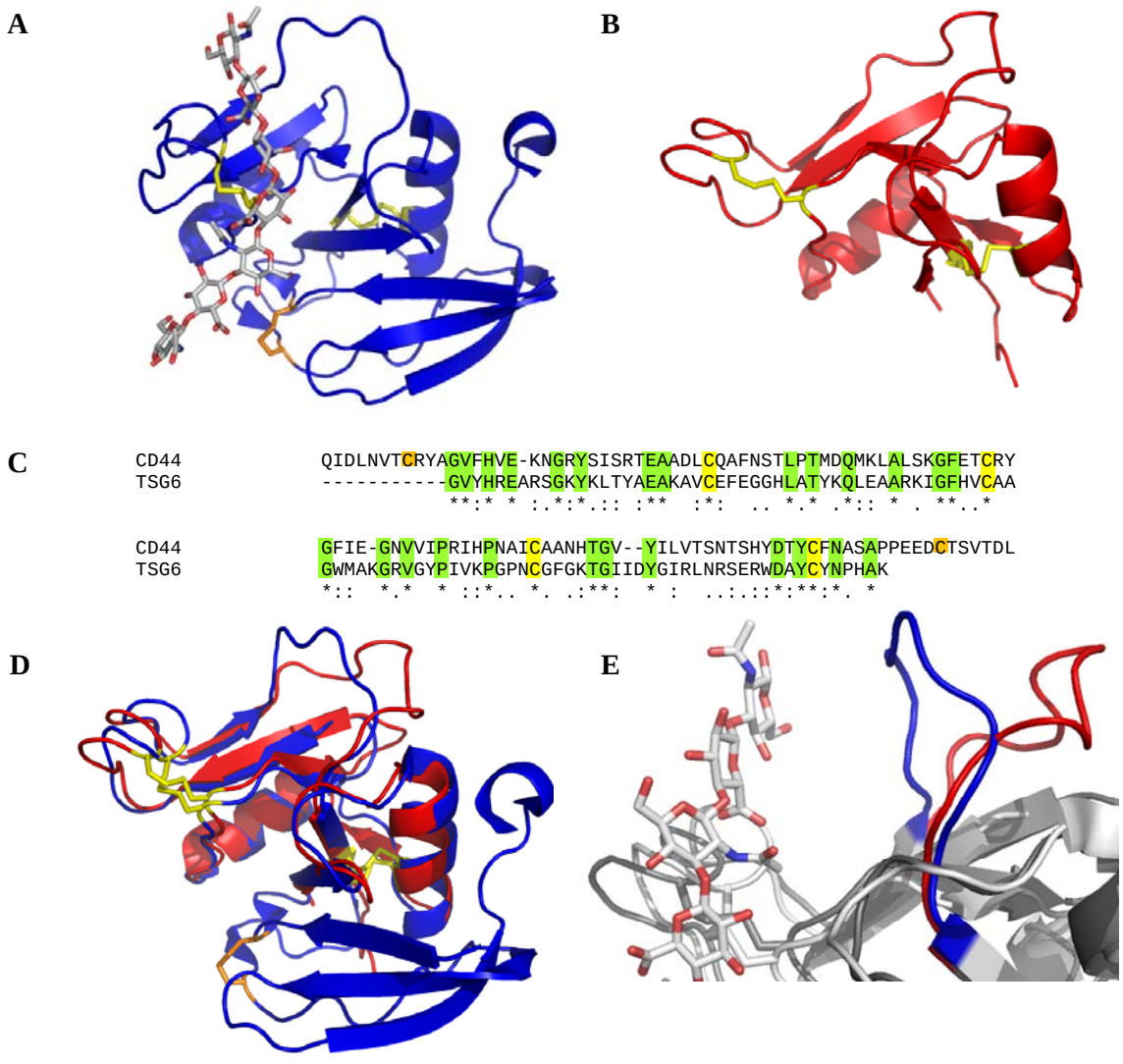

Figure 5-2. Structures of mouse CD44 Link and human TSG-6 Link in hyaluronan bound conformations. A. Structure of mouse CD44 Link (blue ribbon) with hyaluronan oligomer (light gray stick) determined by X-ray crystallagraphy (PDB ID: 2JCR). **B.** Solution structure of TSG-6 Link (red ribbon) determined by NMR (PDB ID: 1O7C). **C.** Primary sequence alignment of the two Link domains. The green blocks show matching residues and yellow blocks represent the conserved cysteine residues in the Link domain. There is an extra disulfide bond in CD44 Link domain (colored orange). **D**. Structure alignment between CD44 Link (blue) and TSG-6 Link (red). RMSD value is at 1.573 Å. **E**. The positions of beta turn loops that are in contact with hyaluronan (CD44 Link loop in blue, and TSG-6Link loop in red). The position of hyaluronan (white stick figure) is with respect to CD44 Link domain. The graphics were reproduced by PyMol software.

The structures of the mouse CD44 Link (PDB 2JCR, Figure 5-2A) and human TSG-6 Link (PDB 1O7C, Figure 5-2B) were aligned together in Figure 5-2D. Both of these structures represent the hyaluronan bound conformations. Although there is only 30% sequence identity between the mouse CD44 Link and human TSG-6 (Figure 5-2C), the overall structures of the Link domains match very well (RMSD 1.573 Å). There is a significant difference in the position of the β3 - β4 turn loop of TSG-6 Link and the corresponding loop of CD44 near the hyaluronan binding groove, where the loop of CD44 is bent towards the hyaluronan (Figure 5-2E). The structure of the bound hyaluronan with CD44 Link is kinked due to the bent conformation of the loop, whereas the bound hyaluronan to TSG-6 Link is straight (based on the docking model described by Blundell et al 2005), presumably because the β3 - β4 turn loop lays backwards relative to the loop of CD44 Link and is not bent towards the binding groove to occupy the surface.

Since CD44 Link domain is structurally similar to TSG-6 Link, it may be possible to rationally design CD44 Link chimeras to increase affinity for hyaluronan. By identifying the key residues of TSG-6 Link for hyaluronan binding from the structure studies, the corresponding amino acids can be located in CD44 Link by a pair-wise sequence comparison between TSG-6 Link and CD44 Link.

A

```
Mouse CD44      -QIDLNVTCRYAGVFHVE-KNGRYSISRTEAADLCQAFNSTLPTMDQMKLALSKGFETCR
Human CD44      AQIDLNITCRFAGVFHVE-KNGRYSISRTEAADLCKAFNSTLPTMAQMEKALSIGFETCR
Human TSG-6     ------------GVYHREARSGKYKLTYAEAKAVCEFEGGHLATYKQLEAARKIGFHVCA
                            **:* * :.*:*.:: :**  :*:  .. *.*  *:: * . **..*

Mouse CD44      YGFIE-GNVVIPRIHPNAICAANHTGV--YILVTSNTSHYDTYCFNASAPPEEDCTSVTD
Human CD44      YGFIE-GHVVIPRIHPNSICAANNTGV--YILT-SNTSQYDTYCFNASAPPEEDCTSVTD
Human TSG-6     AGWMAKGRVGYPIVKPGPNCGFGKTGIIDYGIRLNRSERWDAYCYNPHAK----------
                 *::  *.*  * ::*.. *. .:**:  * :  ..:.::*:**:*. *

Mouse CD44      LPNSFDGPVTITIVNRDGTRYSKKGEYRTHQEDID 150
Human CD44      LPNAFDGPITITIVNRDGTRYVQKGEYRTNPEDIY 150
Human TSG-6     ----------------------------------
```

B **Human CD44 Link**

AQIDLNITCRFAGVFHVEKNGRYSISRTEAADLCKAFNSTLPTMAQMEKALSIGFETCRYGFIEGHVVIPRIHP
NSICAANNTGVYILTSNTSQYDTYCFNASAPPEEDCTSVTDLPNAFDGPITITIVNRDGTRYVQKGEYRTNPED
IY

Mw 16.65 kDa, pI 5.10

C **Chimeric Link1**

AQIDLNITCRFAGVFHVEKNGKYSISRTEAADLCKAFNSTLPTMAQMEKALSIGFETCRAGFIEGHVVYPIIHP
NSICGANKTGVYILRSNTSQWDTYCFNASAPPEEDCTSVTDLPNAFDGPITITIVNRDGTRYVQKGEYRTNPED
IY

Mw 16.61 kDa, pI 5.31

D **Chimeric Link2**

AQIDLNITCRFAGVFHVEKNGRYSISRTEAADLCKAFNSTLPTMAQMEKALSIGFETCRYGFIEGHVVIPRIHP
NSICAANNTGVIDDYGIRLNRSERYDTYCFNASAPPEEDCTSVTDLPNAFDGPITITIVNRDGTRYVQKGEYRT
NPEDIY

Mw 17.23 kDa, pI 5.16

E **Chimeric Link3**

AQIDLNITCRFAGVFHVEKNGKYSISRTEAADLCKAFNSTLPTMAQMEKALSIGFETCRAGFIEGHVVYPIIHP
NSICGANKTGVIDDYGIRLNRSERWDTYCFNASAPPEEDCTSVTDLPNAFDGPITITIVNRDGTRYVQKGEYRT
NPEDIY

Mw 17.14 kDa, pI 5.16

Figure 5-3. The proposed site-directed mutagenesis for creating chimeras of the human CD44 Link domain containing the key hyaluronan binding residues of TSG-6 Link. **A.** Multiple sequence alignment with the key residues of TSG-6 highlighted (green for hyaluronan binding residues, and underline for the β4 - β5 turn loop. **B.** The wild-type sequence of the human CD44 Link. **C.** A chimeric human CD44 Link containing the key residues that are involved in hyaluronan binding (indicated by green). **D.** A chimeric human CD44 Link containing the β4 - β5 turn loop from TSG-6 Link (red, underlined). The green color residues are the two residues that were chosen for mutations from Chimeric Link1. There are two additional residues from TSG-6 Link to fill up the gap sequence from the sequence alignment. **E.** A chimeric human CD44 Link containing the hyaluronan binding residues and the β4 - β5 turn loop from TSG-6 Link. Theoretical Mw and pI values were calculated by ExPASy proteomic server.

5.3.3 Creation of the CD44 Link chimeras based on the key hyaluronan binding residues and the β4 - β5 turn loop sequence from TSG-6 Link

There are 8 residues that make up a hydrophobic pocket for hyaluronan-TSG-6 Link interaction. These residues are C47, A49, Y59, I61, G69, C68, K72, and Y78. There is another hydrophobic pocket, which is made up of W88 and V57. Two other residues that are located in the binding pocket are K11 and R81 (Blundell et al 2005). Some of these residues were previously found to be important in hyaluronan binding in a site-directed mutagenesis study on TSG-6 Link (Mahoney et al 2001). To find the corresponding residues in the human CD44 Link to select mutations for creating chimeras of the CD44 Link with the key residues of TSG-6 Link that are involved in hyaluronan binding, I performed multiple sequence alignment using the sequences from the CD44 Link (human and mouse) and TSG-6 Link (human). Even though the structure comparison was done using mouse CD44 Link, I decided to place the mutation sites on human CD44 Link, to minimize potential immunogenicity problems.

The proposed sequences of the human CD44 Link chimeras are shown in Figure 5-3C through E. The Chimera 1 sequence contains the key residues for hyaluronan binding from TSG-6 Link. By substituting selected residues from TSG-6 Link, one *N*-glycosylation site was removed as a result of N105K mutation (there are three other *N*-glycosylation sites within the CD44 Link domain). The Chimera 2 sequence contains the β4 - β5 turn loop from TSG-6 Link (DYGIRLNRSER), with two additional residues (ID) for filling the gap sequences from the multiple sequence alignment result. Finally,

the Chimera3 sequence contains both the key residues for hyaluronan binding and the β4 - β5 turn loop from TSG-6 Link.

5.3.4 Multiple sequence alignment of selected Link module superfamily proteins

The proposed sequences of CD44 Link chimeras were derived from the direct sequence and structure comparisons between the Link domains of CD44 and TSG-6. But these are only two of many proteins that contain one or more Link domains. These proteins are grouped in the Link module superfamily (reviewed in Day and Prestwich, 2002).

To explore the possibility of finding key residues that are located in the hyaluronan binding groove of the Link domain of either CD44 or TSG-6, I performed global sequence analyses using available bioinformatics software tools. To find other Link domains from the PubMed database, the Link domain sequence of mouse CD44 (residues 23 – 144) was used as the query sequence (i.e., input sequence) for the Position-Specific Iterative Basic Local Alignment Search Tool (PSI-BLAST) program. PSI-BLAST is one of the BLAST algorithms, which is used to search for distantly-related sequences in the database (Altschule et al 1997). Since the four consensus cysteine residues in the Link domain is the only identical residues that are known in the Link domain, PSI-BLAST was an appropriate choice to find other Link domains in the Link module superfamily (BLAST is a program designed to compare a query sequence with all protein sequences in a database to find proteins that match or closely match the query sequence).

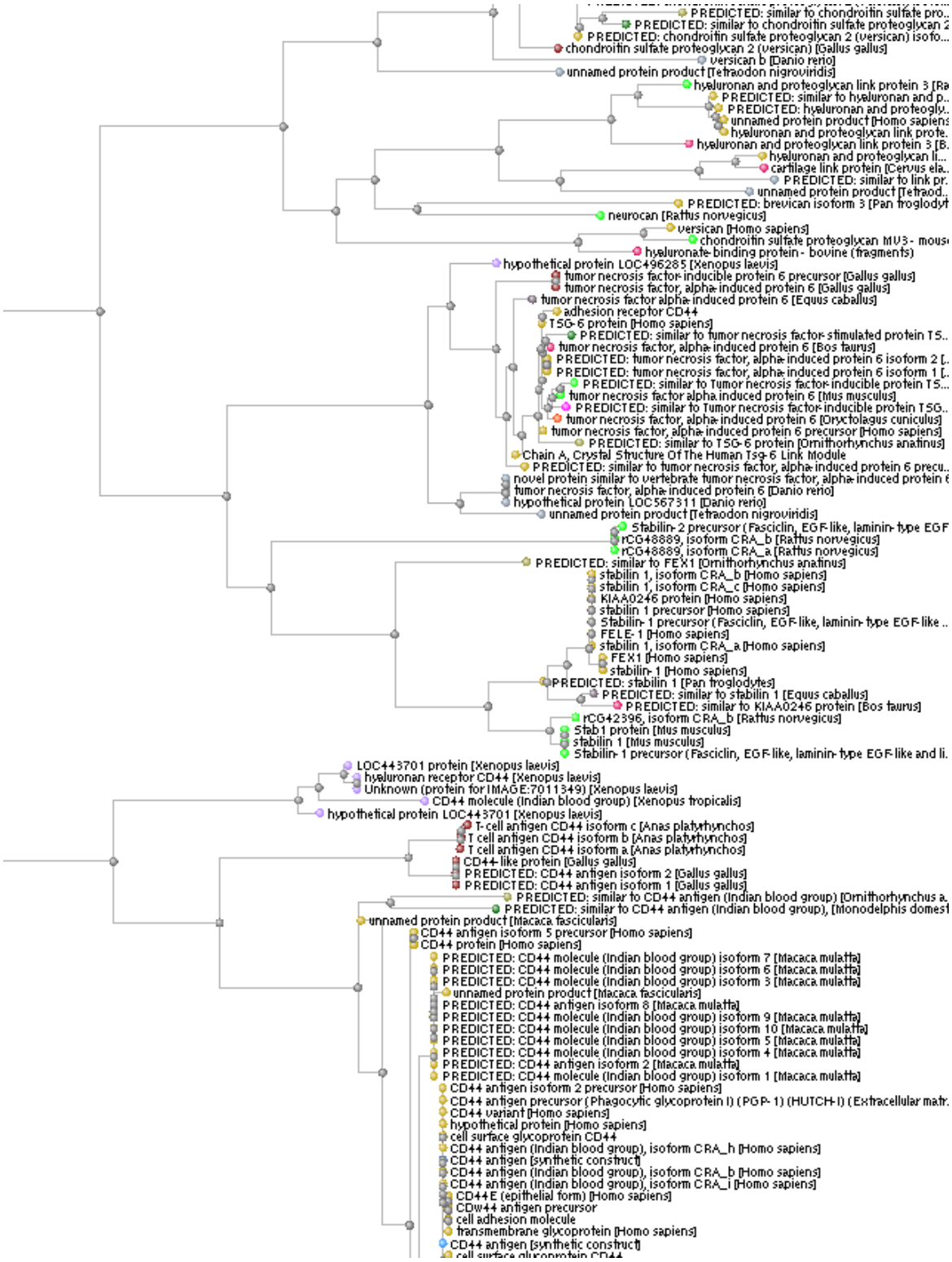

Figure 5-4. A partial tree representation of the PSI-BLAST search using the Link domain sequence of mouse CD44.

Table 5-2. PSI-BLAST results: sequence identity, positive hits, and gaps

Link protein (specie); GenBank ID	Identities	Positives	Gaps
CD44 (human); AAB27919.1	131/149 (87%)	142/149 (95%)	1/149 (0%)
TSG-6 (human); NP00904.2	37/121 (30%)	59/121 (48%)	8/121 (6%)
TSG-6 (mouse); NP033424.1	37/118 (31%)	57/118 (48%)	8/118 (6%)
Lyve-1 (human); NP00682.2	41/131 (31%)	62/131 (47%)	3/131 (2%)
Lyve-1 (mouse); NP444477.2	45/125 (36%)	61/125 (48%)	4/125 (3%)
Stablin-1 (human); EAW65233.1	31/107 (28%)	51/107 (47%)	4/107 (3%)
Stablin-1 (mouse); AAH31166.1	30/107 (28%)	53/107 (49%)	4/107 (3%)
Hapln-1 (human); AAH57808.1	34/135 (25%)	58/135 (42%)	9/135 (6%)
Aggrecan (human); AAH36445.1	23/87 (26%)	41/87 (47%)	9/87 (10%)
Brain link protein-1 (human); NP068589	34/145 (23%)	55/145 (37%)	14/145 (9%)
Brain link protein-1 (rat); NP071621	37/156 (23%)	63/156 (40%)	15/156 (9%)

PSI-BLAST was performed using the protein sequence of mouse CD44 Link. Identities are the identical match between the query sequence (mouse CD44 Link) and the subject sequence. Positives represent the conserved residues. Gaps represent the number of the gap sequences. Notice that the number of amino acid residues for each pair-wise comparison varies.

A partial tree representation of the PSI-BLAST results is shown in Figure 5-4. The distance between a pair of proteins are calculated by the percentages of identical residues, positive residues (i.e. conserved and semi-conserved residues), and gap sequences. After two iterations of PSI-BLAST using the mouse CD44 Link domain sequence, the following Link domain sequences were selected for further analysis: CD44 Link (human), TSG-6 (human and mouse), lyve-1 (human and mouse), stabilin-1 (human and mouse), hapln-1 (human), aggrecan (human), and brain link protein-1 (human and mouse). These proteins were selected because they are known proteins in the Link module superfamily (Day and Prestwich 2002). Since aggrecan and brain link protein-1 both contain more than one Link domain, only the first Link domain sequence from these two proteins was selected. The results of the pair-wise comparisons of the selected Link domains to the query sequence are listed in Table 5-2. The sequence identities to the mouse CD 44 Link varied from only 23% identity for the brain link protein-1 (both human and mouse) to 87% identity for the human CD44 Link. Except for the human CD44 Link domain, the sequence identities for the selected Link domains to the mouse CD44 Link domain were below 40%. Although there were only a small number of identical residues, other conserved residues in these selected Link domains enhanced the positive scores to above 37%. The percentages of gap sequences were at or below 10% levels.

The Link domain sequences of CD44, TSG-6, lyve-1, hapln-1, brain link protein-1, stablin-1, and aggrecan from the PSI-BLAST output were pooled together to perform a multiple sequence alignment using ClustalW2 sequence analysis program

(http://www.ebi.ac.uk/Tools/clustalw2/index.html). The four consensus cysteine residues were found as expected (Figure 5-5A). Surprisingly, four additional identical residues (A, Q, and two G residues in green) and eleven conserved residues were found (blue), even though the sequence identities among these Link domains were low. To my knowledge, these residues have not been reported in the literature. Based on this result, these new identical residues could be considered as consensus residues for the Link module proteins.

To examine whether these residues could be important for the interaction with hyaluronan, the hyaluronan-bound structures of the mouse CD44 Link and human TSG-6 Link were used to locate the new consensus and conserved residues (Figure 5-5B). Most of the residues found in the multiple sequence alignment were located away from the hyaluronan binding groove, except for the Y119 residue of the mouse CD44 Link and W88 of the human TSG-6 Link. Interestingly, W88 residue is one of the residues that were selected for generating a chimera of the human CD44 Link domain (Figure 5-3), which is located in the hydrophobic pocket II (Blundell et al 2005). Y119 residue is relatively further away from the bound hyaluronan. Thus, this is corroborating evidence that Y119W mutation on the CD44 Link domain could lead to tighter ligand binding.

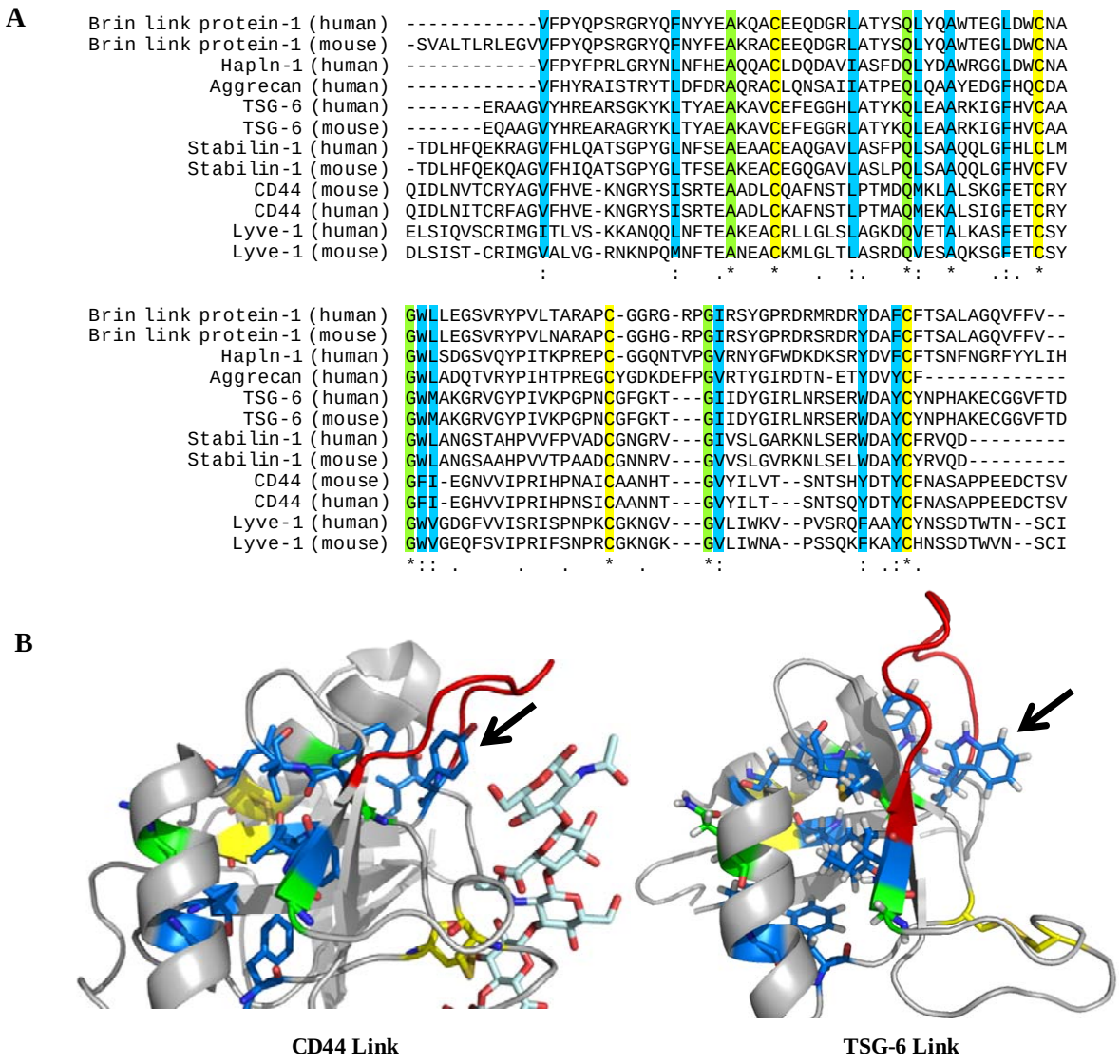

Figure 5-5. Multiple sequence alignment of the proteins containing at least one Link domain. **A.** In addition to the four conserved cysteine residues (highlighted in yellow), there are four additional identical residues that match (green) among the proteins that belong to the Link module superfamily. There are also eleven residues that are matching as conserved substitutions (blue). **B.** The highlighted residues from the multiple sequence alignment are shown on CD44 Link (2JCR, left) and TSG-6 Link (1O7C, right) structures. The hyaluronan binding groove loop is colored in red. Most of the identical or conserved residues found in the multiple sequence alignment are located on away from the hyaluronan binding pocket, except for the Y119 residue of CD44 Link and W88 residue for TSG-6 Link (indicated by arrows). The W88 residue of TSG-6 Link is one of the residues that is involved in the interaction with hyaluronan (Blundell et al 2005).

It is interesting to find that most of the consensus and conserved residues in the Link domain are not located at the hyaluronan binding site. Instead, most of these conserved residues are located on the opposite site of the binding grooves of CD44 Link and TSG-6 Link. None of these residues on TSG-6 Link are involved in the interaction with heparin (Mahoney et al 2005). It is likely that these residues are important for proper folding of the Link domain, rather than being the key residues for the interaction with hyaluronan or heparin. Therefore, it can be hypothesized that most, if not all, Link domains in the Link module superfamily may share similar structures even though there are less than 40% sequence identities among these proteins. In terms of the interaction with hyaluronan, there may be a wide range of affinity within the Link module superfamily since the residues in the binding groove do not appear to be highly conserved.

5.4 Discussion

The objective of the structure and sequence analyses of CD44 Link and TSG-6 Link was to create a CD44 Link chimera that may have better binding affinity towards hyaluronan than the wild-type CD44 Link. A comprehensive *in silico* design of CD44 Link domain is beyond the scope of my thesis research, so I have taken a rational design approach by employing available bioinformatics tools to create chimera sequences of CD44 Link domains. Indeed, further experiments must be carried out to show that a CD44 chimera can be expressed as stable protein, and determine the ligand binding kinetics to show that the interaction between a CD44 chimera and hyaluronan is stronger.

Designing CD44/TSG-6 chimera was previously done by replacing the Link domain of CD44 with that of TSG-6 (Lesley et al 2002). The study found that the resulting chimera of CD44/TSG-6 Link had stronger affinity towards hyaluronan than the wild-type CD44. This chimeric CD44 protein is certainly a good candidate for increasing the affinity to hyaluronan while retaining the CD44 backbone. However, by replacing the entire Link domain with that of TSG-6, four *N*-glycosylation sites on the CD44 Link domain were removed (only one glycosylation site was added from the TSG-6 Link domain). By selecting only the key hyaluronan binding residues from TSG-6, at least three of the four glycosylation sites of the CD44 Link domain remained in the proposed chimera sequences.

It would be interesting to learn whether the designed chimeras of CD44 Link have longer circulation time than the wild-type CD44 Link (or TSG-6 Link). However, preliminary experimental studies must be done to examine the effect of extensive amino acid substitutions on CD44 Link on the overall stability of the protein. Since it may be possible that the substitutions can lead to improper folding of the protein, there may be more substitutions required to make the chimeras more stable and retain function. Also, the circulation time of CD44 Link should be compared to sCD44 *in vivo*—because there are more *N*-glycosylation sites available on sCD44 than CD44 Link, the extra glycosylation could increase the circulation time significantly.

There are several alternative ways to increase the apparent molecular weight of LinkCD to improve the circulation time in the blood: PEGylation, multiple repeating units of the

Link domain, and grafting LinkCD onto a Fc domain of IgG. Also, a library of Link chimeras can be generated by DNA shuffling (Stemmer 1994) or error-prone PCR techniques and screened for the mutations that have desired function, since there is a homologous Link domain that is shared among the proteins in the Link module superfamily. Although this directed-evolution approach is a powerful tool in protein engineering, the lack of a high-throughput screening method is a major limitation to identify promising candidates in the library of CD44 chimeras.

All attempts to increase the circulation time of the LinkCD fusion protein by engineering the Link domain would ultimately fail for cancer therapy, if the duration of the fusion protein function is significantly shorter than the circulation time of the modified fusion protein *in vivo*. The thermostability of the LinkCD fusion protein at 37 ^{o}C is a critical element for the optimization of the blood circulation time of LinkCD. Although the CD enzyme from yeast is relatively thermolabile, the enzymatic function of LinkCD is shown to be more stable than that of CD at 37 ^{o}C (Chapter 3). In addition, there is a well-characterized thermostable mutant of CD enzyme that can be used to increase the duration of catalytic activity, which was created by a computational design approach (Korkegian et al 2005). This thermostable mutant of the CD enzyme was found to have 10 ^{o}C higher melting temperature (T_m) than the wild-type enzyme. Also, the half-life of the activity at 50 ^{o}C was increased by 30-fold over the wild-type enzyme. The structural analysis showed that the thermostable mutant (A23L, I140L, and V108I) has more compact core structure, which resulted in increasing interactions between the side

residues of the adjacent chains within the monomeric unit of the enzyme. The active site structure is unchanged in the mutant version.

Currently, our laboratory is collaborating with Halozyme Therapeutics, Inc. (located in San Diego, CA) to develop several versions of the LinkCD fusion proteins containing either CD44 Link or TSG-6 Link (Figure 5-6). Halozyme Therapeutics is employing the CHO cell expression system for glycosylation of the CD44 and TSG-6 Link domains. Since the protein expression in CHO cells is done at 37 ^{o}C, the thermo-labile nature of the CD enzyme was the major concern. Therefore, all versions of the LinkCD fusion protein being expressed in CHO cells were designed to contain the triple mutations on the CD enzyme that lead to thermostability. Also, the signal peptide sequence from human IgG κ chain was inserted at the N-terminal end to facilitate secretion of the target protein to CHO cell medium. These LinkCD proteins will be used to investigate pharmacokinetics and biodistribution of the glycosylated proteins, as well as the stability of the protein function. The chimeric sequences of CD44 Link could be useful to increase the affinity of the CD44LinkCD fusion protein to hyaluronan.

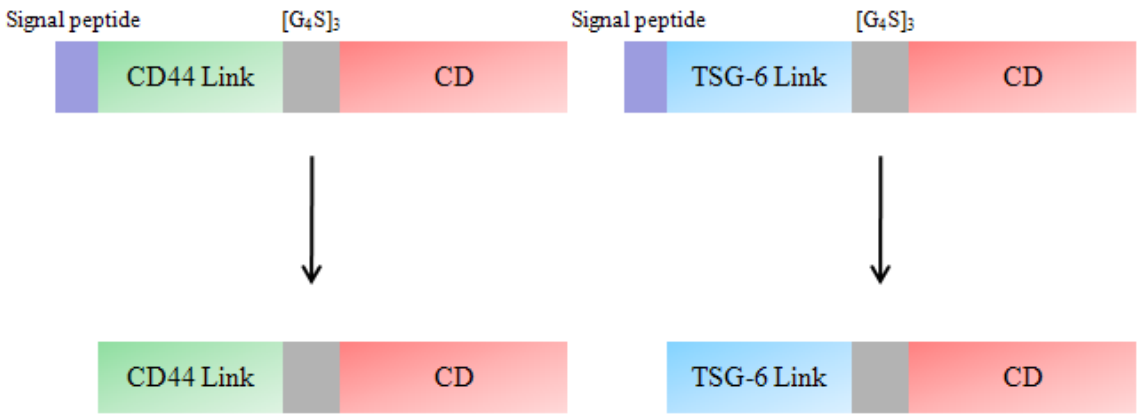

Figure 5-6. Production of the LinkCD fusion proteins using the CHO cell expression system. The two versions of the LinkCD fusion protein for the CHO cell expression. CD44LinkCD and TSG-6LinkCD constructs were designed with the thermostable mutations on the CD enzyme domain. The signal peptide is derived from the human IgG κ chain, which facilitates the secretion of the target protein.

5.5 Conclusions

Although local administration of LinkCD at the tumor site and oral administration of 5-FC prodrug caused an anti-tumor effect, improving pharmacokinetics and biodistribution properties of LinkCD is critical for systemic delivery. Optimization of systemic delivery of LinkCD could move MAT forward to preclinical studies and clinical trials. Replacing the TSG-6 Link domain of LinkCD with glycosylated CD44 Link may increase the circulation time, but the affinity of the resulting fusion protein to hyaluronan may be reduced. By taking a rational design approach, I propose three chimeric sequences of CD44 Link to engineer the hyaluronan binding surface of CD44 Link to enhance the binding activity. This chapter provides the first step towards engineering the hyaluronan binding surface of the CD44 Link for improving hyaluronan binding activity.

APPENDIX:

Preliminary Pharmacokinetics and Biodistribution of ^{125}I-Radiolabeled LinkCD in Normal Mice

A.1 Introduction

The anti-tumor effect of LinkCD/5-FC combination therapy was demonstrated in the C26 tumor model in mice (Chapter 4). If the circulation time of LinkCD is sufficiently long, it may be possible to target the extracellular matrix of tumor via intravenous administration. To examine the circulation time and biodistribution of LinkCD and CD in mice, the proteins were labled with ^{125}I radioisotope and injected into the tail-vein of normal CD-1 mice.

A.2 Methods

A.2.1 Radioiodination of LinkCD and CD enzyme

1,3,4,6-tetrachloro-3α, 6α-diphenylglycouril was used as the iodination reagent for radio-labeling of LinkCD and CD with ^{125}I radioisotope following the manufacturer's instructions (Pierce; Rockford, IL). Each of the radiolabeled proteins was separated from un-reacted free ^{125}I radioisotope by a DG-10 desalting column (Bio-Rad; Hercules, CA). The fractions containing the radio-labeled protein were pooled together and mixed with unlabeled protein. The specific activities of the injected doses were 15 μCi/mL and 19 μCi/mL for LinkCD and CD, respectively.

A.2.2 Pharmacokinetics and biodistribution of ^{125}I radiolabeled LinkCD and CD

^{125}I Radiolabeled LinkCD or CD in 200 μL volume was injected intravenously via the tail-vein of six to eight week old female CD-1 mice. For measurement of the radioactivity in the blood, the blood samples were taken at seven different time points ranging from 15 min to 24 hr via retro-orbital sinus bleeding. The last blood samples at the 24 hr time point were collected by heart puncture when the animals were sacrificed. For the biodistribution study, the animals were sacrificed at three different time points (1.5 hr, 6 hr, and 24 hr) to collect all organs—the heart, lungs, liver, kidneys, stomach, intestines, spleen, and carcass. The animals were housed in metabolic cages to collect urine and feces. The radioactivity of all collected blood and organ samples was detected using a Wallac 1480 Automatic Gamma Counter (PerkinElmer Life and Analytical Sciences; Waltham, MA).

To trace injected ^{125}I radiolabel *in vivo*, the radioactivity of the whole body of a mouse was scanned at 30 min, 3 hr, 6 hr, and 24 hr time points after the tail-vein injection using a Kodak Image Station 4000MM (Carestream Molecular Imaging; New Haven, CT). The animal was anesthetized in the Image Station with isofluorane prior to taking images. The recorded radioactivity and X-ray images were analyzed by Kodak Molecular Imaging Software Standard Edition (version 4.5.0).

A. 3 Results

LinkCD and CD enzyme were radiolabeled with ^{125}I radioisotope to quantify the circulation time in the blood and examine their biodistributions *in vivo*. The reaction mixture containing the radiolabeled protein and free ^{125}I radioisotope was separated by a

DG-10 desalting column, which is the same column used for exchanging buffers during the protein purification step (described in Chapter 3). The samples that eluted at the void volume of the DG-10 column (4 mL with 6-kDa cutoff) had radioactivity, which indicated that the protein was successfully radiolabeled with ^{125}I (Figure A-1). The purified ^{125}I-LinkCD and ^{125}I-CD were mixed with 'cold' proteins and injected into the tail-vein to measure the circulation time and biodistributions.

The circulation time in the blood appeared to be very short for both ^{125}I-LinkCD and ^{125}I-CD (Figure A-2). Only 12% of the total injected dose was found in the collected blood sample after 15 min of the intravenous administration of either ^{125}I-LinkCD or ^{125}I-CD. Thus, ^{125}I-LinkCD and ^{125}I-CD were rapidly cleared from the blood circulation shortly after the intravenous administration; neither protein circulated significantly better than the other in the blood.

The results of the biodistribution study indicated that the accumulation of ^{125}I-LinkCD in the liver and stomach at the 1.5 hr time point were relatively higher than that of ^{125}I-CD enzyme (Figure A-3). Also, it appears that the mice that received the ^{125}I-LinkCD excreted the radioisotope in both urine and feces, whereas the mice that received the ^{125}I-CD enzyme excreted the radioisotope material mostly through urine. However, only 28% of the total radioactivity was recovered from the mice that received the ^{125}I-CD at the 24 hr time point. Therefore, this experiment should be repeated to see whether the ^{125}I-CD is excreted primarily in the urine. Nonetheless, since the level of radioactivity is higher in the urine sample of the mice that received ^{125}I-CD than that of the mice that received

^{125}I-LinkCD at the 1.5 hr time point, the rate of elimination of ^{125}I-CD through the kidneys appears to be more rapid than that of ^{125}I-LinkCD.

There was no significant accumulation in the kidneys in the mice that received either ^{125}I-LinkCD or ^{125}I-CD. However, the radioactivity remained relatively higher in the head/thyroid region than other organs at the 24 hr time point for the mice that received either ^{125}I-LinkCD or ^{125}I-CD. This suggested a possibility that the radioactivity in the urine sample is smaller fragments of ^{125}I radiolabeled protein, or free ^{125}I that was cleaved off from the radiolabeled protein. To examine whether the excreted urine contains the intact ^{125}I radiolabeled protein, 1-ml of the collected urine sample was applied on a DG-10 desalting column with 6-kDa cut-off at the void volume (i.e., sizes greater than 6-kDa would be eluted at the void volume, which is 4-ml). More than 99% of the total activity in the urine came from the small Mw fractions (Figure A-4). There was no cytosine deaminase activity detected in the urine sample (data not shown). Thus, these results confirmed that either the ^{125}I-CD enzyme was degraded or the ^{125}I radioisotope was cleaved off from the labeled protein.

The radioactivity of ^{125}I-LinkCD was traced *in vivo* using a Kodak Image Station (Figure A-5A). After 30 min of intravenous administration of ^{125}I-LinkCD, the radioactivity was detected in three major parts of the body: head/thyroid, torso, and bladder. Most of the radioactivity was detected in the torso region at 30 min time point. At 3 hr and 6 hr time points, most of the measured radioactivity was concentrated in the bladder region. Thus, this *in vivo* imaging provided further evidence that ^{125}I radioisotope was being eliminated

rapidly from the body. At 24 hr time point, the radioactivity was detected only in the head/thyroid region. The intensity of the radioactivity from the head/thyroid region was analyzed to see the time-dependent of accumulation of the radioactivity in this region (Figure A-5B). Just 30 min after the intravenous administration, the intensity of radioactivity reached near the level of intensity recorded at the 6 hr time point. This suggests that the ^{125}I radiolabel was rapidly accumulating in the head/thyroid region, although it is possible that the level of accumulation was at its maximum between 6 hr and 24 hr. The radioactivity from the head/thyroid region gradually decreased from 6 to 24 hr, which is in agreement with the biodistribution study results (Figure A-3).

A.4 Discussion

Although the anti-tumor effect of LinkCD/5-FC was successfully demonstrated in Chapter 4, the preliminary results of pharmacokinetic and biodistribution studies were disappointing. The half-life of ^{125}I-LinkCD appears to be shorter than 15 min, and it did not seem to be any longer than that of ^{125}I-CD. A significant accumulation of radioactivity at the head/thyroid region suggests that the radio-labeled protein was degraded into smaller fragments or the ^{125}I radioisotope was cleaved from the radiolabeled protein. It is also possible that the ^{125}I radioisope was conjugated to the N-terminal His(×6) tag of LinkCD and CD, and the radio-labeled His-tag was cleaved off by thrombin in the body since both LinkCD and CD contained an N-terminal His-tag with a thrombin cleavage site (see Chapter 3).

A recent study reported biodistribution of ^{131}I-radiolabeled scFv-CD antibody-enzyme conjugate in mice (Panjideh et al 2008). The authors used chloramine-T (*N*-chloro tosylamide sodium salt) to label the antibody-enzyme conjugate with the radioisotope. Although this method is certainly an alternative radiolabeling technique that could be used for LinkCD, the harsh reaction conditions could damage the functional protein during the labeling procedure. Therefore, we avoided the chloramine-T method and used 1,3,4,6-tetrachloro-3α, 6α-diphenylglycouril for the iodination of LinkCD and CD under a mild condition.

It is imperative to determine the circulation time and biodistribution of LinkCD to move MAT forward to target the extracellular matrix of tumors via intravenous administration. Thus, these preliminary studies must be re-examined after the radio-labeling technique is validated for LinkCD to substantiate the represented results in this chapter.

A.5 Conclusions

The results of a preliminary pharmacokinetics study show that the circulation times of radio-labeled LinkCD and CD in the blood are very short (less than 15 min), which suggests that the circulation time in the blood needs to be improved for targeting the extracellular matrix of tumor systemically. The biodistribution results suggest the possibility that the ^{125}I radiolabel was cleaved from the radiolabeled protein. Thus, these results must be validated with further pharmacokinetics and biodistribution studies.

A.6 Credits

1. Radioiodination of LinkCD and CD were performed by Professor Frank Szoka.
2. Animals were handled and monitored by Edward Dy.

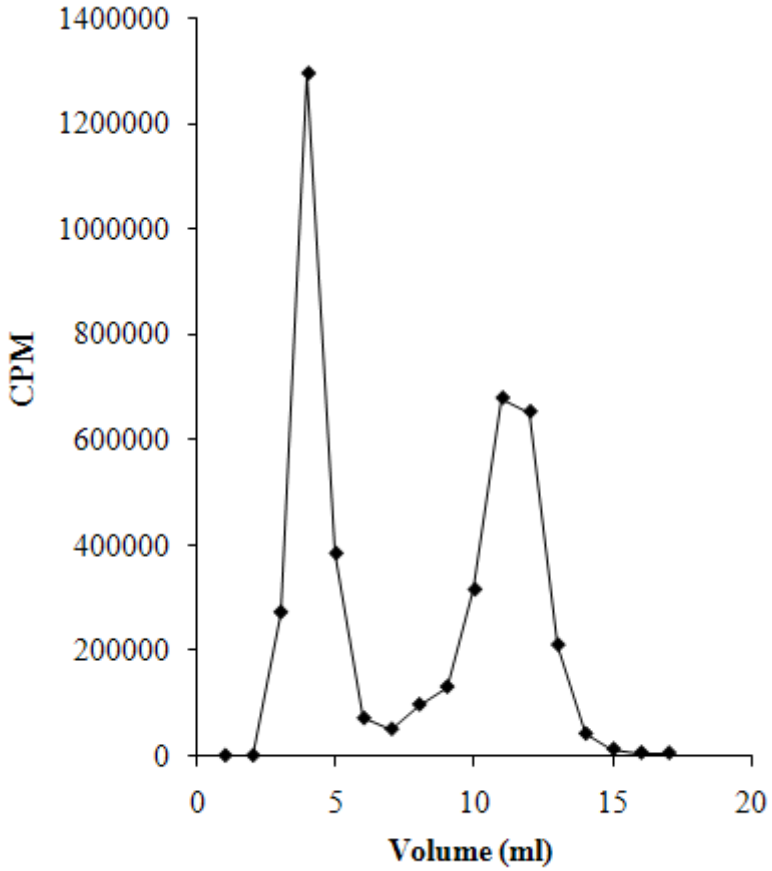

Figure A-1. Separation of ^{125}I radiolabeled protein from the free ^{125}I radioisotope on desalting column. After ^{125}I-iodonation of LinkCD, the reacted product containing the labeled protein and free radioisotope was applied on a DG-10 desalting column with 6 kDa cut-off (the void volume ~ 4 ml). The first peak represents the ^{125}I labeled LinkCD, and the second broad peak is the unreacted free-^{125}I radio isotope. Fractions 3 – 5 were pooled together for pharmacokinetics and biodistribution experiments.

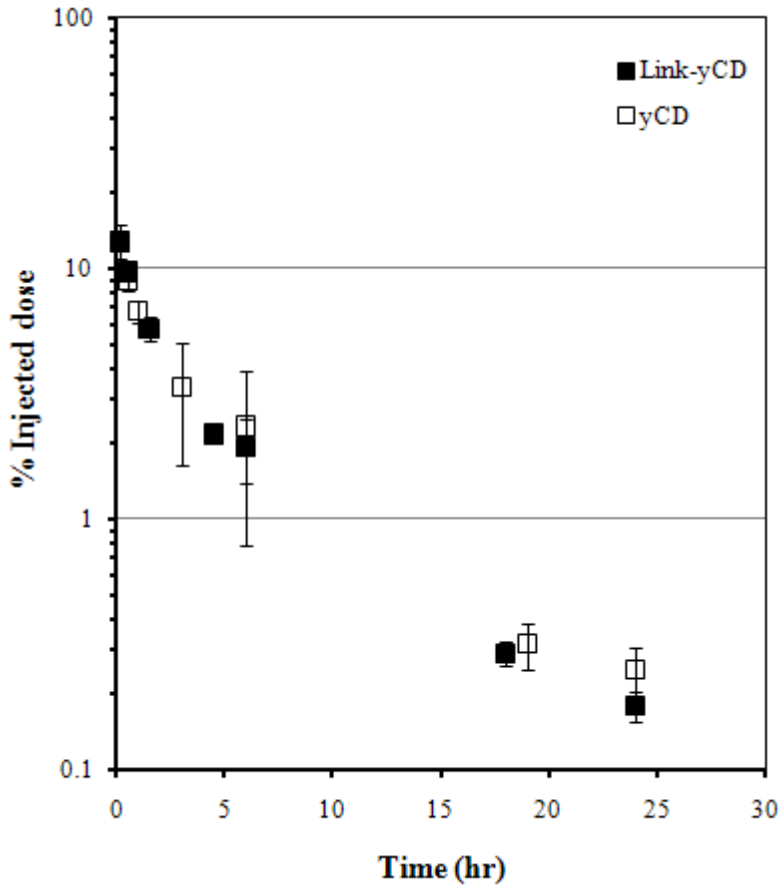

Figure A-2. Pharmacokinetics of ^{125}I radiolabeled LinkCD fusion protein in CD-1 mice. The blood samples were collected at each time point (from 15 min to 24 hr) after the ^{125}I labeled protein injections. The radioactivity in each blood sample was measured by a gamma counter instrument. Only 12% of the injected doses were recovered 15 min after the tail-vein injection. The elimination half-lives of LinkCD and CD are 4.1 and 4.6 hr, respectively. Each time point represent the mean ± sem (n = 3).

A

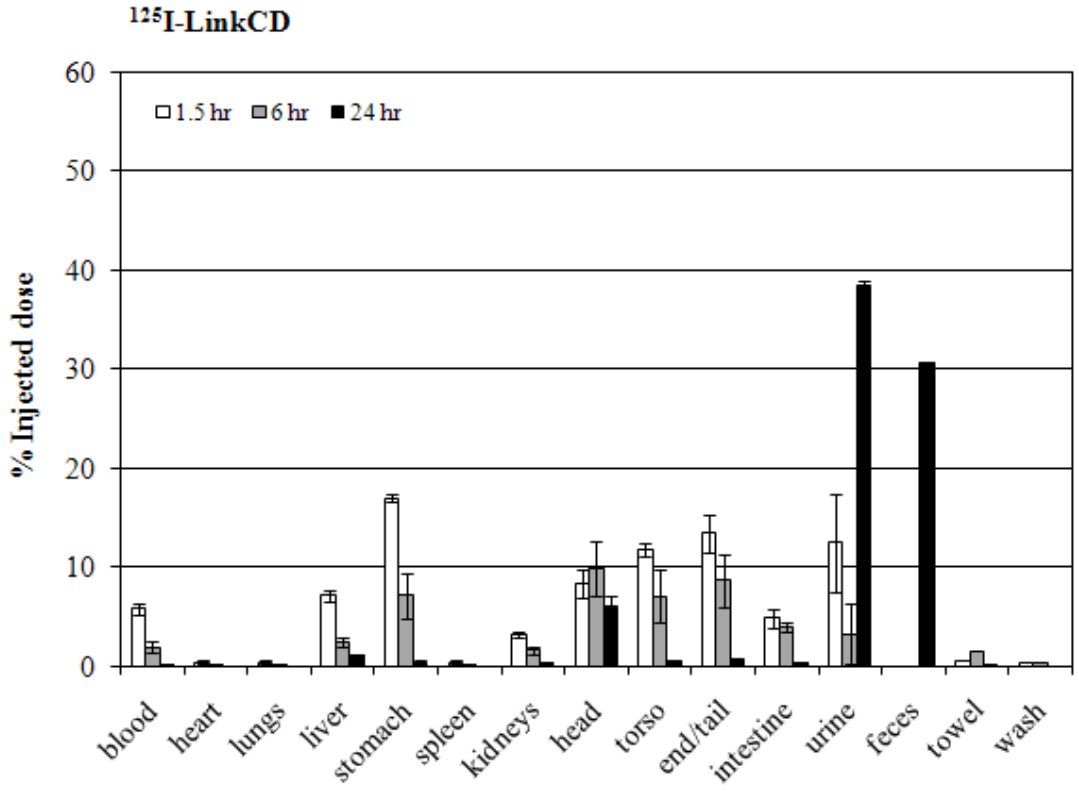
125I-LinkCD
1.5 hr
6 hr
24 hr
% Injected dose
60
50
40
30
20
10
0
blood
heart
lungs
liver
stomach
spleen
kidneys
head
torso
end/tail
intestine
urine
feces
towel
wash

B

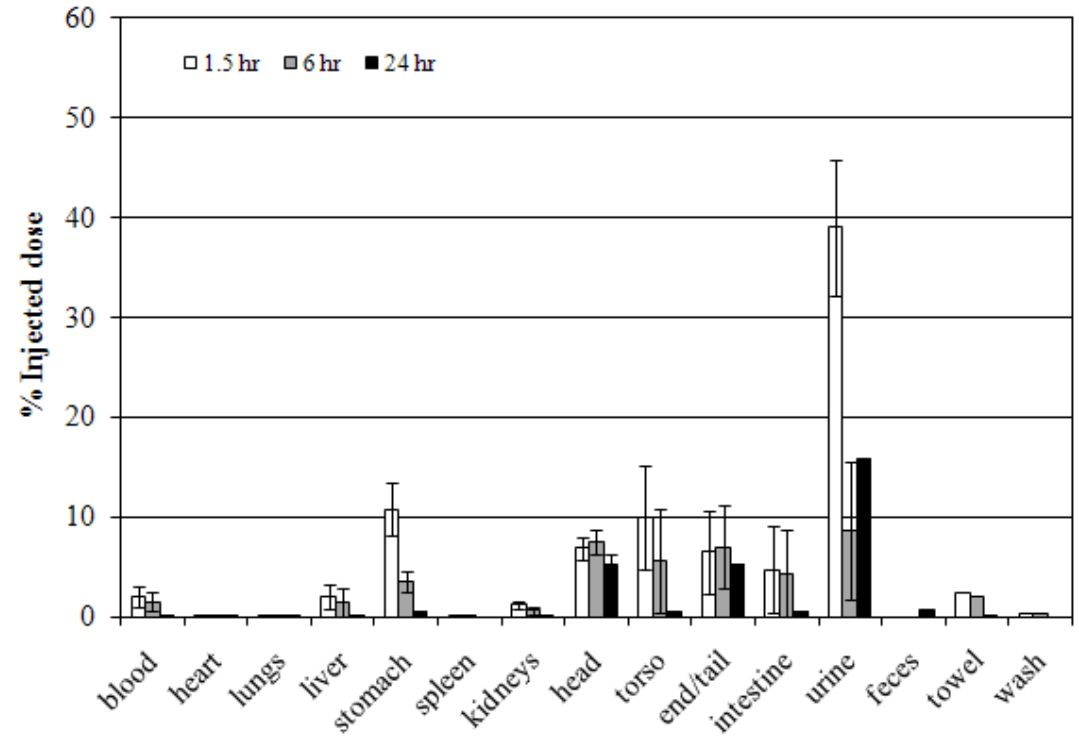
125I-CD
1.5 hr
6 hr
24 hr
% Injected dose
60
50
40
30
20
10
0
blood
heart
lungs
liver
stomach
spleen
kidneys
head
torso
end/tail
intestine
urine
feces
towel
wash

Figure A-3. Biodistribution of ^{125}I labeled -LinkCD fusion protein and the CD enzyme in CD-1 mice. The samples of blood, organs, urine, and feces were collected 1.5 hr, 6 hr, and 24 hr after the ^{125}I labeled-LinkCD fusion protein was injected into the tail-vein. The radio activity in each sample was measured by a gamma counter. Most of the radioactivity was excreted as urine or feces. The head region contained the most radioactivity among the collected organs 24 hr after ^{125}I labeled-LinkCD fusion protein was injected into the tail-vein. Each time point represent the mean ± sem (n = 3).

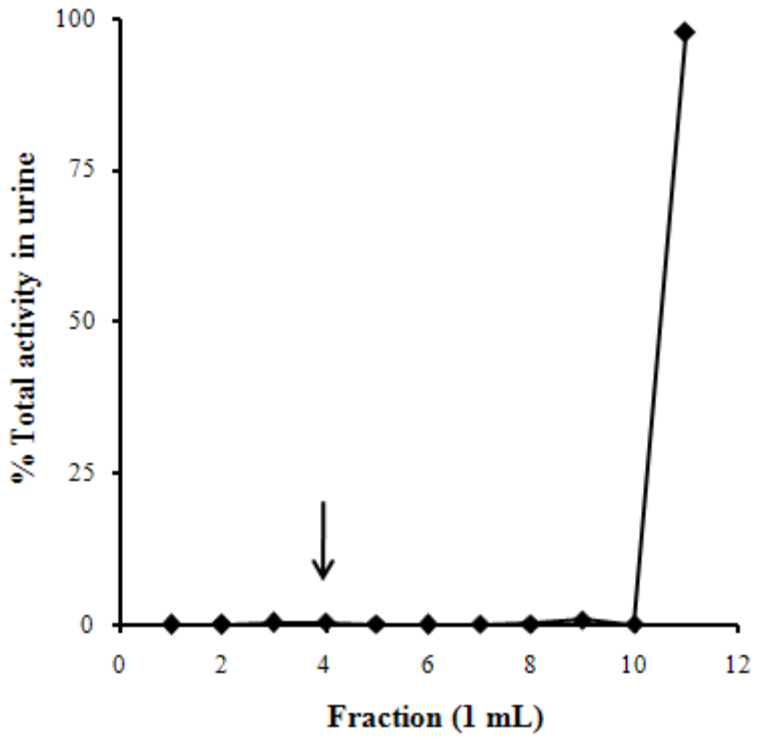

Figure A-4. Analysis of the urine sample of mice injected with the ^{125}I radio-labeled CD enzyme. The collected urine sample (1 ml) from the biodistribution study (24 hr time point) was applied to a DG-10 desalting column. The radio-activities of the collected fractions (1-ml each) were measured. Fraction number 11 (the last fraction) contained a pooled 'wash fraction' (12 mL total). >99 % of activity was eluted after the void volume fraction (Fractions 6 – 11). The arrow indicates the void volume of the column (4 ml), where the intact CD enzyme would elute.

A

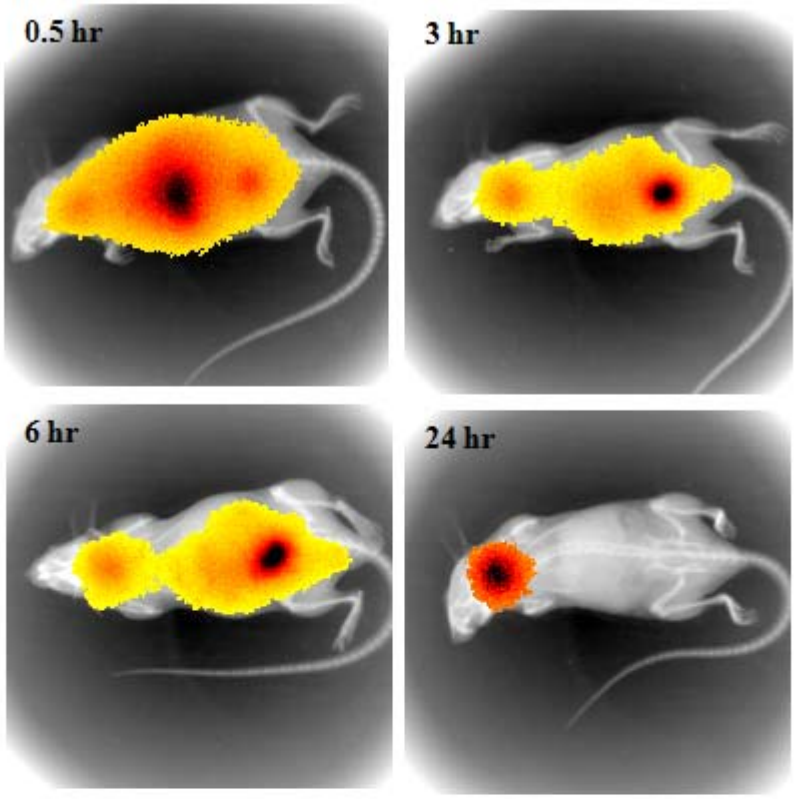
0.5 hr
3 hr
6 hr
24 hr

B

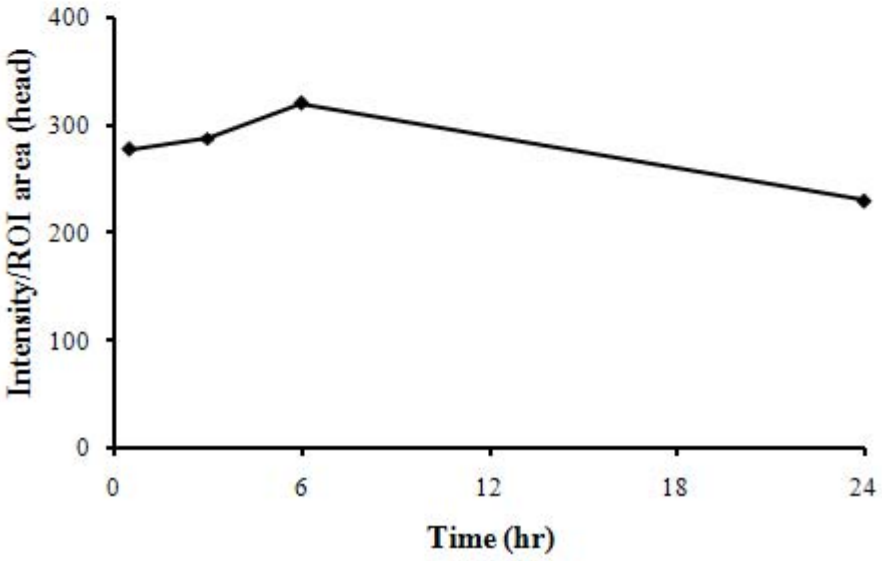
Intensity/ROI area (head)
400
300
200
100
0
0
6
12
18
24
Time (hr)

Figure A-5. ***In vivo*** **images of ^{125}I labeled -LinkCD fusion protein**. **A**. The images were taken 0.5 hr, 3 hr, 6 hr, and 24 hr after the tail-vein injection of ^{125}I labeled-LinkCD fusion protein. The lowest percentage of the radioactivity is colored in yellow, and the highest percentage of radio activity is black (within the image of the animal body). The radio activity is concentrated in the torso region after 0.5 hr. At 24 hr post-injection time point, radio-activity is detected only in the head/thyroid region. **B.** Time-course measurement of the radio-activity accumulation in the head region. The intensity of radio-activity from the head/thyroid region was normalized by the area selected. ROI (region of interest).

REFERENCES

Adachi, Y.; Tamiya, T.; Ichikawa, T.; Terada, K.; Ono, Y.; Matsumoto, K.; Furuta, T.; Hamada, H.; Ohmoto, T. Experimental gene therapy for brain tumors using adenovirus-mediated transfer of cytosine deaminase gene and uracil phosphoribosyltransferase gene with 5-fluorocytosine. *Hum. Gene Ther.* 2000, *11,* 77-89.

Ahrens, T.; Sleeman, J.P.; Schempp, C.M.; Howells, N.; Hofmann, M.; Ponta, H.; Herrlich, P.; Simon, J.C. Soluble CD44 inhibits melanoma tumor growth by blocking cell surface CD44 binding to hyaluronic acid. *Oncogene* 2001, *20,* 3399-3408.

Alderson, R.F.; Toki, B.E.; Roberge, M.; Geng, W.; Basler, J.; Chin, R.; Liu, A.; Ueda, R.; Hodges, D.; Escandon, E.; Chen, T.; Kanavarioti, T.; Babe, L.; Senter, P.D.; Fox, J.A.; Schellenberger, V. Characterization of a CC49-based single-chain fragment-beta-lactamase fusion protein for antibody-directed enzyme prodrug therapy (ADEPT). *Bioconjug. Chem.* 2006, *17,* 410-418.

Allen, T.M. and Cullis, P.R. Drug delivery systems: entering the mainstream. *Science* 2004, *303,* 1818-1822.

Altschul, S.F.; Madden, T.L.; Schaffer, A.A.; Zhang, J.; Zhang, Z.; Miller, W.; Lipman, D.J. Gapped BLAST and PSI-BLAST: a new generation of protein database search programs. *Nucleic Acids Res.* 1997, *25,* 3389-3402.

Anttila, M.A.; Tammi, R.H.; Tammi, M.I.; Syrjanen, K.J.; Saarikoski, S.V.; Kosma, V.M. High levels of stromal hyaluronan predict poor disease outcome in epithelial ovarian cancer. *Cancer Res.* 2000, *60,* 150-155.

Asai, T.; Trinh, R.; Ng, P.P.; Penichet, M.L.; Wims, L.A.; Morrison, S.L. A human biotin acceptor domain allows site-specific conjugation of an enzyme to an antibody-avidin fusion protein for targeted drug delivery. *Biomol. Eng.* 2005, *21,* 145-155.

Auvinen, P.; Tammi, R.; Parkkinen, J.; Tammi, M.; Agren, U.; Johansson, R.; Hirvikoski, P.; Eskelinen, M.; Kosma, V.M. Hyaluronan in peritumoral stroma and malignant cells associates with breast cancer spreading and predicts survival. *Am. J. Pathol.* 2000, *156,* 529-536.

Bagshawe, K.D. Antibody-directed enzyme prodrug therapy (ADEPT) for cancer. *Expert Rev. Anticancer Ther.* 2006, *6,* 1421-1431.

Bagshawe, K.D. Antibody directed enzymes revive anti-cancer prodrugs concept. *Br. J. Cancer* 1987, *56,* 531-532.

Bagshawe, K.D.; Springer, C.J.; Searle, F.; Antoniw, P.; Sharma, S.K.; Melton, R.G.; Sherwood, R.F. A cytotoxic agent can be generated selectively at cancer sites. *Br. J. Cancer* 1988, *58,* 700-703.

Banerji, S.; Day, A.J.; Kahmann, J.D.; Jackson, D.G. Characterization of a functional hyaluronan-binding domain from the human CD44 molecule expressed in Escherichia coli. *Protein Expr. Purif.* 1998, *14,* 371-381.

Banerji, S.; Wright, A.J.; Noble, M.; Mahoney, D.J.; Campbell, I.D.; Day, A.J.; Jackson, D.G. Structures of the Cd44-hyaluronan complex provide insight into a fundamental carbohydrate-protein interaction. *Nat. Struct. Mol. Biol.* 2007, *14,* 234-239.

Blundell, C.D.; Almond, A.; Mahoney, D.J.; DeAngelis, P.L.; Campbell, I.D.; Day, A.J. Towards a structure for a TSG-6.hyaluronan complex by modeling and NMR spectroscopy: insights into other members of the link module superfamily. *J. Biol. Chem.* 2005, *280,* 18189-18201.

Blundell, C.D.; Mahoney, D.J.; Cordell, M.R.; Almond, A.; Kahmann, J.D.; Perczel, A.; Taylor, J.D.; Campbell, I.D.; Day, A.J. Determining the molecular basis for the pH-dependent interaction between the link module of human TSG-6 and hyaluronan. *J. Biol. Chem.* 2007, *282,* 12976-12988.

Board, R.E. and Valle, J.W. Metastatic colorectal cancer: current systemic treatment options. *Drugs* 2007, *67,* 1851-1867.

Bobo, R.H.; Laske, D.W.; Akbasak, A.; Morrison, P.F.; Dedrick, R.L.; Oldfield, E.H. Convection-enhanced delivery of macromolecules in the brain. *Proc. Natl. Acad. Sci. U. S. A.* 1994, *91,* 2076-2080.

Bourquin, C.; Schreiber, S.; Beck, S.; Hartmann, G.; Endres, S. Immunotherapy with dendritic cells and CpG oligonucleotides can be combined with chemotherapy without loss of efficacy in a mouse model of colon cancer. *Int. J. Cancer* 2006, *118,* 2790-2795.

Braybrooke, J.P.; Slade, A.; Deplanque, G.; Harrop, R.; Madhusudan, S.; Forster, M.D.; Gibson, R.; Makris, A.; Talbot, D.C.; Steiner, J.; White, L.; Kan, O.; Naylor, S.; Carroll, M.W.; Kingsman, S.M.; Harris, A.L. Phase I study of MetXia-P450 gene therapy and

oral cyclophosphamide for patients with advanced breast cancer or melanoma. *Clin. Cancer Res.* 2005, *11,* 1512-1520.

Chang, T.S.; Wan, H.M.; Chen, C.C.; Giridhar, R.; Wu, W.T. Fusion protein of the hyaluronan binding domain from human TSG-6 with luciferase for assay of hyaluronan. *Biotechnol. Lett.* 2003, *25,* 1037-1040.

Chu, E.; Drake, J.C.; Koeller, D.M.; Zinn, S.; Jamis-Dow, C.A.; Yeh, G.C.; Allegra, C.J. Induction of thymidylate synthase associated with multidrug resistance in human breast and colon cancer cell lines. *Mol. Pharmacol.* 1991, *39,* 136-143.

Coelho, V.; Dernedde, J.; Petrausch, U.; Panjideh, H.; Fuchs, H.; Menzel, C.; Dubel, S.; Keilholz, U.; Thiel, E.; Deckert, P.M. Design, construction, and in vitro analysis of A33scFv::CDy, a recombinant fusion protein for antibody-directed enzyme prodrug therapy in colon cancer. *Int. J. Oncol.* 2007, *31,* 951-957.

Coussens, L.M.; Fingleton, B.; Matrisian, L.M. Matrix metalloproteinase inhibitors and cancer: trials and tribulations. *Science* 2002, *295,* 2387-2392.

Curreri, A.R.; Ansfield, F.J.; McIver, F.A.; Waisman, H.A.; Heidelberger, C. Clinical studies with 5-fluorouracil. *Cancer Res.* 1958, *18,* 478-484.

Cutler, R.E.; Blair, A.D.; Kelly, M.R. Flucytosine kinetics in subjects with normal and impaired renal function. *Clin. Pharmacol. Ther.* 1978, *24,* 333-342.

Dakappagari, N.K.; Douglas, D.B.; Triozzi, P.L.; Stevens, V.C.; Kaumaya, P.T. Prevention of mammary tumors with a chimeric HER-2 B-cell epitope peptide vaccine. *Cancer Res.* 2000, *60,* 3782-3789.

Dalba, C.; Bellier, B.; Kasahara, N.; Klatzmann, D. Replication-competent vectors and empty virus-like particles: new retroviral vector designs for cancer gene therapy or vaccines. *Mol. Ther.* 2007, *15,* 457-466.

Day, A.J.; Aplin, R.T.; Willis, A.C. Overexpression, purification, and refolding of link module from human TSG-6 in Escherichia coli: effect of temperature, media, and mutagenesis on lysine misincorporation at arginine AGA codons. *Protein Expr. Purif.* 1996, *8,* 1-16.

Day, A.J. and Prestwich, G.D. Hyaluronan-binding proteins: tying up the giant. *J. Biol. Chem.* 2002, *277,* 4585-4588.

Deckert, P.M.; Renner, C.; Cohen, L.S.; Jungbluth, A.; Ritter, G.; Bertino, J.R.; Old, L.J.; Welt, S. A33scFv-cytosine deaminase: a recombinant protein construct for antibody-directed enzyme-prodrug therapy. *Br. J. Cancer* 2003, *88,* 937-939.

Diasio, R.B. and Harris, B.E. Clinical pharmacology of 5-fluorouracil. *Clin. Pharmacokinet.* 1989, *16,* 215-237.

Eliaz, R.E. and Szoka, F.C.,Jr Liposome-encapsulated doxorubicin targeted to CD44: a strategy to kill CD44-overexpressing tumor cells. *Cancer Res.* 2001, *61,* 2592-2601.

Evrard, A.; Cuq, P.; Robert, B.; Vian, L.; Pelegrin, A.; Cano, J.P. Enhancement of 5-fluorouracil cytotoxicity by human thymidine-phosphorylase expression in cancer cells: in vitro and in vivo study. *Int. J. Cancer* 1999, *80,* 465-470.

Fraser, J.R.; Laurent, T.C.; Laurent, U.B. Hyaluronan: its nature, distribution, functions and turnover. *J. Intern. Med.* 1997, *242,* 27-33.

Freytag, S.O.; Stricker, H.; Pegg, J.; Paielli, D.; Pradhan, D.G.; Peabody, J.; DePeralta-Venturina, M.; Xia, X.; Brown, S.; Lu, M.; Kim, J.H. Phase I study of replication-competent adenovirus-mediated double-suicide gene therapy in combination with conventional-dose three-dimensional conformal radiation therapy for the treatment of newly diagnosed, intermediate- to high-risk prostate cancer. *Cancer Res.* 2003, *63,* 7497-7506.

Gavelli, A.; Baque, P.; Brossettej, N.; Bourgeon, A.; Staccini, P.; Rossi, B.; Pierrefite-Carle, V. Per os administration of 5-fluorocytosine is effective in the regression of CD-expressing liver metastases in rats. *Int. J. Mol. Med.* 2004, *14,* 323-325.

Gerweck, L.E. Tumor pH: implications for treatment and novel drug design. *Semin. Radiat. Oncol.* 1998, *8,* 176-182.

Gillet, J.P.; Efferth, T.; Remacle, J. Chemotherapy-induced resistance by ATP-binding cassette transporter genes. *Biochim. Biophys. Acta* 2007, *1775,* 237-262.

Gillies, E.R.; Dy, E.; Frechet, J.M.; Szoka, F.C. Biological evaluation of polyester dendrimer: poly(ethylene oxide) "bow-tie" hybrids with tunable molecular weight and architecture. *Mol. Pharm.* 2005, *2,* 129-138.

Glasgow, J.N.; Everts, M.; Curiel, D.T. Transductional targeting of adenovirus vectors for gene therapy. *Cancer Gene Ther.* 2006, *13,* 830-844.

Greco, O. and Dachs, G.U. Gene directed enzyme/prodrug therapy of cancer: historical appraisal and future prospectives. *J. Cell. Physiol.* 2001, *187,* 22-36.

Hanahan, D. and Weinberg, R.A. The hallmarks of cancer. *Cell* 2000, *100,* 57-70.

Hao, X.K.; Liu, J.Y.; Yue, Q.H.; Wu, G.J.; Bai, Y.J.; Yin, Y. In vitro and in vivo prodrug therapy of prostate cancer using anti-gamma-Sm-scFv/hCPA fusion protein. *Prostate* 2006, *66,* 858-866.

Hasenburg, A.; Fischer, D.C.; Tong, X.W.; Rojas-Martinez, A.; Nyberg-Hoffman, C.; Orlowska-Volk, M.; Kohlberger, P.; Kaufman, R.H.; Ramzy, I.; Aguilar-Cordova, E.; Kieback, D.G. Histologic and immunohistochemical analysis of tissue response to adenovirus-mediated herpes simplex thymidine kinase gene therapy of ovarian cancer. *Int. J. Gynecol. Cancer* 2002, *12,* 66-73.

Helfrich, W.; Haisma, H.J.; Magdolen, V.; Luther, T.; Bom, V.J.; Westra, J.; van der Hoeven, R.; Kroesen, B.J.; Molema, G.; de Leij, L. A rapid and versatile method for harnessing scFv antibody fragments with various biological effector functions. *J. Immunol. Methods* 2000, *237,* 131-145.

Herman, J.R.; Adler, H.L.; Aguilar-Cordova, E.; Rojas-Martinez, A.; Woo, S.; Timme, T.L.; Wheeler, T.M.; Thompson, T.C.; Scardino, P.T. In situ gene therapy for adenocarcinoma of the prostate: a phase I clinical trial. *Hum. Gene Ther.* 1999, *10,* 1239-1249.

Higman, V.A.; Blundell, C.D.; Mahoney, D.J.; Redfield, C.; Noble, M.E.; Day, A.J. Plasticity of the TSG-6 HA-binding loop and mobility in the TSG-6-HA complex revealed by NMR and X-ray crystallography. *J. Mol. Biol.* 2007, *371,* 669-684.

Hirschowitz, E.A.; Ohwada, A.; Pascal, W.R.; Russi, T.J.; Crystal, R.G. In vivo adenovirus-mediated gene transfer of the Escherichia coli cytosine deaminase gene to human colon carcinoma-derived tumors induces chemosensitivity to 5-fluorocytosine. *Hum. Gene Ther.* 1995, *6,* 1055-1063.

Huang, Z.; Park, J.I.; Watson, D.S.; Hwang, P.; Szoka, F.C.,Jr Facile synthesis of multivalent nitrilotriacetic acid (NTA) and NTA conjugates for analytical and drug delivery applications. *Bioconjug. Chem.* 2006, *17,* 1592-1600.

Huber, B.E.; Austin, E.A.; Richards, C.A.; Davis, S.T.; Good, S.S. Metabolism of 5-fluorocytosine to 5-fluorouracil in human colorectal tumor cells transduced with the

cytosine deaminase gene: significant antitumor effects when only a small percentage of tumor cells express cytosine deaminase. *Proc. Natl. Acad. Sci. U. S. A.* 1994, *91,* 8302-8306.

Ireton, G.C.; Black, M.E.; Stoddard, B.L. The 1.14 A crystal structure of yeast cytosine deaminase: evolution of nucleotide salvage enzymes and implications for genetic chemotherapy. *Structure* 2003, *11,* 961-972.

Itano, N.; Sawai, T.; Miyaishi, O.; Kimata, K. Relationship between hyaluronan production and metastatic potential of mouse mammary carcinoma cells. *Cancer Res.* 1999, *59,* 2499-2504.

Jelesarov, I. and Bosshard, H.R. Isothermal titration calorimetry and differential scanning calorimetry as complementary tools to investigate the energetics of biomolecular recognition. *J. Mol. Recognit.* 1999, *12,* 3-18.

Johnston, P.G.; Fisher, E.R.; Rockette, H.E.; Fisher, B.; Wolmark, N.; Drake, J.C.; Chabner, B.A.; Allegra, C.J. The role of thymidylate synthase expression in prognosis and outcome of adjuvant chemotherapy in patients with rectal cancer. *J. Clin. Oncol.* 1994, *12,* 2640-2647.

Jojovic, M.; Delpech, B.; Prehm, P.; Schumacher, U. Expression of hyaluronate and hyaluronate synthase in human primary tumours and their metastases in scid mice. *Cancer Lett.* 2002, *188,* 181-189.

Joyce, J.A. Therapeutic targeting of the tumor microenvironment. *Cancer. Cell.* 2005, *7,* 513-520.

Kahmann, J.D.; Koruth, R.; Day, A.J. Method for quantitative refolding of the link module from human TSG-6. *Protein Expr. Purif.* 1997, *9,* 315-318.

Kahmann, J.D.; O'Brien, R.; Werner, J.M.; Heinegard, D.; Ladbury, J.E.; Campbell, I.D.; Day, A.J. Localization and characterization of the hyaluronan-binding site on the link module from human TSG-6. *Structure* 2000, *8,* 763-774.

Kajita, M.; Itoh, Y.; Chiba, T.; Mori, H.; Okada, A.; Kinoh, H.; Seiki, M. Membrane-type 1 matrix metalloproteinase cleaves CD44 and promotes cell migration. *J. Cell Biol.* 2001, *153,* 893-904.

Kambara, H.; Tamiya, T.; Ono, Y.; Ohtsuka, S.; Terada, K.; Adachi, Y.; Ichikawa, T.; Hamada, H.; Ohmoto, T. Combined radiation and gene therapy for brain tumors with adenovirus-mediated transfer of cytosine deaminase and uracil phosphoribosyltransferase genes. *Cancer Gene Ther.* 2002, *9,* 840-845.

Kan, O.; Griffiths, L.; Baban, D.; Iqball, S.; Uden, M.; Spearman, H.; Slingsby, J.; Price, T.; Esapa, M.; Kingsman, S.; Kingsman, A.; Slade, A.; Naylor, S. Direct retroviral delivery of human cytochrome P450 2B6 for gene-directed enzyme prodrug therapy of cancer. *Cancer Gene Ther.* 2001, *8,* 473-482.

Kanai, F.; Kawakami, T.; Hamada, H.; Sadata, A.; Yoshida, Y.; Tanaka, T.; Ohashi, M.; Tateishi, K.; Shiratori, Y.; Omata, M. Adenovirus-mediated transduction of Escherichia coli uracil phosphoribosyltransferase gene sensitizes cancer cells to low concentrations of 5-fluorouracil. *Cancer Res.* 1998, *58,* 1946-1951.

Katoh, S.; McCarthy, J.B.; Kincade, P.W. Characterization of soluble CD44 in the circulation of mice. Levels are affected by immune activity and tumor growth. *J. Immunol.* 1994, *153,* 3440-3449.

Kawamura, K.; Tasaki, K.; Hamada, H.; Takenaga, K.; Sakiyama, S.; Tagawa, M. Expression of Escherichia coli uracil phosphoribosyltransferase gene in murine colon carcinoma cells augments the antitumoral effect of 5-fluorouracil and induces protective immunity. *Cancer Gene Ther.* 2000, *7,* 637-643.

Kerr, D.E.; Garrigues, U.S.; Wallace, P.M.; Hellstrom, K.E.; Hellstrom, I.; Senter, P.D. Application of monoclonal antibodies against cytosine deaminase for the in vivo clearance of a cytosine deaminase immunoconjugate. *Bioconjug. Chem.* 1993, *4,* 353-357.

Kievit, E.; Bershad, E.; Ng, E.; Sethna, P.; Dev, I.; Lawrence, T.S.; Rehemtulla, A. Superiority of yeast over bacterial cytosine deaminase for enzyme/prodrug gene therapy in colon cancer xenografts. *Cancer Res.* 1999, *59,* 1417-1421.

Kirchhoff, W.H. Exam: A Two-State Thermodynamic Analysis Program. *NIST Tech. Note 1401. U.S. Government Printing Office, Washington, DC. 1–103.* 1993,

Klatzmann, D.; Valery, C.A.; Bensimon, G.; Marro, B.; Boyer, O.; Mokhtari, K.; Diquet, B.; Salzmann, J.L.; Philippon, J. A phase I/II study of herpes simplex virus type 1 thymidine kinase "suicide" gene therapy for recurrent glioblastoma. Study Group on Gene Therapy for Glioblastoma. *Hum. Gene Ther.* 1998, *9,* 2595-2604.

Ko, T.P.; Lin, J.J.; Hu, C.Y.; Hsu, Y.H.; Wang, A.H.; Liaw, S.H. Crystal structure of yeast cytosine deaminase. Insights into enzyme mechanism and evolution. *J. Biol. Chem.* 2003, *278,* 19111-19117.

Kojima, A.; Hackett, N.R.; Crystal, R.G. Reversal of CPT-11 resistance of lung cancer cells by adenovirus-mediated gene transfer of the human carboxylesterase cDNA. *Cancer Res.* 1998, *58,* 4368-4374.

Komura, K.; Sato, S.; Fujimoto, M.; Hasegawa, M.; Takehara, K. Elevated levels of circulating CD44 in patients with systemic sclerosis: association with a milder subset. *Rheumatology (Oxford)* 2002, *41,* 1149-1154.

Korkegian, A.; Black, M.E.; Baker, D.; Stoddard, B.L. Computational thermostabilization of an enzyme. *Science* 2005, *308,* 857-860.

Kosaki, R.; Watanabe, K.; Yamaguchi, Y. Overproduction of hyaluronan by expression of the hyaluronan synthase Has2 enhances anchorage-independent growth and tumorigenicity. *Cancer Res.* 1999, *59,* 1141-1145.

Koyama, F.; Sawada, H.; Hirao, T.; Fujii, H.; Hamada, H.; Nakano, H. Combined suicide gene therapy for human colon cancer cells using adenovirus-mediated transfer of escherichia coli cytosine deaminase gene and Escherichia coli uracil phosphoribosyltransferase gene with 5-fluorocytosine. *Cancer Gene Ther.* 2000, *7,* 1015-1022.

Larsen, R.A.; Bauer, M.; Weiner, J.M.; Diamond, D.M.; Leal, M.E.; Ding, J.C.; Rinaldi, M.G.; Graybill, J.R. Effect of fluconazole on fungicidal activity of flucytosine in murine cryptococcal meningitis. *Antimicrob. Agents Chemother.* 1996, *40,* 2178-2182.

Lee, K.C.; Hamstra, D.A.; Bullarayasamudram, S.; Bhojani, M.S.; Moffat, B.A.; Dornfeld, K.J.; Ross, B.D.; Rehemtulla, A. Fusion of the HSV-1 tegument protein vp22 to cytosine deaminase confers enhanced bystander effect and increased therapeutic benefit. *Gene Ther.* 2006, *13,* 127-137.

Lee, T.H.; Wisniewski, H.G.; Vilcek, J. A novel secretory tumor necrosis factor-inducible protein (TSG-6) is a member of the family of hyaluronate binding proteins, closely related to the adhesion receptor CD44. *J. Cell Biol.* 1992, *116,* 545-557.

Lesley, J.; English, N.M.; Gal, I.; Mikecz, K.; Day, A.J.; Hyman, R. Hyaluronan binding properties of a CD44 chimera containing the link module of TSG-6. *J. Biol. Chem.* 2002, *277,* 26600-26608.

MacKay, J.A.; Deen, D.F.; Szoka, F.C.,Jr Distribution in brain of liposomes after convection enhanced delivery; modulation by particle charge, particle diameter, and presence of steric coating. *Brain Res.* 2005, *1035,* 139-153.

Mahoney, D.J.; Blundell, C.D.; Day, A.J. Mapping the hyaluronan-binding site on the link module from human tumor necrosis factor-stimulated gene-6 by site-directed mutagenesis. *J. Biol. Chem.* 2001, *276,* 22764-22771.

Mahoney, D.J.; Mulloy, B.; Forster, M.J.; Blundell, C.D.; Fries, E.; Milner, C.M.; Day, A.J. Characterization of the interaction between tumor necrosis factor-stimulated gene-6 and heparin: implications for the inhibition of plasmin in extracellular matrix microenvironments. *J. Biol. Chem.* 2005, *280,* 27044-27055.

Martin, J.; Stribbling, S.M.; Poon, G.K.; Begent, R.H.; Napier, M.; Sharma, S.K.; Springer, C.J. Antibody-directed enzyme prodrug therapy: pharmacokinetics and plasma levels of prodrug and drug in a phase I clinical trial. *Cancer Chemother. Pharmacol.* 1997, *40,* 189-201.

Martin, Y.N.; Salavaggione, O.E.; Eckloff, B.W.; Wieben, E.D.; Schaid, D.J.; Weinshilboum, R.M. Human methylenetetrahydrofolate reductase pharmacogenomics: gene resequencing and functional genomics. *Pharmacogenet Genomics* 2006, *16,* 265-277.

Mayer, A.; Francis, R.J.; Sharma, S.K.; Tolner, B.; Springer, C.J.; Martin, J.; Boxer, G.M.; Bell, J.; Green, A.J.; Hartley, J.A.; Cruickshank, C.; Wren, J.; Chester, K.A.; Begent, R.H. A phase I study of single administration of antibody-directed enzyme prodrug therapy with the recombinant anti-carcinoembryonic antigen antibody-enzyme fusion protein MFECP1 and a bis-iodo phenol mustard prodrug. *Clin. Cancer Res.* 2006, *12,* 6509-6516.

McNeish, I.A.; Green, N.K.; Gilligan, M.G.; Ford, M.J.; Mautner, V.; Young, L.S.; Kerr, D.J.; Searle, P.F. Virus directed enzyme prodrug therapy for ovarian and pancreatic cancer using retrovirally delivered E. coli nitroreductase and CB1954. *Gene Ther.* 1998, *5,* 1061-1069.

Meyer, D.L.; Jungheim, L.N.; Law, K.L.; Mikolajczyk, S.D.; Shepherd, T.A.; Mackensen, D.G.; Briggs, S.L.; Starling, J.J. Site-specific prodrug activation by antibody-beta-lactamase conjugates: regression and long-term growth inhibition of human colon carcinoma xenograft models. *Cancer Res.* 1993, *53,* 3956-3963.

Miller, C.R.; Williams, C.R.; Buchsbaum, D.J.; Gillespie, G.Y. Intratumoral 5-fluorouracil produced by cytosine deaminase/5-fluorocytosine gene therapy is effective for experimental human glioblastomas. *Cancer Res.* 2002, *62,* 773-780.

Molica, S.; Vitelli, G.; Levato, D.; Giannarelli, D.; Gandolfo, G.M. Elevated serum levels of soluble CD44 can identify a subgroup of patients with early B-cell chronic lymphocytic leukemia who are at high risk of disease progression. *Cancer* 2001, *92,* 713-719.

Moolten, F.L. An alternative to the magic bullet paradigm for specific cancer therapy. *Med. Hypotheses* 1987, *24,* 43-51.

Mummert, M.E.; Mummert, D.I.; Ellinger, L.; Takashima, A. Functional roles of hyaluronan in B16-F10 melanoma growth and experimental metastasis in mice. *Mol. Cancer. Ther.* 2003, *2,* 295-300.

Navolanic, P.M. and McCubrey, J.A. Pharmacological breast cancer therapy (review). *Int. J. Oncol.* 2005, *27,* 1341-1344.

Nemunaitis, J.; Cunningham, C.; Senzer, N.; Kuhn, J.; Cramm, J.; Litz, C.; Cavagnolo, R.; Cahill, A.; Clairmont, C.; Sznol, M. Pilot trial of genetically modified, attenuated Salmonella expressing the E. coli cytosine deaminase gene in refractory cancer patients. *Cancer Gene Ther.* 2003, *10,* 737-744.

O'Brien, T.A.; Tuong, D.T.; Basso, L.M.; McIvor, R.S.; Orchard, P.J. Coexpression of the uracil phosphoribosyltransferase gene with a chimeric human nerve growth factor receptor/cytosine deaminase fusion gene, using a single retroviral vector, augments cytotoxicity of transduced human T cells exposed to 5-fluorocytosine. *Hum. Gene Ther.* 2006, *17,* 518-530.

O'Connor, S.W. and Bale, W.F. Accessibility of circulating immunoglobulin G to the extravascular compartment of solid rat tumors. *Cancer Res.* 1984, *44,* 3719-3723.

Olumi, A.F.; Grossfeld, G.D.; Hayward, S.W.; Carroll, P.R.; Tlsty, T.D.; Cunha, G.R. Carcinoma-associated fibroblasts direct tumor progression of initiated human prostatic epithelium. *Cancer Res.* 1999, *59,* 5002-5011.

Palmer, D.H.; Mautner, V.; Mirza, D.; Oliff, S.; Gerritsen, W.; van der Sijp, J.R.; Hubscher, S.; Reynolds, G.; Bonney, S.; Rajaratnam, R.; Hull, D.; Horne, M.; Ellis, J.; Mountain, A.; Hill, S.; Harris, P.A.; Searle, P.F.; Young, L.S.; James, N.D.; Kerr, D.J. Virus-directed enzyme prodrug therapy: intratumoral administration of a replication-deficient adenovirus encoding nitroreductase to patients with resectable liver cancer. *J. Clin. Oncol.* 2004, *22,* 1546-1552.

Pandha, H.S.; Martin, L.A.; Rigg, A.; Hurst, H.C.; Stamp, G.W.; Sikora, K.; Lemoine, N.R. Genetic prodrug activation therapy for breast cancer: A phase I clinical trial of erbB-2-directed suicide gene expression. *J. Clin. Oncol.* 1999, *17,* 2180-2189.

Panjideh, H.; Da Silva Coelho, V.C.; Dernedde, J.; Bachran, C.; Forster, G.J.; Franke, J.; Fasold, P.; Fuchs, H.; Thiel, E.; Deckert, P.M. Biodistribution and efficacy of [131I]A33scFv::CDy, a recombinant antibody-enzyme protein for colon cancer. *Int. J. Oncol.* **2008,** *32,* 925-930.

Parkar, A.A.; Kahmann, J.D.; Howat, S.L.; Bayliss, M.T.; Day, A.J. TSG-6 interacts with hyaluronan and aggrecan in a pH-dependent manner via a common functional element: implications for its regulation in inflamed cartilage. *FEBS Lett.* 1998, *428,* 171-176.

Peer, D. and Margalit, R. Loading mitomycin C inside long circulating hyaluronan targeted nano-liposomes increases its antitumor activity in three mice tumor models. *Int. J. Cancer* 2004, *108,* 780-789.

Peters, G.J. Relative role of 5-fluorouracil activation and inactivation pathways on its cytotoxic effects, In *Fluoropyrimidines in Cancer Therapy,* Rustum, Y.M., Ed.; Humana Press, Inc.: Totowa, NJ, 2003; pp. 1-27.

Peterson, R.M.; Yu, Q.; Stamenkovic, I.; Toole, B.P. Perturbation of hyaluronan interactions by soluble CD44 inhibits growth of murine mammary carcinoma cells in ascites. *Am. J. Pathol.* 2000, *156,* 2159-2167.

Portsmouth, D.; Hlavaty, J.; Renner, M. Suicide genes for cancer therapy. *Mol. Aspects Med.* 2007, *28,* 4-41.

Pullarkat, S.T.; Stoehlmacher, J.; Ghaderi, V.; Xiong, Y.P.; Ingles, S.A.; Sherrod, A.; Warren, R.; Tsao-Wei, D.; Groshen, S.; Lenz, H.J. Thymidylate synthase gene polymorphism determines response and toxicity of 5-FU chemotherapy. *Pharmacogenomics J.* 2001, *1,* 65-70.

Rainov, N.G. A phase III clinical evaluation of herpes simplex virus type 1 thymidine kinase and ganciclovir gene therapy as an adjuvant to surgical resection and radiation in adults with previously untreated glioblastoma multiforme. *Hum. Gene Ther.* 2000, *11,* 2389-2401.

Ram, Z.; Culver, K.W.; Oshiro, E.M.; Viola, J.J.; DeVroom, H.L.; Otto, E.; Long, Z.; Chiang, Y.; McGarrity, G.J.; Muul, L.M.; Katz, D.; Blaese, R.M.; Oldfield, E.H. Therapy of malignant brain tumors by intratumoral implantation of retroviral vector-producing cells. *Nat. Med.* 1997, *3,* 1354-1361.

Ramnaraine, M.; Pan, W.; Goblirsch, M.; Lynch, C.; Lewis, V.; Orchard, P.; Mantyh, P.; Clohisy, D.R. Direct and bystander killing of sarcomas by novel cytosine deaminase fusion gene. *Cancer Res.* 2003, *63,* 6847-6854.

Ristamaki, R.; Joensuu, H.; Hagberg, H.; Kalkner, K.M.; Jalkanen, S. Clinical significance of circulating CD44 in non-Hodgkin's lymphoma. *Int. J. Cancer* 1998, *79,* 221-225.

Ropponen, K.; Tammi, M.; Parkkinen, J.; Eskelinen, M.; Tammi, R.; Lipponen, P.; Agren, U.; Alhava, E.; Kosma, V.M. Tumor cell-associated hyaluronan as an unfavorable prognostic factor in colorectal cancer. *Cancer Res.* 1998, *58,* 342-347.

Ruhela, D.; Riviere, K.; Szoka, F.C.,Jr Efficient synthesis of an aldehyde functionalized hyaluronic acid and its application in the preparation of hyaluronan-lipid conjugates. *Bioconjug. Chem.* 2006, *17,* 1360-1363.

Senter, P.D.; Saulnier, M.G.; Schreiber, G.J.; Hirschberg, D.L.; Brown, J.P.; Hellstrom, I.; Hellstrom, K.E. Anti-tumor effects of antibody-alkaline phosphatase conjugates in combination with etoposide phosphate. *Proc. Natl. Acad. Sci. U. S. A.* 1988, *85,* 4842-4846.

Senter, P.D.; Schreiber, G.J.; Hirschberg, D.L.; Ashe, S.A.; Hellstrom, K.E.; Hellstrom, I. Enhancement of the in vitro and in vivo antitumor activities of phosphorylated mitomycin C and etoposide derivatives by monoclonal antibody-alkaline phosphatase conjugates. *Cancer Res.* 1989, *49,* 5789-5792.

Senter, P.D. and Springer, C.J. Selective activation of anticancer prodrugs by monoclonal antibody-enzyme conjugates. *Adv. Drug Deliv. Rev.* 2001, *53,* 247-264.

Senter, P.D.; Su, P.C.; Katsuragi, T.; Sakai, T.; Cosand, W.L.; Hellstrom, I.; Hellstrom, K.E. Generation of 5-fluorouracil from 5-fluorocytosine by monoclonal antibody-cytosine deaminase conjugates. *Bioconjug. Chem.* 1991, *2,* 447-451.

Shand, N.; Weber, F.; Mariani, L.; Bernstein, M.; Gianella-Borradori, A.; Long, Z.; Sorensen, A.G.; Barbier, N. A phase 1-2 clinical trial of gene therapy for recurrent glioblastoma multiforme by tumor transduction with the herpes simplex thymidine kinase gene followed by ganciclovir. GLI328 European-Canadian Study Group. *Hum. Gene Ther.* 1999, *10,* 2325-2335.

Sharma, S.K.; Bagshawe, K.D.; Burke, P.J.; Boden, R.W.; Rogers, G.T. Inactivation and clearance of an anti-CEA carboxypeptidase G2 conjugate in blood after localisation in a xenograft model. *Br. J. Cancer* 1990, *61,* 659-662.

Sjoberg, S.; Fogelstrand, L.; Hulthe, J.; Fagerberg, B.; Krettek, A. Circulating soluble CD44 is higher among women than men and is not associated with cardiovascular risk factors or subclinical atherosclerosis. *Metabolism* 2005, *54,* 139-141.

Slamon, D.J.; Godolphin, W.; Jones, L.A.; Holt, J.A.; Wong, S.G.; Keith, D.E.; Levin, W.J.; Stuart, S.G.; Udove, J.; Ullrich, A. Studies of the HER-2/neu proto-oncogene in human breast and ovarian cancer. *Science* 1989, *244,* 707-712.

Soong, R. and Diasio, R.B. Advances and challenges in fluoropyrimidine pharmacogenomics and pharmacogenetics. *Pharmacogenomics* 2005, *6,* 835-847.

Springer, C.J.; Bagshawe, K.D.; Sharma, S.K.; Searle, F.; Boden, J.A.; Antoniw, P.; Burke, P.J.; Rogers, G.T.; Sherwood, R.F.; Melton, R.G. Ablation of human choriocarcinoma xenografts in nude mice by antibody-directed enzyme prodrug therapy (ADEPT) with three novel compounds. *Eur. J. Cancer* 1991, *27,* 1361-1366.

Stegman, L.D.; Rehemtulla, A.; Beattie, B.; Kievit, E.; Lawrence, T.S.; Blasberg, R.G.; Tjuvajev, J.G.; Ross, B.D. Noninvasive quantitation of cytosine deaminase transgene expression in human tumor xenografts with in vivo magnetic resonance spectroscopy. *Proc. Natl. Acad. Sci. U. S. A.* 1999, *96,* 9821-9826.

Stemmer, W.P. Rapid evolution of a protein in vitro by DNA shuffling. *Nature* 1994, *370,* 389-391.

Stern, R. Hyaluronan catabolism: a new metabolic pathway. *Eur. J. Cell Biol.* 2004, *83,* 317-325.

Stribbling, S.M.; Friedlos, F.; Martin, J.; Davies, L.; Spooner, R.A.; Marais, R.; Springer, C.J. Regressions of established breast carcinoma xenografts by carboxypeptidase G2 suicide gene therapy and the prodrug CMDA are due to a bystander effect. *Hum. Gene Ther.* 2000, *11,* 285-292.

Tai, C.K.; Wang, W.J.; Chen, T.C.; Kasahara, N. Single-shot, multicycle suicide gene therapy by replication-competent retrovirus vectors achieves long-term survival benefit in experimental glioma. *Mol. Ther.* 2005, *12,* 842-851.

Takeda, M.; Ogino, S.; Umemoto, R.; Sakakura, M.; Kajiwara, M.; Sugahara, K.N.; Hayasaka, H.; Miyasaka, M.; Terasawa, H.; Shimada, I. Ligand-induced structural changes of the CD44 hyaluronan-binding domain revealed by NMR. *J. Biol. Chem.* 2006, *281,* 40089-40095.

Teh, B.S.; Ayala, G.; Aguilar, L.; Mai, W.Y.; Timme, T.L.; Vlachaki, M.T.; Miles, B.; Kadmon, D.; Wheeler, T.; Caillouet, J.; Davis, M.; Carpenter, L.S.; Lu, H.H.; Chiu, J.K.; Woo, S.Y.; Thompson, T.; Aguilar-Cordova, E.; Butler, E.B. Phase I-II trial evaluating combined intensity-modulated radiotherapy and in situ gene therapy with or without hormonal therapy in treatment of prostate cancer-interim report on PSA response and biopsy data. *Int. J. Radiat. Oncol. Biol. Phys.* 2004, *58,* 1520-1529.

Teriete, P.; Banerji, S.; Noble, M.; Blundell, C.D.; Wright, A.J.; Pickford, A.R.; Lowe, E.; Mahoney, D.J.; Tammi, M.I.; Kahmann, J.D.; Campbell, I.D.; Day, A.J.; Jackson, D.G. Structure of the regulatory hyaluronan binding domain in the inflammatory leukocyte homing receptor CD44. *Mol. Cell* 2004, *13,* 483-496.

Tlsty, T.D. Stromal cells can contribute oncogenic signals. *Semin. Cancer Biol.* 2001, *11,* 97-104.

Toole, B.P. Hyaluronan: from extracellular glue to pericellular cue. *Nat. Rev. Cancer.* 2004, *4,* 528-539.

Van Hal, N.L.; Van Dongen, G.A.; Ten Brink, C.B.; Heider, K.H.; Rech-Weichselbraun, I.; Snow, G.B.; Brakenhoff, R.H. Evaluation of soluble CD44v6 as a potential serum marker for head and neck squamous cell carcinoma. *Clin. Cancer Res.* 1999, *5,* 3534-3541.

Voges, J.; Reszka, R.; Gossmann, A.; Dittmar, C.; Richter, R.; Garlip, G.; Kracht, L.; Coenen, H.H.; Sturm, V.; Wienhard, K.; Heiss, W.D.; Jacobs, A.H. Imaging-guided convection-enhanced delivery and gene therapy of glioblastoma. *Ann. Neurol.* 2003, *54,* 479-487.

Voges, J.; Weber, F.; Reszka, R.; Sturm, V.; Jacobs, A.; Heiss, W.D.; Wiestler, O.; Kapp, J.F. Clinical protocol. Liposomal gene therapy with the herpes simplex thymidine kinase gene/ganciclovir system for the treatment of glioblastoma multiforme. *Hum. Gene Ther.* 2002, *13,* 675-685.

Wallace, P.M.; MacMaster, J.F.; Smith, V.F.; Kerr, D.E.; Senter, P.D.; Cosand, W.L. Intratumoral generation of 5-fluorouracil mediated by an antibody-cytosine deaminase conjugate in combination with 5-fluorocytosine. *Cancer Res.* 1994, *54,* 2719-2723.

Wallace, P.M. and Senter, P.D. In vitro and in vivo activities of monoclonal antibody-alkaline phosphatase conjugates in combination with phenol mustard phosphate. *Bioconjug. Chem.* 1991, *2,* 349-352.

Wei, X.; McLeod, H.L.; McMurrough, J.; Gonzalez, F.J.; Fernandez-Salguero, P. Molecular basis of the human dihydropyrimidine dehydrogenase deficiency and 5-fluorouracil toxicity. *J. Clin. Invest.* 1996, *98,* 610-615.

Wisniewski, H.G.; Snitkin, E.S.; Mindrescu, C.; Sweet, M.H.; Vilcek, J. TSG-6 protein binding to glycosaminoglycans: formation of stable complexes with hyaluronan and binding to chondroitin sulfates. *J. Biol. Chem.* 2005, *280,* 14476-14484.

Wolfe, L.A.; Mullin, R.J.; Laethem, R.; Blumenkopf, T.A.; Cory, M.; Miller, J.F.; Keith, B.R.; Humphreys, J.; Smith, G.K. Antibody-directed enzyme prodrug therapy with the T268G mutant of human carboxypeptidase A1: in vitro and in vivo studies with prodrugs of methotrexate and the thymidylate synthase inhibitors GW1031 and GW1843. *Bioconjug. Chem.* 1999, *10,* 38-48.

Xiong, M.P. and Kwon, G.S. PEGylation of yeast cytosine deaminase for pretargeting. *J. Pharm. Sci.* 2005, *94,* 1249-1258.

Xu, X.M.; Chen, Y.; Chen, J.; Yang, S.; Gao, F.; Underhill, C.B.; Creswell, K.; Zhang, L. A peptide with three hyaluronan binding motifs inhibits tumor growth and induces apoptosis. *Cancer Res.* 2003, *63,* 5685-5690.

Yao, L.; Yan, H.; Cukier, R.I. A molecular dynamics study of the ligand release path in yeast cytosine deaminase. *Biophys. J.* 2007, *92,* 2301-2310.

Zafir-Lavie, I.; Michaeli, Y.; Reiter, Y. Novel antibodies as anticancer agents. *Oncogene* 2007, *26,* 3714-3733.

Zhang, X. and Diasio, R.B. Regulation of human dihydropyrimidine dehydrogenase: implications in the pharmacogenetics of 5-FU-based chemotherapy. *Pharmacogenomics* 2007, *8,* 257-265.

Publishing Agreement

It is the policy of the University to encourage the distribution of all theses and dissertations. Copies of all UCSF theses and dissertations will be routed to the library via the Graduate Division. The library will make all theses and dissertations accessible to the public and will preserve these to the best of their abilities, in perpetuity.

Please sign the following statement:

I hereby grant permission to the Graduate Division of the University of California, San Francisco to release copies of my thesis or dissertation to the Campus Library to provide access and preservation, in whole or in part, in perpetuity.

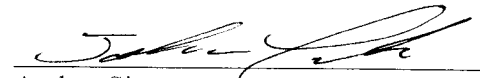

Author Signature

May 28, 2008

Date